

THE CHEMICAL GENETIC
INTERACTIONS OF STATIN
DRUGS WITH THEIR TARGET
GENES IN *Saccharomyces cerevisiae*

Bede P. Busby

A thesis submitted to Victoria University of Wellington in fulfilment of the requirements for the degree of Masters of Science in Cell and Molecular Bioscience

School of Biological Sciences
Victoria University of Wellington 2009

Abstract

Statins, competitive inhibitors of the rate limiting cholesterol/ergosterol enzymes HMG-CoA reductase (HMG1 and HMG2), are the most widely prescribed human therapeutic drugs. They are effective in lowering cholesterol levels in atherosclerosis and related syndromes. However, statins exhibit a range of pleiotropic side effects whose mechanisms are poorly understood.

This study investigates statin pleiotropy by analysis of genetic interaction networks in yeast, *Saccharomyces cerevisiae*, which shows high homology to mammalian pathways affected by statins. Synthetic genetic array (SGA) analysis allows elucidation of functional genetic networks of genes of interest (“query genes”) by measurement of genetic epistasis in double mutants of the query gene with the genome - wide deletion mutant array of ~4800 non-essential strains. Chemical-genetic profiling is similar where a SMP may effectively replace the query gene in genome wide epistatic analysis.

The genetic interaction networks resulting from use of *HMG1* and *HMG2* as query genes for SGA analysis were compared to the chemical-genetic profiles of *atorvastatin*, *cerivastatin* and *lovastatin*. The genes *ARV1*, *BTS1*, *OPI3* displaying phenotypic enhancements (i.e. their deletion caused major *growth inhibition*) with statins became essential in the presence of all the statins. Two mitochondrial genes, *COX17* and *MMMI*, showed phenotypic suppressions (i.e. their deletion allowed *better growth*) in common to all three statin drugs. An attractive hypothesis is that

major pleiotropic effects of statins could be due to variation in function or expression of these enhancing or suppressing genes.

Other processes compensating statin use were also elucidated. For example, when HMG1 and its epistatically interacting genes are shut down by deletion coupled with inhibition of HMG2 with statin, there is strong evidence that the cell attempts to maintain membrane/lipid homeostasis via anterograde and retrograde transport mechanisms, including the mobilisation of lipid storage droplets.

To aid refinement of genetic analysis in this and future studies, a more direct phenotypic assay was developed for quantifying ergosterol. Such an assay may be used as a phenotype to map the effect of up - and downstream - genes, or network genes affecting ergosterol levels. This assay was used to quantify ergosterol in a drug - resistant mutant developed by others aiding confirmation of the drug target.

Acknowledgements

I would like to thank Professor Paul Atkinson for his supervision, scientific guidance and hard work throughout the course of this thesis.

I also extend my appreciation to Dr David Maass for all the help with the experimental design, especially the molecular biology aspect of this study.

I would also like to thank the following people for their helpful advice Dr. David Bellows for all the intricate yeast genetics and especially James Matthews for all his help, support and motivation throughout the course of this thesis, also a big thank you to all those in the chemical genetics laboratory.

Finally, I would like to acknowledge my Mum, Dad, Grandma and Ingrid for all their encouragement, patience and support throughout the course of this work.

List of Tables

Table 2.1 Deletion PCR Reaction Conditions.....	21
Table 2.2 Primers used for <i>Δhmg2</i> query strain construction	22
Table 2.3 Conformation PCR conditions.....	24
Table 3.1 <i>Δhmg1</i> PE query gene interactions..	40
Table 3.2 Linkage group genes surrounding HMG1.....	40
Table 3.3 <i>Δhmg2</i> PE query gene interactions.	44
Table 3.4 Linkage group genes surrounding HMG2.....	45
Table 4.1 <i>Atorvastatin</i> chemical genetic PE interactions.	56
Table 4.2 <i>Atorvastatin</i> chemical genetic PS interactions	57
Table 4.3 <i>Cerivastatin</i> chemical genetic PE interactions	63
Table 4.4 <i>Cerivastatin</i> chemical genetic PS interactions.	68
Table 4.5 <i>Lovastatin</i> chemical genetic PE interactions.....	71
Table 4.6 <i>Lovastatin</i> chemical genetic PS interactions.	72
Table 6.1 Ergosterol content of wild-type and mutant strains	106
Table 6.2 Ergosterol content of <i>molr1</i> and <i>molr2</i> mutants	109
Table A.1 Ergosterol quantification data analysis.....	147

List of Figures

Figure 1.1 World Health Organisation human disease mortality.....	1
Figure 1.2 Salicylate example of drug target networks.....	3
Figure 1.3 Structural formulae of statin drugs	5
Figure 1.4 The mevalonate pathway in mammalian cells.	7
Figure 1.5 Bi-modal feedback regulation of HMG-CoA reductase	8
Figure 1.6 Details of the mevalonate pathway.....	9
Figure 1.7 Structural difference of ergosterol and cholesterol	10
Figure 1.8 Summary of yeast cell biology processes directly involved in this study	15
Figure 1.9 Diagrammatic comparison of genetic and chemical genetic interactions	18
Figure 2.1 PCR-mediated gene deletion used to construct the non-essential query strains.....	20
Figure 2.2 Synthetic genetic array methodology.	25
Figure 3.1 HMG2 query strain construction.....	37
Figure 3.2 Example of HMG1 SGA showing linkage group genes.....	41
Figure 3.3 Example of HMG2 SGA showing linkage group genes.....	45
Figure 3.4 Cytoscape network graph showing HMG1 and HMG2 screens	48
Figure 4.1 Spot assays for statin drug working concentrations.	52
Figure 4.2 Cytoscape network graph showing the phenotypic enhancement interactions from the chemical genetic screens performed on <i>atorvastatin</i> , <i>cerivastatin</i> and <i>lovastatin</i>	75
Figure 4.3 Cytoscape network graph showing the phenotypic suppression interactions from the chemical genetic screens performed on <i>atorvastatin</i> , <i>cerivastatin</i> and <i>lovastatin</i>	76
Figure 5.1 Double mutant chemical-genetic screen pilot for <i>atorvastatin</i> working concentrations in robotically pinned SGA formatted $\Delta hmg1 \Delta his3$	81
Figure 5.2 Double mutant chemical-genetic screen pilot for <i>cerivastatin</i> working concentrations in robotically pinned SGA formatted $\Delta hmg1 \Delta his3$	81

Figure 5.3 Double mutant chemical-genetic screen pilot for <i>lovastatin</i> working concentrations in robotically pinned SGA formatted $\Delta hmg1 \Delta his3$	82
Figure 5.4 Double mutant chemical-genetic screen pilot for <i>atorvastatin</i> working concentrations in robotically pinned SGA formatted $\Delta hmg2 \Delta his3$	82
Figure 5.5 Double mutant chemical-genetic screen pilot for <i>cerivastatin</i> working concentrations in robotically pinned SGA formatted $\Delta hmg2 \Delta his3$	82
Figure 5.6 Double mutant chemical-genetic screen pilot for <i>lovastatin</i> working concentrations in robotically pinned SGA formatted $\Delta hmg2 \Delta his3$	83
Figure 5.7 HMG1 based interactions. Cytoscape network graph showing the phenotypic enhancement interactions from the chemical genetic screens performed on <i>atorvastatin</i> , <i>cerivastatin</i> and <i>lovastatin</i>	94
Figure 5.8 HMG2 based interactions. Cytoscape network graph showing the phenotypic enhancement interactions from the chemical genetic screens performed on <i>atorvastatin</i> , <i>cerivastatin</i> and <i>lovastatin</i>	98
Figure 5.9 Graph of GO processes involving HMG1 showing enrichment for vesicle mediated transport genetic interactions.	100
Figure 6.1 Ergosterol standard HPLC chromatographs.....	104
Figure 6.2 Ergosterol Concentration Standardisation.	105
Figure 6.3 Ergosterol quantification results in different sample sizes	108
Figure 6.4 Ergosterol quantification <i>molliside</i> resistant mutants <i>molr1</i> and <i>molr2</i> compared to wild type (BY7092).	109

List of Abbreviations

µg	microgram
µL	micro litre
ATP	Adenosine triphosphate
bp	base pair
CoA	Co-enzyme A
CVD	Cardiovascular disease
DAG	Diacylglycerol
DMA	Deletion mutant array
DMSO	Dimethyl sulfoxide
DNA	Deoxyribonucleic acid
ER	Endoplasmic reticulum
ERAD	ER associated protein degradation
FPP	Farnesyl pyrophosphate
GARP	Golgi assisted retrograde protein
gDNA	Genomic DNA
GET	Golgi - ER trafficking
GGPP	Geranylgeranyl pyrophosphate
GO	Gene ontology
GTP	Guanine Triphosphate
HDL	High density lipoprotein
HMG-CoA	3-hydroxy-3-methylglutaryl-coenzyme A
HPLC	High performance liquid chromatography

HRD	HMG-CoA reductase degradation
HT	High throughput
IPP	Isopentyl pyrophosphate
LDL	Low density lipoprotein
LG	Linkage group
LiAc	Lithium acetate
M	Mole
MDR	Multi drug resistant
MIC	Minimum inhibitory concentration
mL	millilitre
MVB	Multi vesicular body
NADPH	Nicotinamide adenine dinucleotide phosphate
NAT	Nourseothricin
NatR	Nourseothricin resistance cassette
nM	nanomole
OD	Optical density
ORF	Open reading frame
PCR	Polymerase chain reaction
PEG	Polyethylene glycol
PE	Phenotypic enhancement
PS	Phenotypic suppression
QTL	Quantitative trait loci
SC	Synthetic complete
SD	Synthetic drop-out
SESA	SGA experiment set analyser

SGA	Synthetic genetic array analysis
SL	Synthetic lethality
SMP	Small molecule perturbagen
SNARE	Soluble NSF Attachment Protein
SS	Synthetic sick
TAG	Triacylglycerol
TGN	Trans Golgi network
UPR	Unfolded protein response
UV	Ultraviolet
WHO	World Health Organisation
YGDS	Yeast gene deletion set
YPD	Yeast peptone dextrose

Table of Contents

Abstract	II
Acknowledgements	IV
List of Tables	V
List of Figures	VI
List of Abbreviations	VIII
Chapter 1. Introduction	1
1.1. Cardiovascular disease	1
1.2. Statin drugs	2
1.3. Mevalonate pathway	6
1.4. HMG-CoA reductase in yeast and humans	9
1.5. Pleiotropic effects of statins	11
1.6. Adverse effects of statin drugs	12
1.7. Cellular networks	14
1.8. Disease networks - genetic interactions	15
1.9. Yeast as a model organism	16
Chapter 2. Methods	19
2.1. Query strain construction	19
2.2. PCR amplification	21
2.3. Transformation	22
	XI

2.4.	PCR confirmation	23
2.5.	Synthetic genetic array	24
2.6.	SGA analysis	28
2.7.	SGA scoring epistatic interactions in high-throughput	29
2.8.	Gene ontology	30
2.9.	Chemical genetic profiling	31
2.10.	Chemicals and media for chemical genetic profiling	32
2.11.	Spot dilution assays	33
2.12.	Chemical genetic screens	33
2.13.	Ergosterol quantification	34
Chapter 3. Results of SGAs		36
3.1.	Query strain construction	36
3.2.	HMG1 SGA	38
3.3.	HMG2 SGA	42
3.4.	HMG1 and HMG2 SGA Discussion	47
Chapter 4. Chemical genetic interactions of statin drugs		50
4.1.	Spot dilution assays	51
4.2.	Chemical genetic screens	52
4.3.	Discussion	74

Chapter 5. Double mutant chemical genetic interactions of statin

drugs with their target genes 79

5.1. Pilot Study: double mutant growth on statin drugs	80
5.2. <i>Atorvastatin</i> + $\Delta hmg1$ Δxxx double mutant chemical genetic screens	84
5.3. <i>Atorvastatin</i> + $\Delta hmg2$ Δxxx double mutant chemical genetic screens	85
5.4. <i>Cerivastatin</i> + $\Delta hmg1$ Δxxx double mutant chemical genetic screens	87
5.5. <i>Cerivastatin</i> + $\Delta hmg2$ Δxxx double mutant chemical genetic screens	88
5.6. <i>Lovastatin</i> + $\Delta hmg1$ Δxxx double mutant chemical genetic screens	90
5.7. <i>Lovastatin</i> + $\Delta hmg2$ Δxxx double mutant chemical genetic screens	91
5.8. Discussion: statins + $\Delta hmg1$ Δxxx double mutant chemical genetic screens	93
5.9. Discussion: statins + $\Delta hmg2$ Δxxx double mutant chemical genetic screens	96

Chapter 6. Ergosterol quantification 102

6.1. Ergosterol standard	103
6.2. Method optimisation	106
6.3. <i>Molliside</i> resistant mutants	109
6.4. Discussion	110

Chapter 7. General discussion, conclusions and future directions

111

7.1. Epistasis	111
7.2. Isoprenoid compensatory pathways within the mitochondria	112
7.3. Statin compensating genes	113
7.4. Vesicular transport	114
7.5. Other lipid synthesis genes	116
7.6. The HRD – ubiquitin pathway	116
7.7. Statins and quantitative traits	118
7.8. Overall conclusions	119
7.9. Future directions	120

References

123

Appendix 1 Media and components

144

YPD (Agar)	144
SD complete (Agar)	144
Enriched Sporulation (Agar)	145
Antibiotics	145

Appendix 2: Ergosterol quantification data

146

Appendix 3: Double mutant chemical genetic interactions of statin drugs with their target genes

Chapter 1. Introduction

1.1. Cardiovascular disease

This study focuses on key enzymes of sterol synthesis and statin inhibitors, in light of the importance of sterol metabolism in diseases. Cardiovascular disease (CVD), for example, accounted for 41% of all deaths in New Zealand in 2000 (MOH, 2003). CVD is now recognised as a global epidemic, equalling infectious disease as the leading cause of death and disability worldwide (Fig.1.1, reproduced from WHO 2001) and is expected to surpass infectious diseases in the next 15 years (WHO, 2001). High levels of total cholesterol (hypercholesterolemia) and low-density lipoprotein cholesterol (LDL-C) with low levels of high-density lipoprotein cholesterol (HDL-C) are important risk factors for coronary heart disease (Yusuf, et al., 2001).

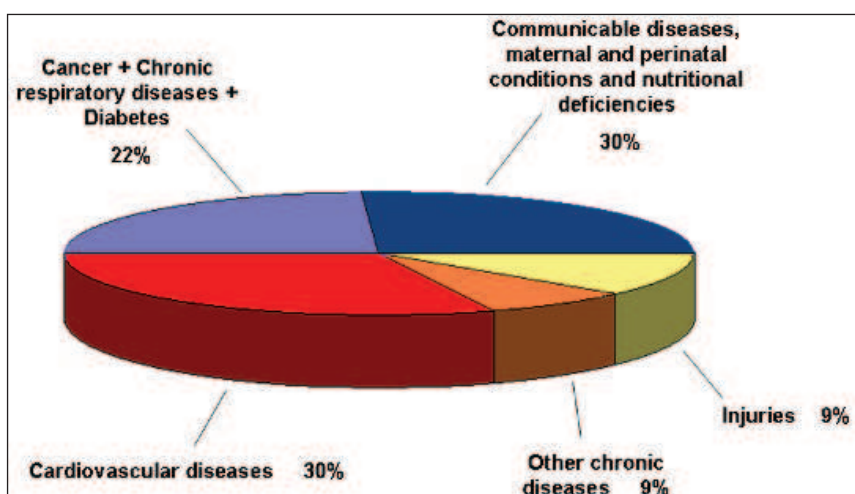


Figure 1.1 World Health Organisation human disease mortality.

Hypercholesterolemia is characterised by an increase in low density lipoprotein (LDL) and a decrease in high density lipoprotein (HDL) caused by a combination of genetic and environmental factors that disturb the transport of apolipoprotein B-100 in plasma (Austin, et al., 2004). Familial hypercholesterolemia is an autosomal dominant disorder of lipoprotein metabolism characterised by mutations of the LDL receptor resulting in an accumulation of LDL cholesterol in the plasma. It has been estimated that familial hypercholesterolemia affects approximately one in 500 of the British population and carries with it an increased risk of CVD (Broome, 1991). It is the aim of this dissertation to assemble genetic interaction networks around the genes of the mevalonate pathway and of their statin inhibitors in order to better understand the mechanism of the drugs.

1.2. Statin drugs

Mammalian and yeast 3-hydroxy-3-methylglutaryl-coenzyme A (HMG-CoA) reductase is an integral membrane glycoprotein of the endoplasmic reticulum (ER) which catalyses the rate determining reaction in cholesterol biosynthesis namely the conversion of HMG-CoA to mevalonate (Fig.1.4). Statin drugs are HMG-CoA reductase inhibitors that are effective and reasonably safe drugs used for the prevention and treatment of atherosclerosis. Statins inhibit cholesterol synthesis, increase LDL uptake, improve endothelial function and prevent thrombus formation. They are currently the most widely prescribed class of all therapeutic drugs with sales (of *atorvastatin*) in the order of \$US12b pa.

However, it is unsurprising given the central role sterol metabolism in cell processes and physiology that statins display side-effects. In addition to their cholesterol lowering effects, statins also exhibit a range of pleiotropic effects including nitric oxide mediated promotion of blood vessel growth, stimulation of bone formation, protection against oxidative modification of LDL and anti-inflammatory effects (Liao and Laufs, 2005). It is an aim of this study to understand the network effects of statins in genetic interaction networks. As an example as to what is meant by ‘network effects’ the effects of aspirin (Fig.1.2, reproduced from Huang 2002) are a good illustration (Huang, 2002). Salicylate has network effects across a number basic pathways of importance in cell physiology as can be seen in the figure. However, even salicylate is not without side-effects.

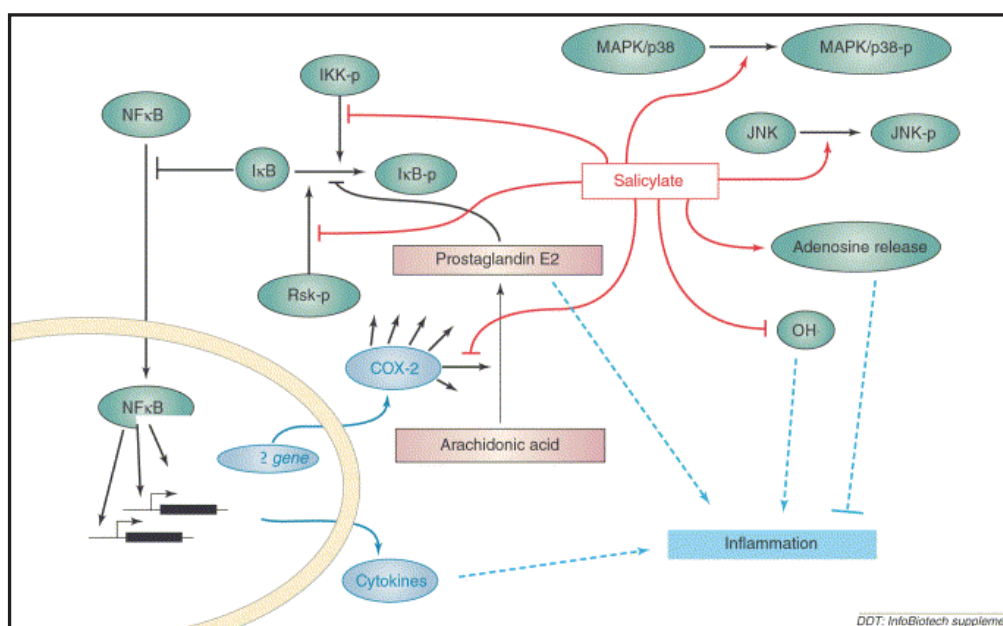


Figure 1.2 Salicylate example of drug target networks (Huang, 2002).

An example is Reyes syndrome that may appear in children suffering from acute viral infections. Reyes syndrome results from damage to cellular mitochondria (Gosalakkal and Kamoji, 2008) – a side-effect that might not be immediately

evident in the main (anti - inflammatory) mechanism of aspirin action. Statins may also have pleiotropic effects across pathways (this thesis), including mitochondrial effects and given the therapeutic value of statins such network effects should be studied.

Statins are competitive inhibitors of HMG-CoA reductase (Fig. 1.4) possessing an HMG-like moiety (Schachter, 2005) inhibiting the deacylation of HMG-CoA to form CoA and mevalonate (Istvan and Deisenhofer, 2001):



Type one fungal derived statins contain rigid hydrophobic groups that are covalently linked to the HMG-like moiety (Fig. 1.3A, adapted from Istvan, 2001 and Schachter, 2005). In contrast type two statins are fully synthetic with larger groups linked to the HMG-like moiety (Fig. 1.3B). The additional groups range from very hydrophobic (*cerivastatin*) to partially hydrophobic (*rosuvastatin*). Type 1 and type 2 statins inhibit binding of the substrate HMG-CoA, but not co-enzyme NADPH to the enzyme. Statins can also exist as ‘pro drugs’ (*lovastatin*) in their inactive lactone form which is hydrolysed *in vivo* (in mammals) to the active hydroxy acid form, whereas the other statins exist freely in the active hydroxy acid form (Istvan and Deisenhofer, 2001; Schachter, 2005).

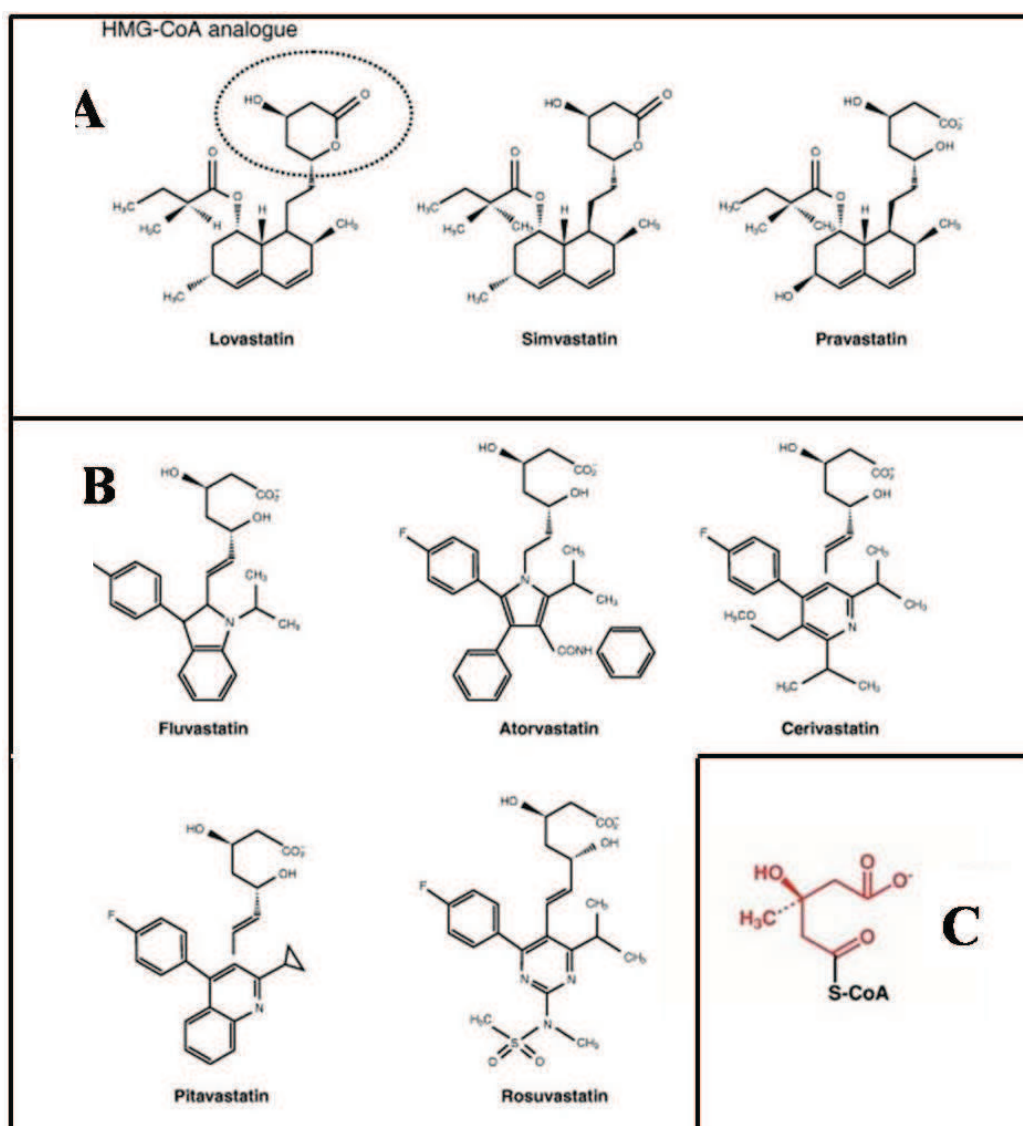


Figure 1.3 Structural formulae of statin drugs. A. Type one statins *Lovastatin*, *Simvastatin* and *Pravastatin*. B. Type Two Statins, *Fluvastatin*, *Atorvastatin*, *Cerivastatin*, *Pitavastatin* and *Rosuvastatin*. C. Structure of HMG-CoA. (Istvan and Deisenhofer, 2001; Schachter, 2005)

1.3. Mevalonate pathway

In addition to cholesterol synthesis, mevalonate is the precursor of multiple isoprenoid compounds that become incorporated into many end products (Fig.1.4, reproduced from Goldstein, 1990) including haem A and ubiquinone (electron transport), polyisoprenoid biosynthesis (Basson, et al., 1988), dolichol (glycoprotein synthesis), isopentyladenine (tRNA) and intracellular messengers such as cytokines in plants, farnesylated mating factors in fungi, hormones in insects and steroid hormones in mammals (Brown and Goldstein, 1980; Goldstein and Brown, 1990). Cellular cholesterol is also derived from plasma LDL in mammals and to maintain sterol homeostasis, cells must balance and maintain equilibrium between sterol biosynthesis, uptake, transport, utilisation, efflux and storage of the sterol products. Aberrations in any of these processes may lead to multiple human disease pathologies including atherosclerosis and neurodegeneration (Sturley, 2000). The balance within the pathway is coordinated mainly through feedback regulation from HMG-CoA reductase (Goldstein and Brown, 1990; White, 1972).

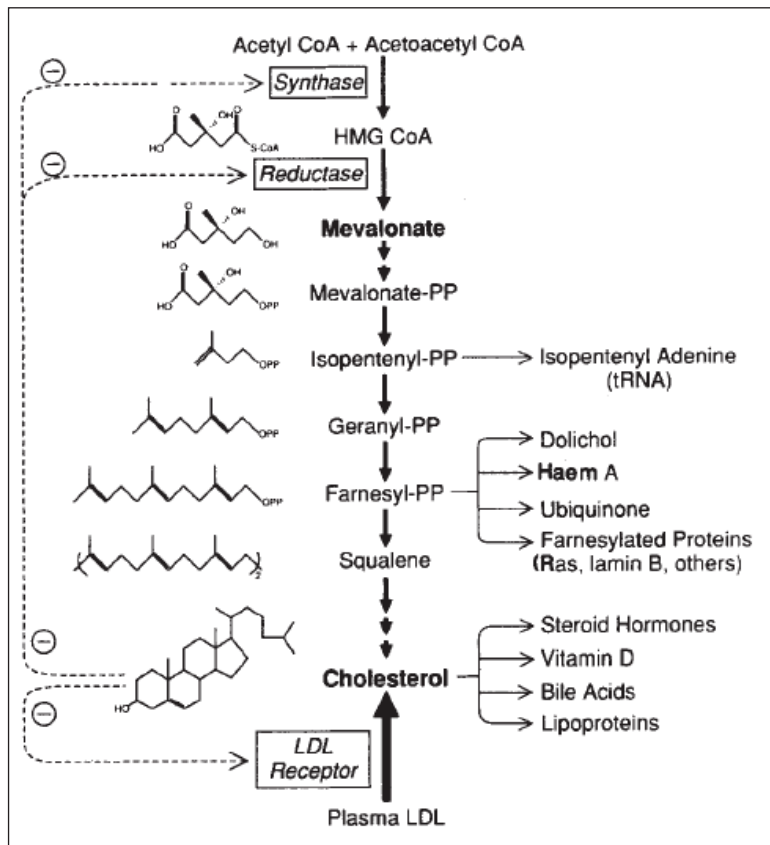


Figure 1.4 The mevalonate pathway in mammalian cells (Goldstein and Brown, 1990).

Mevalonate synthesis is predominately regulated by feedback inhibition from the sequential enzymes HMG-CoA synthase and HMG-CoA reductase but is also regulated by LDL receptors (Brown and Goldstein, 1980). In the presence of exogenous LDL and/or mevalonate, HMG-CoA synthase and HMG-CoA reductase activities can decrease to under 10% with the cells producing only the minuscule amounts of mevalonate needed for non sterol products. Conversely, when exogenous LDL is absent, animal cells maintain high activities of the two enzymes (Fig. 1.5) and the ER degradation is decreased (Goldstein and Brown, 1990; Hampton and Rine, 1994).

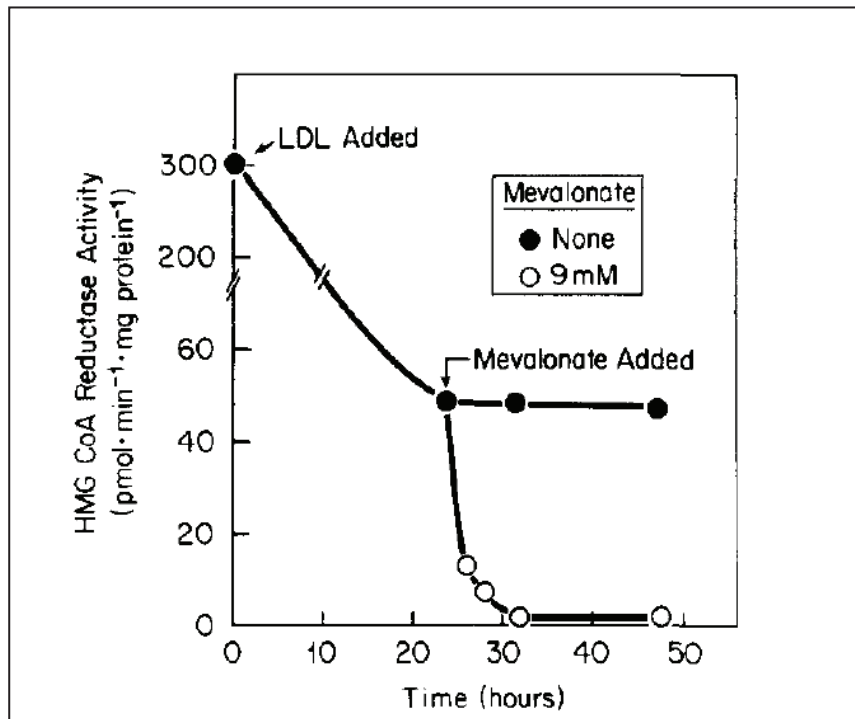


Figure 1.5 Bi-modal feedback regulation of HMG-CoA reductase (Brown and Goldstein, 1980).

Figure 1.5 (reproduced from Brown, 1980) shows that cells require mevalonate and cholesterol for HMG-CoA reductase to be suppressed. Because cholesterol may be supplied exogenously from LDL or endogenously from mevalonate, high levels of mevalonate alone are required to completely suppress the enzyme (Brown and Goldstein, 1980). This bimodal feedback regulation of HMG-CoA reductase is an important mechanism for therapeutic intervention to inhibit cholesterol production and also plasma LDL levels. In addition to regulation of mevalonate synthesis, cells also regulate mevalonate use between sterol and non-sterol pathways. The enzymes of the non – sterol pathways (Figs.1.4 and 1.6) have much higher affinities for mevalonate than those of the sterol derived substrates. Thus, when mevalonate is sparse, it is preferentially shunted into the higher affinity non sterol pathways (Goldstein and Brown, 1990).

1.4. HMG-CoA reductase in yeast and humans

The mammalian genome contains a single gene encoding HMG-CoA reductase (Basson, et al., 1988). In contrast, yeast (*Saccharomyces cerevisiae*) has two genes, designated HMG1 and HMG2 (Fig.1.6). Cells containing an inoperative mutant allele of HMG1 or HMG2 show only a subtle growth defect, whereas cells containing null mutant alleles for both HMG1 and HMG2 show a synthetic lethal phenotype (Basson, et al., 1986). This phenotype can be rescued with the insertion of the human HMG gene demonstrating the aptness of the yeast model. The functional conservation (in the catalytic domain) between yeast and human HMG-CoA reductase allows the use of yeast cells in the identification of drugs with therapeutic value in the treatment of diseases such as hypercholesterolemia (Basson, et al., 1988).

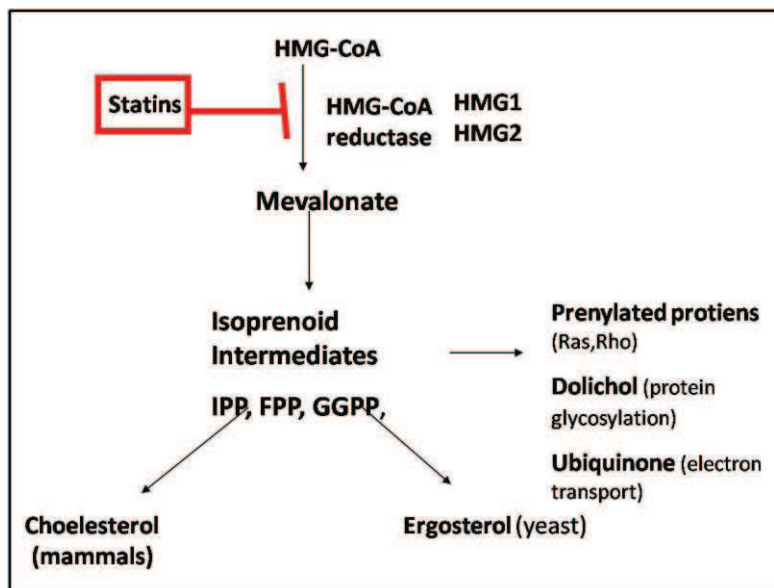


Figure 1.6 Details of the mevalonate pathway. The bulk product of mevalonate synthesis in mammals is cholesterol, whereas the end product in yeast is ergosterol. Adapted from (Brown and Goldstein 1980; Goldstein and Brown 1990; Bammert and Fostel 2000).

Ergosterol differs from cholesterol in that it contains two extra double bonds and a methyl group (Fig. 1.7). However, ergosterol is synthesised, regulated and esterified in very similar processes as mammalian cells. Mevalonate biosynthesis and signalling pathways are also highly conserved between yeast and humans (Smith, et al., 1996; Veen and Lang, 2005).

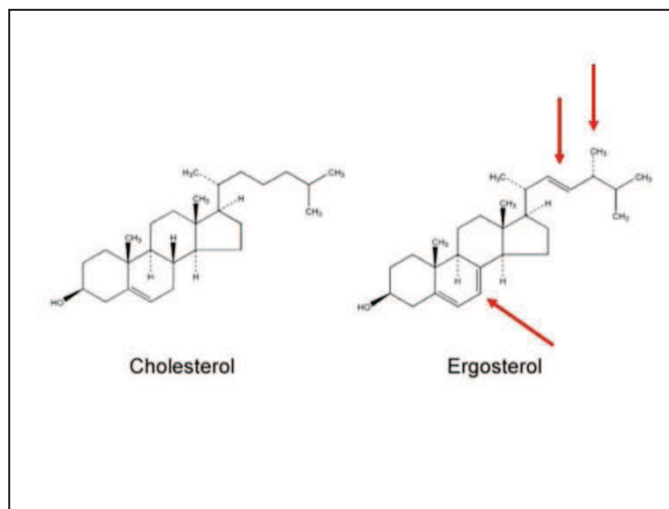


Figure 1.7 Structural difference of ergosterol and cholesterol with double bonds at C7 and C22 and an additional methyl group at C28 (Smith, Crowley et al. 1996; Veen and Lang 2005).

1.5. Pleiotropic effects of statins

Though statins are structurally different, they all possess the HMG-CoA-like domain (Fig.1.3), these various statins differ in their tissue permeability and metabolism and entail different potencies for HMG-CoA reductase inhibition. However, it was thought that the pleiotropic effects of statins were primarily mediated by the inhibition of mevalonate synthesis, with other unidentified mechanisms playing an important role (Laufs, et al., 1998; Liao and Laufs, 2005). By inhibiting mevalonate synthesis statins also prevent *de novo* synthesis of isoprenoid intermediates (see Mevalonate Pathway) as shown in Figures 1.4 and 1.6.

These intermediates provide lipid moieties in the post-translational modification of a variety of proteins affecting intracellular trafficking, such as found in the gamma subunit of heterotrimeric G-proteins, Heme-a, nuclear lamins, the small guanosine triphosphate (GTP)-binding protein RAS, and the RAS like proteins Rho, Rab, Rac, Ral and Rap (Van Aelst and Dae Souza-Schorey, 1997). In endothelial cells Ras translocation from the cytoplasm to the plasma membrane is dependent on farnesylation, whereas Rho translocation is dependent of geranylgeranylation. Thus statins inhibit both Ras and Rho isoprenylation which leads to the accumulation of inactive Ras and Rho in the cytoplasm (Liao and Laufs, 2005).

Rho inhibition by statins also leads to inhibition of the downstream target Rho-kinase. Members of the Rho GTPase family play important roles in cell shape,

motility, secretion and proliferation. The distinct functions of Rho proteins also exhibit cell signalling effects. When cells reorganise their cytoskeleton in response to extracellular signals, they alter the co-localisation of intracellular proteins (Van Aelst and Dae Souza-Schorey, 1997). Therefore, these changes can also affect intracellular transport, membrane trafficking, mRNA stability and gene transcription. This suggests that some of the non-sterol associated effects caused by statin drugs could be due to the inhibition of isoprenylation of Rho and Ras proteins (Liao and Laufs, 2005; Van Aelst and Dae Souza-Schorey, 1997), however, the mechanisms are not well understood (Liao and Laufs, 2005). Another example of non-sterol effects is statin binding to an allosteric site within the $\beta 2$ integrin function associated antigen-1, which appears to occur independently of mevalonate synthesis (Weitz-Schmidt, et al., 2001).

1.6. Adverse effects of statin drugs

Despite the favourable overall health benefits of statins, they have adverse effects of unknown molecular origins such as hepatotoxicity, renal dysfunction, muscular myopathies and in extreme cases fatal rhabdomyolysis (Gilles Labbe, 2008; Kromer and Moosmann, 2009). Hepatotoxicity seems to involve mitochondrial dysfunction as a major side-effect ultimately triggering apoptosis or necrosis of hepatocytes in cytolytic hepatitis conditions. Mitochondrial perturbations can also lead to diverse extrahepatic ailments such as hyperlactatemia, lactic acidosis, myopathy, rhabdomyolysis, pancreatitis, neuropathy or lipodystrophy (Dyken and Will, 2007; Gilles Labbe, 2008). Muscular myopathies are commonly seen in

statin use presenting in approximately 10% of patients undergoing treatment with statin drugs. *Cerivastatin* was voluntarily withdrawn from the market by Bayer Pharmaceuticals in 2001 due to increased cases of rhabdomyolysis (Furberg and Pitt, 2001).

While muscular myopathies have been reported in all the statins on the market, the myotoxicity for *Cerivastatin* was higher than the other statins, perhaps related to their physiochemical properties (Fig.1.3). Such properties can alter the kinetic behaviour of drugs, including bioavailability, tissue distribution and metabolism - which may affect statin toxicity on muscular tissue. For example, inhibition of cytochrome P450 isozymes can lead to increased bioavailability of the lipophilic statins, hence increasing the potential for myotoxicity (Gilles Labbe, 2008; Kaufmann, et al., 2006).

Isopentenyl pyrophosphate is required for the post-transcriptional maturation of selenocysteine-tRNA (an essential component of selenoprotein biosynthesis) and is inhibited by pharmacological perturbation of the mevalonate pathway by statin drugs. It has been noted that statin treatment of human HepG2 cells alters glutathione peroxidase expression, enzyme activity and steady state. The authors noted that there is limited crosstalk between the two pathways and therefore further investigation is needed into the hepatic side effects exhibited with the use of statin drugs (Kromer and Moosmann, 2009).

1.7. Cellular networks

It is clear from the foregoing review that statins, like any useful therapeutic agent, affect numerous biochemical pathways in addition to their major target (HMG-CoA-reductase). It is likely that tailoring their use will require a cross-pathway analysis as in the example of aspirin described above.

It is a tenet of this thesis that molecular mechanisms underlying complex biochemical phenotypes across pathways may emerge from such genetic interaction studies. These novel approaches may indeed permit a more comprehensive prediction of gene function in cross-pathway networks (Boone, et al., 2007; Schadt and Lum, 2006; Tong, et al., 2004). Focussing more on statin mechanisms, Figure 1.8 is a summary diagram adapted from the literature of known sterol involvement in yeast (Henneberry and Sturley, 2005; Schekman, 2002). Involved sub cellular organelles include the endoplasmic reticulum, Golgi apparatus, mitochondria and vacuole are intimately involved in these processes. HMG1 and HMG2, located in the ER, when inhibited by statin drugs may disrupt the cellular sterol homeostasis. It is unknown what effect that statin drugs have on related processes such as glycosylation, protein folding and degradation. This study attempts to identify some of the genetic interactions affecting the processes shown in Figure 1.8 thereby adding new data and a systematic approach to a better understanding of the mechanism and the pleiotropic effects of statin drugs.

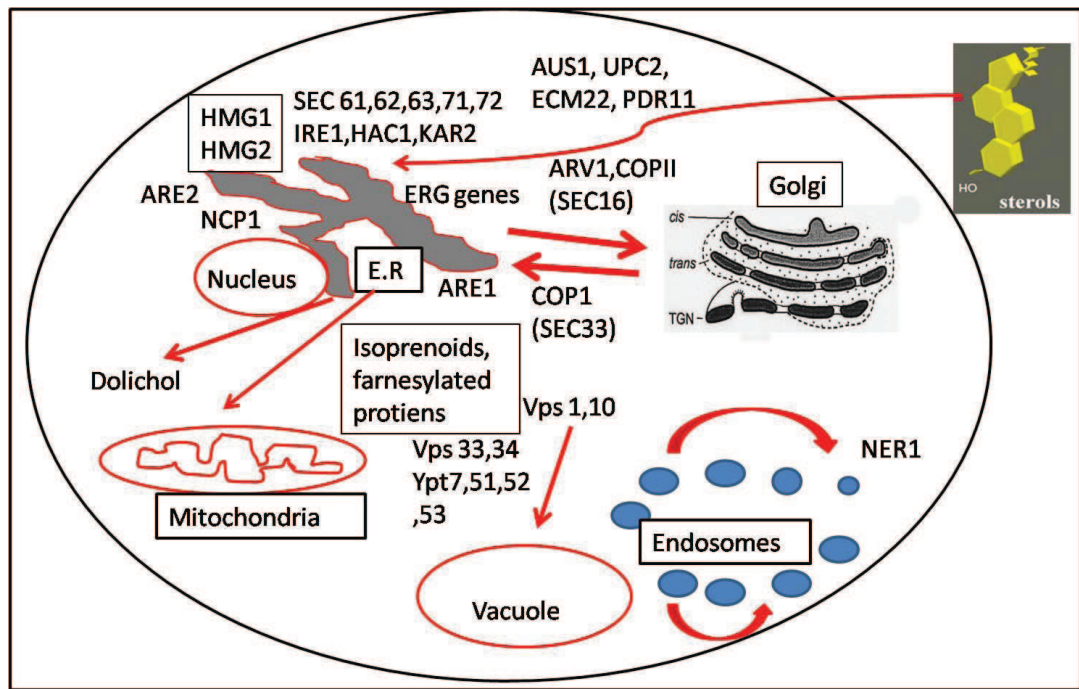


Figure 1.8 Summary of yeast cell biology processes directly involved in this study. Namely those involved in sterol import, synthesis and trafficking, protein folding, protein trafficking and degradation, intracellular vesicle transport and the transport of isoprenoids (FPP, IPP and GGPP), and isoprenylated proteins such as Ras and Ras like proteins Rho, Rab, Rac, Ral and Rap (Henneberry and Sturley, 2005; Schekman, 2002; Sturley, 2000; Van Aelst and Dae Souza-Schorey, 1997)

1.8. Disease networks - genetic interactions

Complex human diseases, such as cardiovascular disease and atherosclerosis, are known to involve partial contribution of numerous genes that are often unrelated by biochemical pathway as seen in increasing numbers of QTL (quantitative trait loci) studies (Hopkins, 2008; Schadt, et al., 2009; Schadt and Lum, 2006). The problem with QTL studies is that they lack resolution to single genes. Alternative approaches of studying complexity such as genetic interaction networks may allow higher resolution. High-throughput screening tools have allowed the

assembly of genetic interaction networks on a genome-wide basis, such that a genetic interaction observed between two genes indicates functionality whether or not it is within known biochemical pathways. Genetic interactions observed in this study are mostly of the epistatic enhancement type that in its extreme form is called “synthetic lethality” (Boone, et al., 2007; Tong, et al., 2001; Tong, et al., 2004).

1.9. Yeast as a model organism

Saccharomyces cerevisiae is a powerful model organism because of its comparatively simple genome, its genetic tractability and a range of unsurpassed genetic tools that can be applied, such as the yeast genome deletion set (YGDS) (Tong, et al., 2001; Tong, et al., 2004; Winzeler, et al., 1999). It is possible to uncover redundant and unknown cellular functions using high throughput genetics from which genetic interaction networks can be deduced, such as those described in Tong et al 2004.

The YGDS comprises ~6300 gene-deleted strains of which ~1000 genes are termed “essential” as the strains are inviable and ~5000 are termed “non-essential” since these deletion strains are viable (Winzeler, et al., 1999). Each strain in the YGDS has had a specific gene deleted and replaced by a gene cassette (KanMX4) conferring resistance to kanamycin. This deletion cassette has a unique molecular bar code surrounding every gene deletion. Construction of the YGDS has led to the development of a number of high-throughput assays which can be used to screen for particular phenotypes under a variety of growth

conditions. *S. cerevisiae* is an apt model organism for the study of human genetic diseases because up to 30% of genes implicated in human disease, contain a homologue in yeast (Bassett, et al., 1997; Foury, 1997).

Synthetic genetic array analysis (SGA) allows systematic assessment of synthetic genetic interactions between a chosen query gene deletion strain and the entire “non-essential” genome. It relies on the ability of yeast to grow as haploids, mate to form diploids, undergo meiosis allowing selection of double-mutant haploids. Some of these non-essential gene double-mutants will result in unviable or less-viable meiotic progeny (Boone, et al., 2007; Tong, et al., 2001; Tong, et al., 2004) defining a genetic interaction. A small molecule inhibitor may take the place of one of the deletion mutants also defining a genetic interaction as explained in the following diagram (Fig 1.9), reproduced from Parsons et al., 2004).

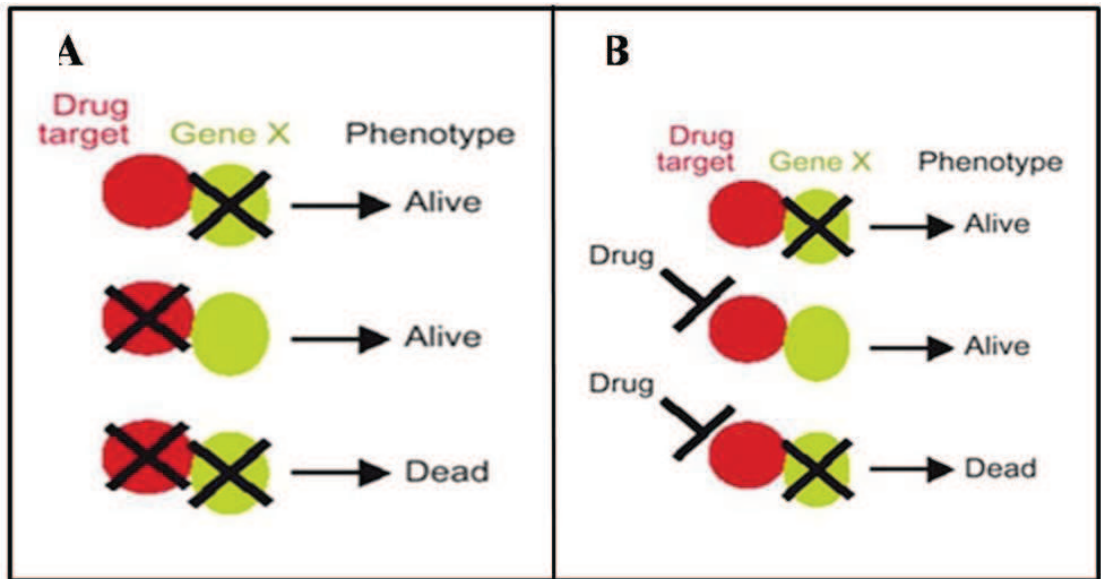


Figure 1.9 Diagrammatic comparison of genetic and chemical genetic interactions. Panel A shows a synthetic-lethal genetic interaction in which two single deletions which are individually viable but are inviable a double-mutant combination. Panel B shows a chemical–genetic interaction, in which a deletion mutant, which lacks the product of the deleted gene is hypersensitive to a normally sub lethal concentration of a small molecule inhibitor (Boone, et al., 2007; Parsons, et al., 2004).

Chapter 2. Methods

2.1. Query strain construction

The strategy in this thesis used to discern genetic interactions is to create double deletion mutants from viable non-essential deletion mutant strains and test whether their combination is viable (no interaction) or non-viable (genetic interaction). Since only about 2-3% of all possible non-essential deletion strain double mutants are likely to be non-viable i.e. likely to interact (Tong, et al., 2001) searching for evidence of genetic interactions is best done on a high-throughput basis. This is achieved by creating “query strains” utilising a deletion strain of a gene of interest of the opposite mating type to the YGDS and provided with a distinct (to the YGDS) selectable marker. The query strain (with a NatR marker) can then be mated *en masse* with the YGDS (with a KanR marker) and the appropriate double mutants selected by a combination of antibiotic selections.

HMG1 and HMG2 that encode HMG-CoA reductase are both “non essential” genes therefore the “one – step polymerase chain reaction gene disruption” method (Fig. 2.2) was used to generate HMG1 and HMG2 null mutants in query strains. The HMG1 query deletion was provided by J.T. Rauniyar from her Honours thesis work (Rauniyar and Atkinson, 2007, unpublished). Two gene deletion primers were constructed (HMG2 forward and reverse deletion) containing 55 base pairs (bp) of sequence homology to either the flanking

upstream (forward deletion primer) or downstream region (reverse deletion primer) of the HMG2 gene, excluding the start and stop codons, in addition to 22bp of sequence homology at the 3' end that is specific for the amplification of the cassette template (p4339, Invitrogen; Table 2.2). The resultant NatR (nourseothricin resistance) PCR product is thus contained within 55bp target sequences that are homologous for the flanking region of the HMG2 open reading frame (Fig. 2.2, adapted from Tong. 2005). This PCR product is transformed into the SGA starting strain Y7092 (*MAT α can1 Δ ::STE2pr-Sp_his5 lyp1 Δ his3 Δ 1 leu2 Δ 0 ura3 Δ 0 met15 Δ 0*), with the transformants selected on YPD + nourseothricin (NAT) media. The correct targeting of the deletion cassette is verified by PCR using transformed genomic DNA as a template and external and internal cassette PCR primers (HMG2 confirmation forward and reverse, Table 2.2) (Tong and Boone, 2005).

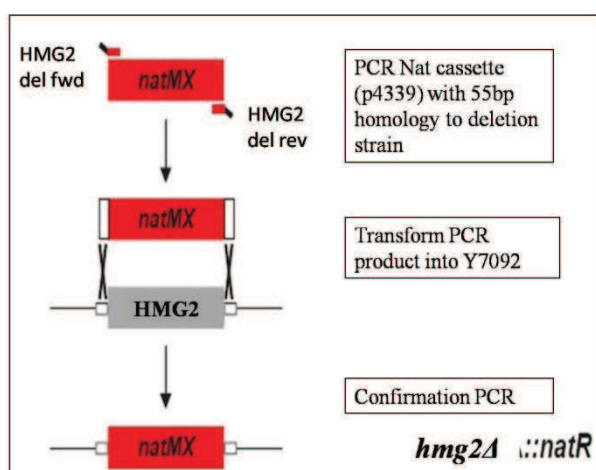


Figure 2.1 PCR-mediated gene deletion used to construct the non-essential query strains. The lines outside of the boxes represent the primers used for the PCR reaction. The red lines represent the primer sequences (table 2.2) that anneal to the *natMX4* cassette, the black lines represent the 55bp-sequence specific to the upstream or downstream sequences of HMG2.

2.2. PCR amplification

The HMG2 query strain PCR (see Table 2.1) was performed using the Qiagen Hotstar Taq DNA polymerase Kit, with the following PCR cycling conditions: 15 min initial denaturation at 94°C, then 35 cycles of 1 min at 94°C (denaturation), 1 min at 54°C (annealing), 1 min at 72°C (extension), followed by final extension for 10 min at 72°C. The resulting PCR product (4µL) were run on a 2% agarose gel, stained with ethidium bromide and visualised under UV (ultraviolet) light.

Reagent	Volume
10X PCR Buffer	10 µL
dNTPs (5mM)	2 µL
Forward primer(100pm)	2 µL
Reverse primer (100pm)	2 µL
Hotstar Taq	1 µL
dd H ₂ O	82 µL
P4339	1 µL
Total	100 µL

Table 2.1 Deletion PCR Reaction Conditions.

Primer	Sequence
HMG2 Deletion Forward	ACTTAATTGTGTTCTTTCCAAATTAGTTCAACAAGGTTCCCA CATACAACCTCAAACATGGAGGCCCAAGAATACCCT
HMG2 Deletion Reverse	TTAGAATAGCTAGACAATACAAAGATATAAAGTATCACCAT GTAAACTACAAGAGCAGTATAGCGACCAGCATTAC
HMG2 confirm Forward	TCCCTTTCAACAGCGCGACA
HMG2 confirm Reverse	AGCGCAGTGCTAGGCGATAA
NAT confirm Reverse	TACGAGACGACCACGAAGC
NAT confirm Forward	TGGAACCGCCGGCTGACC

Table 2.2 Primers used for *Δhmg2* query strain construction

2.3. Transformation

50 ml of YPD media was inoculated with Y7092 cells (5×10^6 cells/mL) and grown for 12 h at 30°C on a shaker. When the cells reached an optical density (OD) of 1.13 at 600 nm (2.3×10^7 cells/mL) they were spun for five min at 2500 rpm and washed twice with 10 mL 0.1 M lithium acetate and resuspended in 500 μ L of 0.1 M lithium acetate. Salmon sperm DNA (90 mg/mL) was denaturated by boiling for 10 min and placed on ice. Denatured salmon sperm DNA (10 μ L) and HMG2 query strain PCR product (20 μ L) were added to yeast cells (90 μ L) and incubated at 30°C for 15 minutes. 600 μ L Li-PEG solution (0.1 mM LiAc/ 5%

PEG) was added and the cells were incubated at 30°C for 30 min, at which time 68µL dimethyl sulfoxide (DMSO) was added and the yeast subjected to heat shock at 42°C for 15 min. The cells were then spun down at 1000 rpm for 2 min, the supernatant was removed and the yeast cells were resuspended in 800 µL of YPD and incubated at 30°C for 4 h to allow expression of the antibiotic resistance gene product. Finally, to concentrate the cells, the tube was centrifuged at 2000 rpm, the supernatant was removed and the cells were resuspended in 200 µL YPD. 100 µL of cell suspension was spread onto YPD plates containing the NAT antibiotic (100 µg/mL) to select for the resistant transformants (Gietz and Schiestl, 2007).

2.4. PCR confirmation

PCR on the transformed genomic DNA (gDNA) was performed to confirm the correct integration of the HMG2 query strain PCR product. Genomic DNA was extracted using the Zymo Research fungal/bacterial DNA kit from Nat-resistant colonies. The gDNA was used as the template in PCR utilising the confirmation HMG2 forward and reverse PCR primers which flank each integration site with an internal NatR cassette primer (Table 2.3). The following PCR cycling conditions: 15 min at 94°C, then 10 cycles of 30 s at 94°C, 30 s at 54°C, 2 min at 72°C, followed by 25 cycles of: 30 s at 94°C, 30 s at 54°C, 2 min (plus 10 s each cycle) at 72°C followed by a final extension for 10 min at 78°C.

Reagent	Volume (μl)
10x Buffer	2.5
dNTP (5mM)	0.8
Fwd Primer HMG2 5'	0.2
Rev Primer Nat	0.2
Hotstar Taq	0.2
ddH ₂ O	16.1
Template	5
Total	25

Table 2.3 Conformation PCR conditions. The initial primers were substituted for: HMG2 3' (reverse) paired with the NAT forward primers in a separate reaction as in Table 2.2.

2.5. Synthetic genetic array

The *MATa* DMA is the YGDS maintained in 1536 format (384 strains in quadruplicate colonies) with a control border strain *MATa his3Δ::kanR* to ensure that colony sizes were not biased (Tong and Boone, 2005; Tong, et al., 2001; Tong, et al., 2004). Replica plating (pinning) was performed using an automated robotic system - the Singer RoToR HDA (Singer Instrument Co. Ltd, Somerset, UK). All media compositions and antibiotics are listed in Appendix 1.

Mating the Query Strain with the DMA: The HMG1 or HMG2 *MATa* query strains (Nat resistant; *hmg1Δ::NatR*, *hmg2Δ::NatR*) were grown as a 1536 array format on rich media with antibiotic (YPD+NAT). The *MATa* deletion mutant array (DMA; G418 resistant) was also grown on rich media with the selective antibiotic (YPD+G418). The query strain was mated with the DMA by pinning

each deletion of the DMA on top of the query strain and incubated on rich media to produce diploid cells.

***MATa/α* diploid selection.** The resulting diploids (query + DMA) are then selected by pinning onto YEPD+G418/NAT media. This media allows only the diploids to grow, as haploids will only be either G418 or NAT resistant, not both, and thus will be inviable.

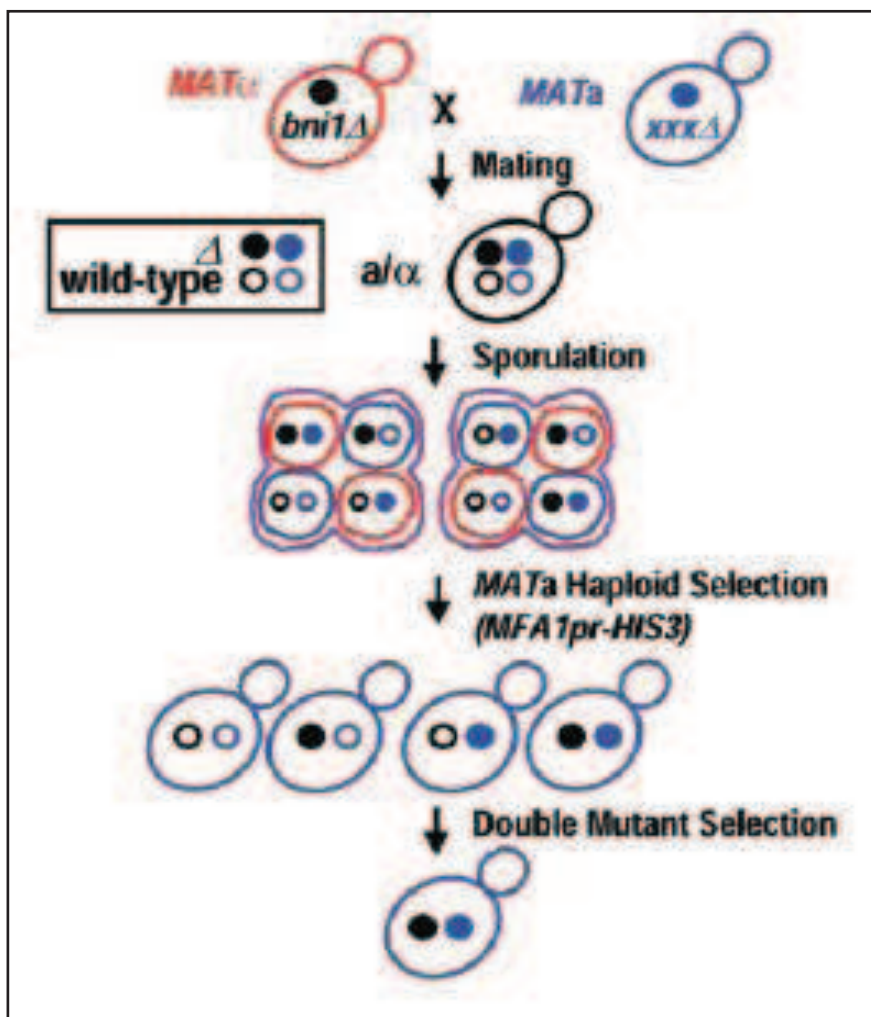


Figure 2.2 Synthetic genetic array methodology (reproduced from Tong and Boone 2005).

Sporulation. The resulting diploids are then pinned onto media deficient in nutrients required for growth and incubated at a lower temperature to induce sporulation of the diploids. The resultant haploid spores will be a combination of wild-type, single or double mutants due to independent assortment of the chromosomes and recombination within the chromosomes.

***MATa* progeny selection.** The spores are transferred onto synthetic media (SC – His/Arg/Lys + canavanine/thialysine) to allow for the selective germination of *MATa* meiotic progeny. To ensure selectivity, *HIS3*, a gene required for histidine biosynthesis, is deleted from both the *MATa* query strain and *MATa* deletion mutant array strains thus they require histidine supplementation for survival. Furthermore, the use of the *STE2pr* promoter linked to the *Sch. pombe HIS5* gene (*can1Δ::STE2pr-Sp_his5*), which is able to complement *S. cerevisiae HIS3*, allows for specific selection of *MATa* haploids in media lacking histidine. *STE2* encodes the α -factor pheromone receptor which is only expressed in *MATa*, thus *S. pombe his5* is only expressed in *MATa* cells and able to survive without the addition of histidine. Moreover, this genetic selection also prevents mating between *MATa* and *MATa* haploid cells.

However, mitotic recombination can occur between homologous chromosomes, in *MATa/a* diploids, a crossover event can result in *MATa/a* or *MATa/a* diploids. To prevent this rare event from occurring, two recessive markers are introduced (*can1Δ* and *lyp1Δ*). The *CAN1* gene encodes an arginine permease which allows canavanine (a toxic analogue of arginine) to enter the cells causing cell death. The *LYP1* gene encodes a lysine permease that allows thialysine (a toxic analogue of lysine) to enter the cells causing cell death. The presence of wild type *LYP1* and

CAN1 genes allows the respective antibiotics to enter the cells resulting in cell death. Whereas, *Δlyp1* and *Δcan1* cells do not have these permeases present, therefore, the cells are able to live in the presence of these toxic analogues. Including these genetic mutations into the query strains ensures the specific selection of *MATa* haploid progeny and substantially reduces the potential for false positives - this step is also repeated twice to assure *MATa* haploid selection.

Double mutant selection. The *MATa* meiotic progeny undergoes two rounds of selection, first selecting for the DMA deletion mutants (G418 alone) and the second selecting for the query and DMA double mutants (G418 and NAT together).

The selection of the DMA deletion mutants is achieved by pinning the *MATa* meiotic progeny onto SC - His/Arg/Lys + canavanine/thialysine/G418 media. Where, the G418 selects for the *MATa* DMA deletions ($\Delta\text{Gene}_{1...5000}::\text{KanR}$). The second selection for the DMA + Query deletions is achieved by pinning the resulting *MATa* progeny onto SD/MSG – His/Arg/Lys + canavanine/thialysine/G418/NAT media, thus selecting for double deletions containing the query deletion (NatR) and DMA deletions. The progeny resulting from this step are the *MATa* (haploid) double mutants of every non-essential gene with the query gene mutation in which synthetic lethal interactions are observed and analysed.

Haploid double mutants containing the query gene and the DMA (~5000 non essential genes) occupy fourteen 1536 colony plates where each individual strain

is pinned in quadruplicate. The neutral strains at the plate borders are excluded from the subsequent analysis to prevent the growth bias of more accessible nutrients at this plate location. The colonies are then scored for fitness.

2.6. SGA analysis

The fitness of each strain was determined by SESA (SGA Experiment Set Analyser; developed by Cameron Jack, Chemical Genetics VUW) which analyses the images of the final *MATa* double mutant SGA plates. The SGA results were compared against a control set of SGA results, *ura3Δ::NatR (MATa ura3Δ::NatR can1Δ::STE2pr-his5 lyp1Δ)*. The genetic background of *hmg1Δ::NatR* and *hmg2Δ::NatR* query strains included a *URA3* deletion, therefore the deletion of HMG1 or HMG2 is the only variable in genetic background between the query strain and control. Comparison of *hmg1Δ* or *hmg2Δ* SGA results to the *ura3Δ* SGA results allows for the filtering of non-specific genetic interactions (frequent flyers). Also, any hits that have appeared in 3 or more previous independent SGA screens are deemed to be ‘frequent flyers’ and are discounted from the results. The frequent flyer hits can be explained by genes that are involved with mating or the sporulation process, therefore are uninformative to the assay. Finally the linkage genes (the genes that are in close physical proximity to the query gene locus) are also discounted as the genes around the query locus are expected to show no growth due to the decreased ability of genetic recombination to occur between these loci. This pattern of no growth of loci flanking the query gene is another method for confirming the query gene.

2.7. SGA scoring epistatic interactions in high-throughput

Synthetic lethal (SL) and synthetic sick (SS) genetic interactions were inferred from reduced colony growth in which double mutants grew less than the expected combination of parental phenotypes (epitasis). 1536-colony plates were photographed and images analysed (gridding, segmenting and digitizing) and colony sizes recorded using ColonyHT software (Collins, et al., 2006; Collins). Colony size data were uploaded into a MySQL database that contained the standardised known colony position of each gene in the yeast deletion mutant array (DMA).

Interactions were scored in high – throughput utilising a robust statistical algorithm for assessing epistatic colony sizes. Our colony size analysis software, SESA, combines replicate experiment and control data sets that were performed under the same growth conditions as the query and control respectively. Plate-to-plate variation was controlled through calculating relative colony growth by taking the ratio of mutant colony area to the median control colony area on each plate, where each plate contained 144 $\Delta his3$ mutants as controls (border strain). Experimental colony growth ratios were then compared to control plates where 1536-colony plates of the DMA as an SGA using *ura3* Δ as a query gene (Tong, et al., 2001). Controls currently comprise 8 independent *ura3* Δ SGA's (no expected interactions) and experimental SGAs comprised 3 independent experiments.

To improve statistical robustness against pinning errors, genetic drift and random growth defects, robust statistics of the form median $\pm 3 \times \text{MAD}$ (median absolute deviation) were used throughout. In SESA, confidence intervals were compared as per the (directional) standard method, forming each confidence interval by smoothed bootstrapping (two-tailed, $\alpha < 0.01$, $r = 1500$), where the bandwidth of the smoothing function (Epanechnikov kernel) (Silverman, 1990) was inversely proportional to the number of independent replicates (Schenker, 2001). Such bootstrapping data were sampled from all available data from either control or experimental sets to better resolve the true distribution function. All test results were output to a text file along with a separate list of significant results.

2.8. Gene ontology

Gene Ontology (GO) is a controlled vocabulary used to describe the biology of a gene product in any organism. GO annotations are able to compare functional, process or cellular localisation associations made between gene products and the GO terms that describe them (Ashburner, et al., 2000; Gene Ontology Consortium, 2004). Statistically significant changes in GO term distribution compared to that of the whole genome suggest enrichment in the number of genes evolved in that particular process. The BiNGO plug-in (Maere, et al., 2005) for Cytoscape (Cline, et al., 2007) and the yeast GO Slim Mapper (SGD, 2009) were used for functional analysis of SGA and chemical genetic ‘hit’ genes. The fold change differences in distribution of GO terms for the ‘hit’ genes were compared to that of the whole genome.

2.9. Chemical genetic profiling

The field of chemical genetics is based on the principle that small molecules can mimic the effects of genetic mutations (Fig 1.9). A loss-of-function mutation in the gene encoding a compound target can be mimicked by an inhibitory compound and vice versa. In chemical genetic profiling, YGDS strains are screened for hypersensitivity to a compound where the compound is present at a concentration that slightly inhibits wild-type growth. Genes identified in a chemical genetic screen will identify pathways that buffer the cell from the growth inhibitory effect of the drug. The chemical genetic profile of a drug is thus expected to have significant overlap with the genetic interaction profile generated by SGA analysis of the drug target (Boone, et al., 2007; Parsons, et al., 2004; Parsons, et al., 2006).

2.10. Chemicals and media for chemical genetic profiling

Atorvastatin (Inter Chemical Hong Kong Ltd; WanChai, Hong Kong), was dissolved in dimethyl sulfoxide (DMSO, Sigma) at a stock concentration of 50mM (Blank, et al., 2007). *Cerivastatin* (Chengdu Caikun Biological Products Co., Ltd.; Chengdu, Sichuan, China) was dissolved in DMSO at 10 mM (Yoshida, et al., 2001). *Lovastatin* (Ivychem; New Jersey, USA) exists in its inactive lactone form and is hydrolysed *in vivo* to its active hydroxy acid form in mammals, not fungi, therefore this drug must be hydrolysed prior to use in our assays. *Lovastatin* was dissolved in 100% ethanol and 0.25% wt/v NaOH, at 25 mM and hydrolysed at 60°C for 1 h (Lorenz and Parks, 1990). All stock solutions were stored at -20°C. DMSO was used as a vehicle control in *atorvastatin* and *cerivastatin* chemical genetic screens while ethanolic NaOH was used as a vehicle control in *lovastatin* chemical genetic screens.

SC media was chosen over standard rich (YPD) yeast media for use in all chemical experiments as it is chemically defined and does not contain yeast extract. Yeast extract is a major component of YPD and is made from concentrations of autolysed yeast. Yeast extract contains a variety of soluble peptides, amino acids and vitamins which could interfere with drug activity. Use of SC over YPD allows for alleviation of drug interactions with media components instead of cellular targets.

2.11. Spot dilution assays

Serial spot dilution assays were performed to identify the minimal inhibitory drug concentration (MIC) to be used in the chemical genetic screen (Parsons, et al., 2004). Haploid wild-type yeast strain BY4741 (*MATa*), *hmg1Δ* (*MATa* *hmg1Δ::NatR can1Δ::STE2pr-his5 lyp1Δ*), *hmg2Δ* (*MATa* *hmg2Δ::NatR can1Δ::STE2pr-his5 lyp1Δ*) and *his3Δ* (*MATa* *his3Δ::KanR*) were used in this assay. The BY4741 strain contains the same genetic background as the non-essential haploid YGDS. Cultures were grown overnight to saturation ($\sim 2 \times 10^8$ cells/mL) and diluted by eight serial 10-fold dilutions in a 96-well plate. 5 μ l of each cell dilution was spotted onto SC agar plates containing varying concentrations of *atorvastatin*, *cerivastatin* or *lovastatin*. The plates were incubated for 48 h at 30°C after which images were taken and growth was compared by SESA to non-treated control plates.

2.12. Chemical genetic screens

The haploid non-essential YGDS (*MATa*) was maintained on SC+G418 agar and replicated onto SC plates containing 25 μ M *atorvastatin*, 20 μ M *cerivastatin* or 150 μ M *lovastatin*. Sensitivity of each deletion strain is assayed by comparison to no drug diluent controls after 48 h (30°C) using Colony HT and SESA. These screens were repeated in triplicate. Double mutant chemical screens were also performed using the resulting double mutants obtained from the *hmg1Δ* and *hmg2Δ* SGA (*MATa* *xxxΔ::KanR his3Δ1 leu2Δ0 met15Δ0 hmg1Δ::NatR*

can1Δ::STE2pr-his5 lyp1Δ0). The double mutants were then pinned onto *atorvastatin* (*hmg1Δ* 7μM, *hmg2Δ* 17.5μM), *cerivastatin* (*hmg1Δ* 3μM, *hmg2Δ* 10μM) or *lovastatin* (*hmg1Δ* 30μM, *hmg2Δ* 80μM) and compared to that of the *hmg1Δ* and *hmg2Δ* SGA for phenotypic enhancement (Parsons, et al., 2004).

2.13. Ergosterol quantification

Yeast strains were grown to saturation in synthetic complete media at 30°C harvested by centrifugation at 4°C and washed 3 times with ddH₂O and stored at -80°C. The pellet was lyophilised, weighed, re-suspended in 20 mL distilled H₂O with 10 g of potassium hydroxide and refluxed for 3 h. Non saponifiable lipids were extracted from the cooled mixture three times with 100 mL diethyl ether (Scharlau, analytical grade), the combined extracts washed 3 times with distilled H₂O (50 mL) and dried with anhydrous Na₂SO₄ (Scharlau, analytical grade). The dried ether fraction was then evaporated and the residue kept at -20°C. Prior to HPLC analysis the dried extracts were resuspended in 100% methanol (Scharlau, HPLC grade) and passed through a 0.22 μm filter. Sterols were separated by HPLC using an Agilent 1200 series chromatograph fitted with a Phenomenex Gemini 5μM octadecysilyl - silica column and an Agilent 1100 series diode array detector. Methanol: H₂O (95:5, v/v) was used as the mobile phase with a flow rate of 1 mL/min. The HPLC separation was performed at 40°C and ergosterol was detected by absorbance at 282 nm. Ergosterol was quantified by comparing to that seen in a purified ergosterol standard (Sigma) (Bocking, et al., 2000; Gessner and

Schmitt, 1996; Jedlickova, et al., 2008; Lamacka and Sajbidor, 1997; Yuan, et al., 2008; Zhou, et al., 2002).

Chapter 3. Results of SGAs

3.1. Query strain construction

Genetic interactions surrounding *HMG1* and *HMG2* using SGA analysis were elucidated with specific query strains comprising the deletion strain of the gene of interest (query gene) provided with a selectable marker in place of the query gene. The commercially available yeast deletion set does not provide query strains which must be constructed *de novo* with the appropriate antibiotic marker to provide for mating strain and haploid selection. In this chapter the query strains were $\Delta hmg1::\text{NatR}$ and $\Delta hmg2::\text{NatR}$. The query strains may be robotically mass mated to the YGDS creating haploid double mutants allowing discernment of those displaying epistatic genetic interactions.

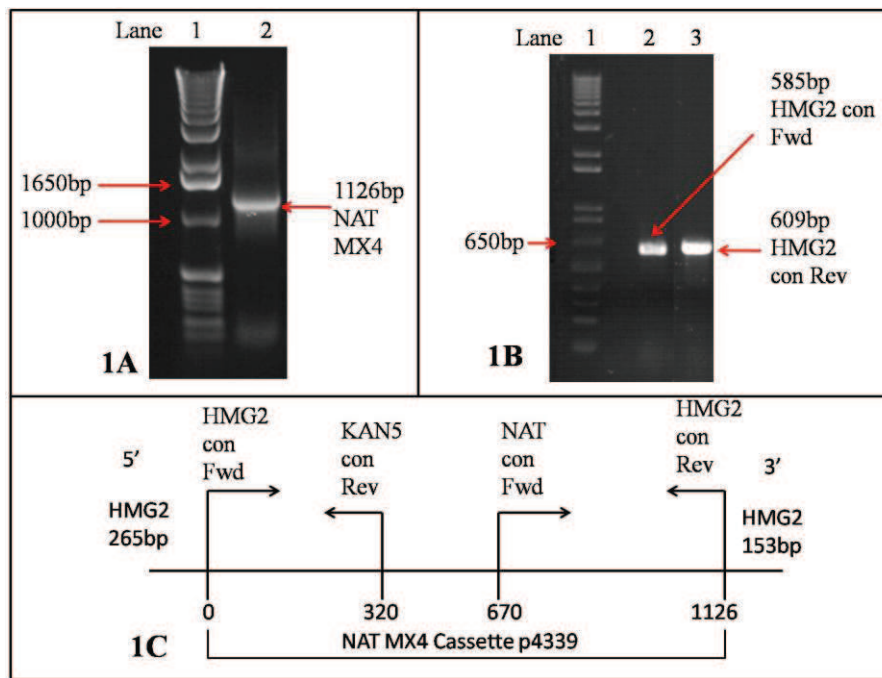


Figure 3.1 HMG2 query strain construction. 1A 1% agarose gel, lane 1 1Kb+ DNA ladder (Invitrogen), lane 2 the 1126bp nat MX4 cassette (p4339). 1B HMG2 query strain confirmation, lane one 1Kb+ DNA ladder, lane 2 *hmg2Δ::NAT* confirmation forward 585bp, lane 3 *hmg2Δ::NAT* confirmation reverse 609bp. 1C schematic diagram of the resulting *hmg2Δ::NAT* PCR.

The *HMG1* and *HMG2* query strains were constructed using the PCR mediated gene disruption method (see Chapter 2). Specific PCR products were generated using primers specific for each gene (see Table 2.2, Chapter 2). These primers were utilised in PCR using the template p4339 which contains the nat MX4 cassette. The correct size 1126bp PCR product is shown in Fig 3.1. This PCR product was used to transform Y7092 and NAT resistant (NatR) colonies were obtained. To confirm correctness of the insert in genomic DNA, flanking primers were used to generate a confirmation PCR product. As seen in Fig 3.1, the PCR products of the correct size (585bp and 609bp of *HMG2* forward and *HMG2* reverse respectively) were obtained verifying that the constructed strains could be used as query strains.

3.2. HMG1 SGA

The *Δhmg1* query strain was mass mated with all the other deletion strains of the non essential set creating a genome-wide SGA. 50 phenotypic enhancement (PE) interactions were scored (hits) and are shown in Table 3.1. These hits appeared in 4 independent SGA screens performed (3 screens were previously performed by J.T Rauniyar, 2007) noting that each SGA is done in triplicate. A SGA typically displays a chromosomally contiguous set of genes that are physically adjacent to the query gene locus (YML075C) that do not recombine and therefore appear to be in linkage disequilibrium. Genes of this linkage group (LG) are not counted as SGA epistatic hits but are a useful indication that the SGA is working correctly. The LG (Table 3.2, Fig. 3.2) for *Δhmg1* appeared in all four SGA screens, thus confirming the HMG1 gene was the gene that was replaced with the nat MX4 cassette (*hmg1Δ::NatR*). Note the contiguous numbering of the genes in the LG observed in Table 3.2.

Table 3.1: *Δhmg1* PE query gene interactions

ORF	Gene	Process	Description
YLR131C	ACE2	Cytoskeleton assembly	Transcription factor/cytokinesis
YOR058C	ASE1	Cell Cycle	mitotic spindle
YPL069C	BTS1	Lipid Biosynthesis	Geranylgeranyl diphosphate synthase
YNL275W	BOR1	Transport	Boron efflux
YER061C	CEM1	Lipid biosynthesis	mitochondrial/fatty acid synthase
YNL130C	CPT1	Lipid biosynthesis	Phosphatidylcholine biosynthesis
YNR010W	CSE2	Cell Cycle	Transcription factor/RNA pol II
YGR092W	DBF2	Cell Cycle	Transcription factor/ mitosis
YDR440W	DOT1	Protein modification	Gene silencing
YGL222C	EDC1	RNA processing	mRNA decapping
YNL080C	EOS1	Glycosylation	N-Glycosylation
YNL280C	ERG24	Lipid biosynthesis	Ergosterol Biosynthesis
YGL002W	ERP6	Transport	Er/Golgi Traffic
YML094W	GIM5	Cytoskeleton assembly	Translocation- heterohexameric cochaperone prefoldin complex
YLR192C	HCR1	Translation	subunit of eIF3
YLR450W	HMG2	Lipid biosynthesis	Subunit of HMG-CoA reductase
YNL106C	INP52	Lipid biosynthesis	Polyphosphatidylinositol phosphatase
YGL016W	KAP122	Transport	Karyopherin β nuclear transport/ poss PDR
YGL173C	KEM1	RNA processing	mRNA decay, Ribosomal maturation
YGL236C	MTO1	RNA processing	Translation/Mitochondria tRNA
YGL221C	NIF3	Unknown	detected in mitochondria
YEL016C	NPP2	other	Nucleotide pyrophosphatase/phosphodiesterase
YGL248W	PDE1	other	cAMP phosphodiesterase - cAMP signalling
YMR201C	RAD14	other	Nucleotide excision repair factor 1
YER162C	RAD4	other	Nucleotide excision repair factor 2
YNL294C	RIM21	other	cell wall construction/pH response
YHL025W	SNF6	RNA processing	Transcriptional regulation/chromatin remodelling
YKL081W	TEF4	Translation	Translation elongation factor
YGR138C	TPO2	Transport	Polyamine transport protien
YGR072W	UPF3	RNA processing	nonsense mediated mRNA decay

YKL041W	VPS24	Transport	ESCRT III - transmembrane proteins to MVB
YDR369C	XRS2	Cell cycle	DNA repair/Meiotic recombination
YNL064C	YDJ1	Transport	Protein chaperone
YFR057W		Unknown	Putative protein unknown function
YGR012W		Unknown	Putative cystine synthase/ localised to Mitochondria
YLR200W	YKE2	Protein Modification	folding of α/β tubulin and actin
YLR346C		Unknown	putative protein unknown function found in mitochondria
YNL241C	ZWF1	Other	G6PD 1st step in PPP

Table 3.1 *Δhmg1* PE query gene interactions. GO terms and annotations are extracts from the Saccharomyces Genome Database (SGD, 2009).

ORF	Gene
YML066C	SMA2
YML067C	ERV41
YML068W	ITT1
YML070W	DAK1
YML071C	COG8
YML072C	TCB5
YML074C	FPR3
YML075C	HMG1
YML076C	WAR1

Table 3.2 Linkage group genes surrounding HMG1.

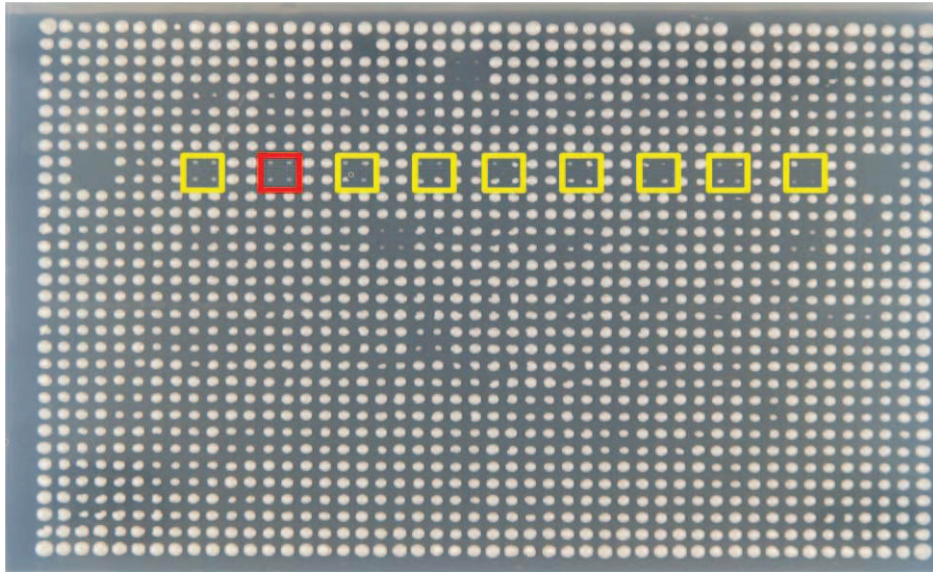


Figure 3.2 Example of HMG1 SGA showing linkage group genes. From left: YML066C, YML067C, YML068W, YML070W, YML071C, YML072C, YML074C, **YML075C**, YML076C.

The *HMG1* SGA resulted in 50 PE interactions, eight of which are linkage genes. Interestingly, when analysed with BiNGO (Maere, et al., 2005), only six (BTS1, CEM1, CPT1, ERG24, HMG2, INP52) out of 42 genes are involved in lipid metabolism (P-value 0.0024) , however, there is a group of nine gene products (BTS1, CEM1, ERP6, HMG2, MTO1, NIF3, TEF4, YGR012W, YLR346C) which are localized to the mitochondria (P-value = 0.21) . BTS1 is of particular interest as, it encodes geranylgeranyl diphosphate synthase which synthesises geranylgeranyl pyrophosphate (Jiang, et al., 1995) located downstream of HMG-CoA reductase (Fig1.4) and is involved in geranylgeranylation of small GTP binding proteins that mediate vesicular traffic.

There are also ten (BOR1, CPT1, EOS1, ERP6, HMG2, KAP122, RIM1, TPO2, VPS24 and YGR012W) membrane localized gene products (P-value=0.25), six genes (BOR1, ERP6, KAP122, TPO2, VPS24, and YDJ1) involved in cellular

transport/ trafficking (P-value = 0.089) and four (CPT1, EOS1, ERG24 and HMG2) gene products localized to the endoplasmic reticulum (P-value = 0.12).

3.3. HMG2 SGA

Using *Δhmg2* as a query strain, 56 phenotypic enhancement interactions were scored (hits) and are shown in Table 3.3. These hits appeared across 3 SGA screens. The LG genes close to the HMG2 locus (YLR450W, Table 3.4, Fig. 3.3) as previously explained has been discounted from the list of epistatic genetic enhancement interactions.

Table 3.3: *Δhmg2* PE query gene interactions

ORF	Gene	Process	Description
YPL069C	BTS1	Lipid Biosynthesis	Geranylgeranyl diphosphate synthase
YCR063W	BUD31	RNA processing	cell cycle/budding
YIR023W	DAL81	RNA processing	Nitrogen degradation pathway
YGR092W	DBF2	Cell Cycle	Transcription factor/ mitosis
YBR078W	ECM33	Other	GPI anchored/unknown function/phos. In mitochondria
YNL080C	EOS1	Glycosylation	N-Glycosylation
YLR192C	HCR1	Translation	subunit of eIF3
YML075C	HMG1	Lipid biosynthesis	Subunit of HMG-CoA reductase
YLR384C	IKI3	RNA processing	subunit of elongator complex
YOL108C	INO4	Lipid biosynthesis	Transcription factor - depression of inositol-cholene reg. genes
YNL106C	INP52	Lipid biosynthesis	Polyphosphatidylinositol phosphatase
YHR082C	KSP1	Protein Modification	Ser/Thr kinase - nuclear translocation
YLL006W	MMM1	Transport	import and assembly of mitochondrial outer membrane proteins
YGL136C	MRM2	RNA processing	Mitochondrial 2' O-ribose methyltransferase
YEL016C	NPP2	other	Nucleotide pyrophosphatase/phosphodiesterase
YOL044W	PEX15	Transport	Peroxisomal biogenesis
YBR093C	PHO5	Other	Repressible acid phosphatase/secretory pathway
YNL294C	RIM21	Other	cell wall construction/pH response
YLR048W	RPS0B	Cell Cycle	RIM101 pathway - cell wall construction
YOR293W	RPS10A	Translation	Component of 40S ribosomal subunit
YLR441C	RPS1A	Translation	Ribosomal protein of the 40S ribosomal subunit
YML063W	RPS1B	Translation	Ribosomal protein of the 40S ribosomal subunit
YLL002W	RTT109	Protein Modification	Cell cycle/DNA damage
YKL212W	SAC1	Transport	Phosphatidylinositol phosphate phosphatase/ER + Golgi

YNL236W	SIN4	RNA processing	Subunit of RNA pol II
YDR073W	SNF11	RNA processing	Chromatin remodelling/transcriptional regulation
YHR066W	SSF1	RNA processing	Constituent of 66S pre - ribosomal particles
YLR452C	SST2	Other	GTPase activating protein/mating
YHR181W	SVP26	Transport	COP II/golgi + ER
YDR126W	SWF1	Protein Modification	Palmitoyl transferase acts on SNAREs
YPL180W	TCO89	Other	subunit of TORC1
YDR207C	UME6	Cell Cycle	Transcriptional regulator of meiotic genes
YGR105W	VMA21	Protein Modification	Assembly of V-ATPase/localised to \ER
YOR083W	WHI5	Cell Cycle	Repressor of G1 transcription
YHR138C		Unknown	Putative protein of unknown function
YLR200W		Protein Modification	folding of α/β tubulin and actin
YLR455W		Unknown	Putative protein of unknown function
YLR460C		Unknown	Putative protein of unknown function
YPR024W	YME1	Protein Modification	degradation of misfolded/unfolded mitochondrial gene products
YNL241C	ZWF1	Other	G6PD 1st step in PPP

Table 3.3 *Δhmg2* PE query gene interactions. Go terms and annotations are extracts from the Saccharomyces Genome Database (SGD, 2009).

ORF	Gene
YLR441C	RPS1A
YLR444C	
YLR 446W	
YLR448W	RPL6B
YLR449W	FPR4
YLR450W	HMG2
YLR451W	LEU3
YLR452C	SST2
YLR453C	RIF2
YLR454W	FMP27
YLR455W	
YLR460C	

Table 3.4 Linkage group genes surrounding HMG2

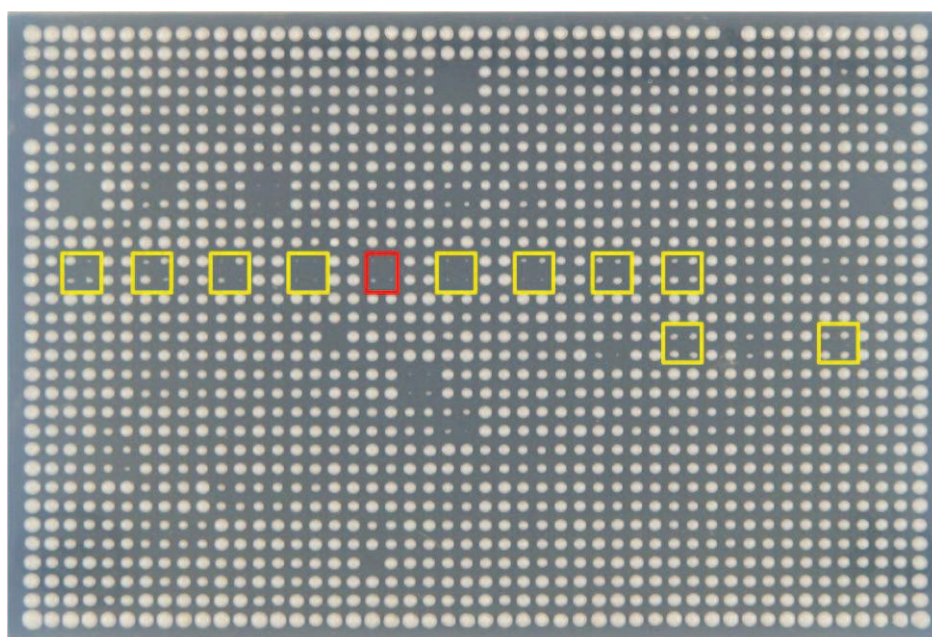


Figure 3.3 Example of HMG2 SGA showing linkage group genes. From top left: YLR441C, YLR444C, YLR 446W, YLR448W, YLR449W, **YLR450W**, YLR451W, YLR452C, YLR453C, YLR454W, YLR455W, YLR460C

The *HMG2* SGA resulted in 56 PE interactions, 12 of which are linkage genes. When analysed with BiNGO (Maere, et al., 2005) five (BTS1, HMG1, INO4, INP52 and SAC1) out of 44 genes are involved in lipid metabolism (P-value = 0.024) and there is a group of seven genes (BTS1, ECM33, HMG1, MMM1, MRM2, SAC1 and YME1) which are localized to the mitochondria (P-value = 0.5). BTS1 (see *HMG1* SGA) is located 'downstream' of the HMG-CoA reductase genes in the mevalonate pathway (Fig1.4) (Garza, et al., 2009b; Jiang, et al., 1995).

There are also 15 (ECM33, EOS1, HMG1, MMM1, NPP2, PEX15, RIM21, SAC1, SST2, SVP26, SWF1, TCO89, VMA21, YME1 and YNL080C) membrane localized genes (P-value = 0.23), six genes (MMM1, IKI13, BTS1, PEX15, RPS0B, and SVP26) involved in cellular transport/ trafficking (P-value = 0.09), 12 genes (DAL81, IKI3, INO4, RTT109, SIN4, UME6, WHI5, HCR1, RPS0B, RPS10A, RPS1A and RPS1B) involved in transcription/translation (P = 0.004) and seven genes (PEX15, HMG1, SAC1, SVP26, SWF1, VMA21 and YNL080C) localized to the endoplasmic reticulum (P-value = 0.0032).

3.4. HMG1 and HMG2 SGA Discussion

The genes that appeared as hits in both HMG1 and HMG2 are depicted in a network graph shown in Figure 3.4, generated by Cytoscape (Cline, et al., 2007). Cytoscape was used as it is freely available and the BiNGO plugin (Maere, et al., 2005) was used as its ability to characterize and group genes based on their GO terms exceeds that of other available software.

The network diagram (Fig. 3.4) shows although HMG1 and HMG2 are duplicated genes, they are non – essential. However, the gene product HMG-CoA reductase is essential, thus a haploid strain carrying a null mutation for both HMG1 and HMG2 enzymes is inviable. When there is a null mutation in either HMG1 or HMG2 the other is able to fully compensate HMG-CoA reductase activity for the null mutation (Basson, et al., 1987; Musso, et al., 2008; Scannell, et al., 2007). There is a small overlap (10/86 genes, ZWF1, RIM21, YNL080C, NPP2, BTS1, INP52, YKE2, HCR1, YEL014C and DBF2) of shared synthetic lethal connections between $\Delta hmg1$ and $\Delta hmg2$, reflecting common functions of the duplicated genes, that share 93% homology at the COOH- terminal region residues 618-1026 of HMG1 and 614-1022 of HMG2 at the catalytic domain (Basson, et al., 1988). Apart from this small overlap the two genes encoding the same enzyme have totally different SL genetic profiles, suggesting that during the whole genome duplication (known to have occurred in yeast) (Musso, et al., 2008) they each developed individual cellular roles.

Federovitch, et al., 2008 have investigated the protein products of HMG1 and HMG2, observing that Hmg1p and Hmg2p have mechanistically distinct roles with respect to ER remodelling. They suggest that these observations may underlie the known coupling of sterol synthesis to phospholipid synthesis seen in mammalian cells (Federovitch, et al., 2008).

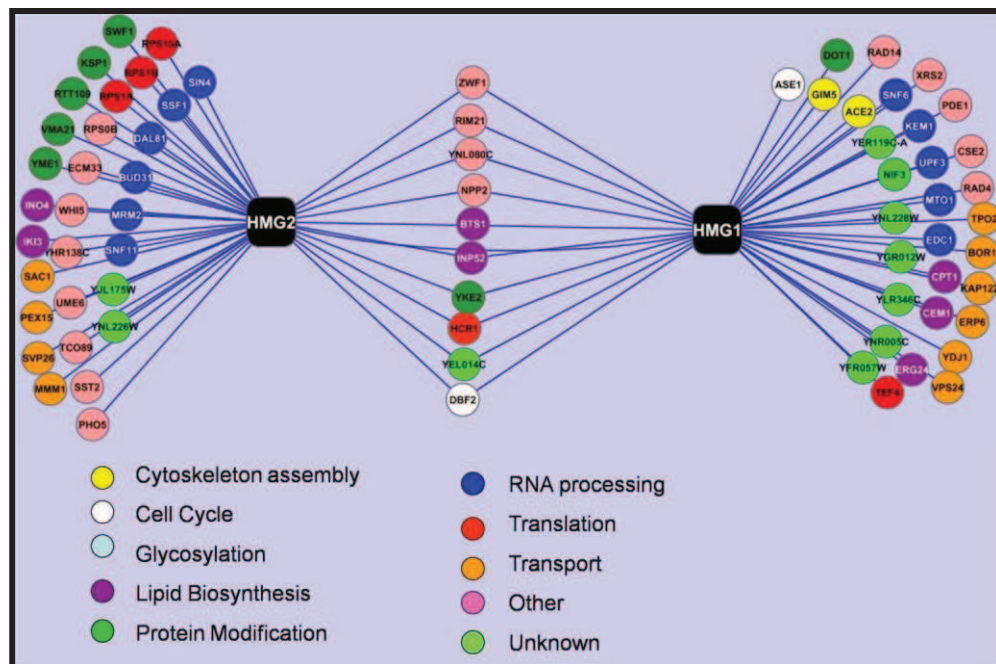


Figure 3.4 Cytoscape network graph showing HMG1 and HMG2 screens. The genes are grouped based on their GO terms (cellular process) generated with BiNGO.

The increased mitochondrial enrichment of genetic interactions in the HMG1 and HMG2 SGA's may play an important role in the mitochondrial electron transport chain. The isoprenoid intermediates farnesyl pyrophosphate and geranylgeranyl pyrophosphate (BTS1) are precursors of isoprenoid end products including ubiquinone, which the highest concentration found in the mitochondrial inner membrane (Dimster-Denk, et al., 1999). BTS1 has recently been described as a potent regulator of HMG-CoA reductase degradation in yeast (Garza, et al., 2009b) and has been reported to cause increased ubiquitination and degradation of

Hmg2p. Hmg1p is stable, whereas Hmg2p undergoes sterol pathway regulated degradation via the HMG-CoA reductase degradation (HRD) pathway (see chapter 7 for further discussion). SAC1, ERG24 and INO4 are of interest because they are involved in phosphatidylinositol synthesis.

ZWF1, appeared in both *HMG1* and *HMG2* SGA's and encodes the cytoplasmic protein Zwf1p (glucose-6-phosphate dehydrogenase, EC 1.1.1.49) which catalyses the first step of the pentose phosphate pathway (PPP). The primary role of the PPP in yeast when grown on a fermentable carbon source is to produce NADPH. When *ZWF1* is inhibited, this decreases the cells ability to generate NADPH from NADP⁺. The production of the malic enzyme up-regulated to compensate and increase the rate of NADPH synthesis in the mitochondria (Blank, et al., 2005). Increased enrichment for mitochondrial hit genes that appear in both the *HMG1* and *HMG2* SGA screens may be due to oxidative damage caused by the increased amount of NADP⁺ within the mitochondria.

Chapter 4. Chemical-genetic interactions of statin drugs

The central assumption of the newly described field of chemical genetics (Hillenmeyer, et al., 2008; Parsons, et al., 2004; Parsons, et al., 2006) is that a ‘small molecule perturbagen’ (SMP) binds specifically to a gene product and alters its function, mimicking a mutation in the corresponding gene. Thus, epistatic interactions between a mutant and an SMP may be defined and further used to define functional genetic interaction networks. To pursue this approach, it is necessary to define a SMP (i.e. inhibitor drug) concentration that slightly inhibits growth, but does not kill cells. In the following results, therefore, the term “*chemical-genetic screens*” is used to describe this mode of epistatic measurement. For the sake of clarity in the following description, “phenotypic enhancements” are growth reducing epistatic interactions and are the main focus of this dissertation where ‘synthetic lethality’ is an extreme form of phenotypic enhancement reduced growth. On the other hand, the term “phenotypic suppression” refers to enhanced growth (cf wild type) of a double deletion mutant combination. The literature at times uses the terms and “*alleviating*” and “*aggravating*” for phenotypic suppression and phenotypic enhancement epistatic interactions respectively (Boone, et al., 2007), bearing in mind that the phenotype being a enhanced or aggravated is reduced growth.

4.1. Spot dilution assays

Spot dilution assays are standard yeast protocols that encompass two variables, namely drug concentration and the number of cells spotted as a colony grown on solid agar. The two-way variation allows a better estimate of the drug concentration that is inhibitory rather than overtly toxic. Use of drugs at less than an LD₅₀ was deemed optimal to estimate PE chemical genetic interactions in subsequent chemical genetic screens. Thus, prior to chemical genetic screening, spot dilution assays were used as a pilot study to assess the growth inhibitory effects of *atorvastatin* and *cerivastatin* on wild type cells (BY4741), and on the deletion strains *Δhmg1* and *Δhmg2* (Fig 4.1). *Lovastatin* spot assays had previously been performed by J.T. Rauniyar in her honours thesis in 2007. Based on the results from the spot assays, concentrations were selected for the chemical-genetic screens that reduced growth. On this basis, *atorvastatin* was used at 25 μM, *cerivastatin* at 20 μM and *lovastatin* at 150 μM as these concentrations showed approximately 20% growth inhibition compared to wild type yeast.

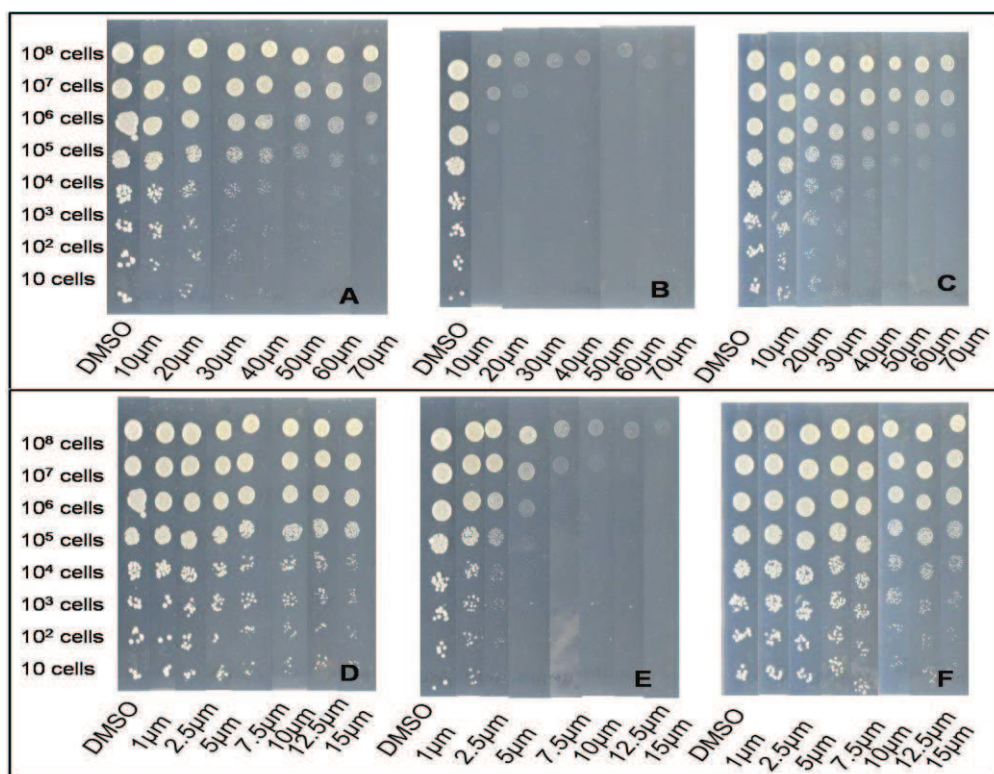


Figure 4.1 Spot assays for statin drug working concentrations. 10×10^8 - 10×10^1 cells/mL serially diluted onto SC media containing varying concentrations of *Atorvastatin* or *Cerivastatin*. A-C, *Atorvastatin* 10 μ M - 70 μ M, A = BY4741, B = Δ hmg1, C = Δ hmg2. D-F, *Cerivastatin* 1 μ M - 15 μ M. D = BY4741, E = Δ hmg1, F = Δ hmg2.

4.2. Chemical genetic screens

Statin drugs were used as SMPs in chemical genetic screens mimicking the effects of double haploid mutants that occur in SGA analysis. All chemical genetic screens were performed by robotically pinning the formatted non-essential gene deletion set (YGDS) of approximately 4800 strains onto solid agar plates containing the drug in 1536 colony format, followed by incubation for 48 h at 30°C. Plates were imaged utilising Colony HT (Collins) in the Chemical Genetics Laboratory's digital imaging system – a system capable of segregating and

measuring the size of colonies on the 1536-format solid media plates. Images were further analyzed with SESA, to assess the statistical significance of colony size differences as epistatic events. Controls for the drugs were DMSO for *atorvastatin* and *cerivastatin* or ethanol for *lovastatin*. SESA produced a list of PE “hits” which was then manually edited for deletion-gene combinations that tend to show up whatever the screen, termed ‘*frequent flyers*’, which were removed. Genes reported as multidrug resistant, “*MDR*”, (Hillenmeyer, et al., 2008; Parsons, et al., 2004; Parsons, et al., 2006) were noted by bold-formatting in Tables 4.1 - 4.6. The results from three independent experiments are shown in Tables 4.1 – 4.6 and are shown in graphical format in Figs. 4.2 & 4.3.

Table 4.1: *Atorvastatin* chemical genetic PE interactions

ORF	Gene	Process	Description
YLR242C	ARV1	Lipid Biosynthesis	Transport of Glycosylphosphatidylinositol intermediates; sterol distribution and sphingolipid metabolism
YNL242W	ATG2	Transport	Membrane protein, Vesicle formation
YJL095W	BCK1	Protein modification	MAP KKK; PKC signalling
YER155C	BEM2	Cytoskeleton assembly	Rho GTPase activating protein; cytoskeleton organisation
YNL271C	BNI1	Cell cycle	Formin linear actin filament formation
YNL233W	BNI4	Cell cycle	Targeting subunit for Glc7p protein phosphatase
YPL069C	BTS1	Lipid Biosynthesis	Geranylgeranyl diphosphate synthase
YGR217W	CCH1	Transport	Voltage gated Ca channel
YKL190W	CNB1	Other	Calcineurin B; stress response TF
YGR092W	DBF2	Cell cycle	Ser/Thr kinase: transcription and stress response
YAL026C	DRS2	Transport	Aminophospholipid translocase (flippase); post golgi secretory vesicles
YML008C	ERG6	Lipid Biosynthesis	Δ -sterol C-methyltransferase, converts zymosterol to fecosterol
YCR089W	FIG2	Cell cycle	Cell wall adhesion; expressed during mating
YEL042W	GDA1	Transport	Guanosine diphosphate located in golgi
YPR160W	GPH1	Metabolite Biosynthesis	Glycogen phosphorylase
YML075C	HMG1	Lipid Biosynthesis	One of two isoenzymes encoding HMG-CoA reductase
YJR075W	HOC1	Other	α -1,6-mannosyltransferase-cell wall mannan biosynthesis
YNL291C	MID1	Transport	N-Glycosylated protein of ER membrane
YLR332W	MID2	Transport	O-Glycosylated PM protein, cell wall integrity sensor

YDR245W	MNN10	Protein modification	Golgi mannosyltransferase complex; elongation of mannan backbone
YKL098W	MTC2	Unknown	Protein of unknown function
YBL024W	NCL1	RNA Processing	S-adenosyl-L-methionine-dependent tRNA; m5C-methyltransferase
YJR073C	OPI3	Lipid Biosynthesis	Phospholipid methyltransferase; phosphatidylcholine biosynthesis
YJL212C	OPT1	Transport	Proton coupled oligopeptide transporter of the PM
YDR071C	PAA1	Other	polyamine acetyltransferase
YOR265W	RBL2	Cytoskeleton assembly	Microtubule morphogenesis
YJL204C	RCY1	Transport	F-Box protein recycling PM proteins
YOR035C	SHE4	Cytoskeleton assembly	Regulates myosin function/endocytosis/actin polarization
YHR030C	SLT2	Protein modification	Ser/Thr kinase MAP kinase; PKC1 signalling; cell cycle
YEL031W	SPF1	Protein modification	P-type ATPase; ion transporter of the ER membrane; Ca ²⁺ homeostasis
YHL022C	SPO11	Cell cycle	Meiosis; meiotic recombination - forms DSB's
YDR293C	SSD1	Other	Cell integrity; TOR pathway
YDR297W	SUR2	Lipid Biosynthesis	Sphinganine C4-hydroxylase; sphingolipid biosynthesis
YJL187C	SWE1	Cell cycle	Protein kinase; regulated G2/M transition
YPL105C	SYH1	Unknown	May interact with ribosomes
YGR105W	VMA21	Other	Membrane protein required for vacuolar H ⁺ ATPase function
YJR099W	YUH1	Protein modification	Ubiquitin C-terminal hydrolase; generates monoubiquitin
YDR541C		Unknown	Putative dihydrokaempferol 4-reductase

YLR346C		Unknown	Putative protein of unknown function
YPL272C		Unknown	Putative protein of unknown function

Table 4.1 *Atorvastatin* chemical genetic PE interactions, bold indicate MDR genes. GO process and annotations were retrieved from the Saccharomyces Genome Database.

The three chemical genetic screens performed on 25 μ M *atorvastatin* resulted in 41 PE interactions (table 4.1) when analysed with SESA, the *atorvastatin* plates were compared to that of a DMSO (solvent) control and assessed for growth. The 41 genes were then analysed based on gene ontology. GO is useful for grouping genes but is a work in progress as its localisation category of genes is not yet agreed on – for example ERG6 in some GO databases is located to the ER where it is known to also to be located in lipid droplets (Maass, et al., 2009; Zehmer, et al., 2008). Eight of 41 genes (ARV1, ERG6, HMG1, MID1, OPI3, SPF1, SUR2 and VMA21) were annotated as being localised to the endoplasmic reticulum, Six of 41 genes (ARV1, BTS1, ERG6, HMG1, OPI3, and SUR2) are genes involved in lipid synthesis carried out in the ER, which is also the main location of the target enzyme HMG-CoA reductase.

Furthermore, there are seven genes displaying PE interactions (BEM2, BTS1, ERG6, HMG1, OPI3, SPF1, and SYH1) that are localised to the mitochondria. These are likely due to inhibition of isoprenylated proteins namely those involved in the electron transport chain (ubiquinone) and small GTP binding proteins which mediate intracellular membrane vesicular traffic (Jiang, et al., 1995). BTS1 (see Chapter 3) reflects the activities of other (non-sterol) enzymes in the HMG-CoA reductase pathway as described in the Introduction (Chapter 1), this gene has

been described by Garza et al. 2009 as a potent regulator of HMG-CoA reductase and would be a most interesting gene to follow-up in further studies.

Table 4.2: *Atorvastatin* chemical genetic PS interactions

ORF	Gene	Process	Description
YLL006W	MMM1	Transport	Mitochondrial outer membrane; import and assembly of outer membrane β barrel proteins
YLL009C	COX17	Other	Cu metallochaperone
YCR063W	BUD31	RNA Processing	Cell cycle/budding
YLR114C	AVL9	Transport	Exocytic transport form Golgi
YKR024C	DBP7	RNA Processing	Putative ATP dependent RNA helicase of the DEAD box family
YJL131C	AIM23	Unknown	Putative protein of unknown function
YKL098W	YKL098W	Unknown	Protein of unknown function
YLR410W	VIP1	Other	Inositol hexakisphosphate and inositol heptakisphosphate kinase
YLL041C	SDH2	Metabolite Biosynthesis	Iron sulfur protein subunit of succinate dehydrogenase
YKL037W	YKL037W	Unknown	Putative protein of unknown function
YLR038C	COX12	Other	Subunit Vib of cyc c oxidase
YLR024C	UBR2	Protein modification	Cytoplasmic E3 ligase
YOL004W	SIN3	Protein modification	Histone deacetylase transcriptional repression; meiosis

Table 4.2 *Atorvastatin* chemical genetic PS interactions, GO process and annotations were retrieved from the Saccharomyces Genome Database

The enrichment in ER/lipid synthesis genes in statin chemical genetic interactions suggests that the unknown genes displaying interactions in the chemical genetic tables also belong in these same categories – a useful hypothesis that could be tested in follow on work to this dissertation.

The three independent chemical-genetic screens performed on 25 μ M *atorvastatin* resulted in 14 PS interactions (Table 4.2) as analysed with SESA. The 14 genes were then analysed based on gene ontology, with 5/14 genes (AIM23, COX12, COX17, MMM1 and SDH2) being found to localise to the mitochondria, four of which (COX12, COX17, MMM1 and SDH2) are in the outer membrane. This is a significant enrichment of chemical genetic interactions implying that enzymes/functions probably occur in the isoprene pathways, known to be inhibited by statins, resulting in a compensating up-regulation.

Table 4.3: *Cerivastatin* chemical genetic PE interactions

ORF	Gene	Process	Description
YOR141C	ARP8	Other	nuclear actin related protein; Chromatin remodeling
YLR242C	ARV1	Lipid Biosynthesis	Transport of Glycosylphosphatidylinositol intermediates
YNL242W	ATG2	Transport	Membrane protein, Vesicle formation
YBL089W	AVT5	Transport	Putative transporter; GABA glycine transport
YJL095W	BCK1	Protein modification	MAP KKK; PKC signaling
YER155C	BEM2	Cytoskeleton assembly	Rho GTPase activating protein; cytoskeleton organisation
YNL271C	BNI1	Cell cycle	Formin linear actin filament formation
YNL233W	BNI4	Cell cycle	Targeting subunit for Glc7p protein phosphatase
YPL069C	BTS1	Lipid Biosynthesis	Geranylgeranyl diphosphate synthase
YOR026W	BUB3	Cell cycle	Kinetochore checkpoint WD40; prophase/metaphase
YGR217W	CCH1	Transport	Voltage gated Ca channel
YLR330W	CHS5	Transport	Golgi to PM transport; exomer complex
YKL190W	CNB1	Other	Calcineurin B; stress response TF
YJR084W	CSN12	Other	Subunit of Cop9 signalosome
YGL110C	CUE3	Protein modification	Protein of unknown function; Poss. intramolecular monoubiquitination
YGR092W	DBF2	Cell cycle	Ser/Thr kinase: transcription and stress response
YAL026C	DRS2	Transport	Aminophospholipid translocase (flippase); post golgi secretory vesicles
YGL043W	DST1	RNA Processing	Transcription elongation factor TFIIS
YGL054C	ERV14	Transport	COPII coated vesicles
YCR089W	FIG2	Cell cycle	Cell wall adhesion; expressed during mating

YEL042W	GDA1	Transport	Guanosine diphosphate located in golgi
YPR160W	GPH1	Metabolite Biosynthesis	Glycogen phosphororylase
YJR090C	GRR1	Protein modification	F-Box component of SCF Ubiquitin ligase complex
YML075C	HMG1	Lipid Biosynthesis	One of two isoenzymes encoding HMG-CoA reductase
YJR075W	HOC1	Other	α -1,6-mannosyltransferase-cell wall mannan biosynthesis
YOL108C	INO4	Lipid Biosynthesis	transcription factor - depression of inositol-choline reg. genes
YJL124C	LSM1	RNA Processing	LSM protein; cytoplasmic mRNA degradation
YOR306C	MCH5	Transport	PM riboflavin transporter
YNL291C	MID1	Transport	N-Glycosylated protein of ER membrane
YLR332W	MID2	Transport	O-Glycosylated PM protein, cell wall integrity sensor
YDR245W	MNN10	Protein modification	Golgi mannosyltransferase complex; elongation of mannan backbone
YPR118W	MRI1	Other	5'- methylthioribose-1-phosphate isomerase; methionine salvage pathway
YBL024W	NCL1	RNA Processing	S-adenosyl-L-methionine-dependent tRNA; m5C-methyltransferase
YMR145C	NDE1	Metabolite Biosynthesis	Mitochondrial external NADH dehydrogenase; type II NADPH quinone oxireductase
YJR073C	OPI3	Lipid Biosynthesis	Phospholipid methyltransferase; phosphatidylcholine biosynthesis
YGR038W	ORM1	Protein modification	required for resistance to UPR inducing agents
YDR071C	PAA1	Other	polyamine acetyltransferase
YCR077C	PAT1	RNA Processing	Topo II associated deadenylation dependent mRNA decapping

YCR020C	PET18	Metabolite Biosynthesis	Respiratory growth and stability of mitochondrial genome
YOL001W	PHO80	RNA Processing	Cyclin; regulates phosphate metabolism
YNL201C	PSY2	Other	subunit of protein phosphatase complex
YER162C	RAD4	Other	subunit of Nuclear excision repair factor 2
YDL090C	RAM1	Protein modification	β subunit of CAAX farnesyltransferase; a-factor and Ras proteins
YJL204C	RCY1	Transport	F-Box protein recycling PM proteins
YGL045W	RIM8	Cell cycle	Unknown function - essential for anaerobic growth
YLL046C	RNP1	RNA Processing	Ribonucleoprotein contains 2 RNA recognition motifs
YBL027W	RPL19B	Translation	Component of 60s ribosomal subunit
YNL096C	RPS7B	Translation	Component of 40s ribosomal subunit
YOR035C	SHE4	Cytoskeleton assembly	Regulates myosin function/endocytosis/actin polarization
YBR103W	SIF2	Cell cycle	WD40 repeat subunit of SET3 Histone deacetylase complex; sporulation
YNL236W	SIN4	RNA Processing	RNA pol II mediator complex; transcriptional regulation
YBL007C	SLA1	Cytoskeleton assembly	Cytoskeletal protein binding protein; assembly of cortical actin cytoskeleton
YHR030C	SLT2	Protein modification	Ser/Thr kinase MAP kinase; PKC1 signaling; cell cycle
YMR016C	SOK2	Other	Regulation of cAMP PKA signal transduction pathway
YEL031W	SPF1	Protein modification	P-type ATPase; ion transporter of the ER membrane; Ca ²⁺ homeostasis
YCR081W	SRB8	RNA Processing	Subunit of RNA pol II; glucose repression
YDR293C	SSD1	Other	Cell integrity; TOR pathway

YJL187C	SWE1	Cell cycle	Protein kinase; regulated G2/M transition
YPL105C	SYH1	Unknown	May interact with ribosomes
YDR213W	UPC2	Lipid Biosynthesis	SREBP - induces transcription of sterol biosynthetic genes
YEL013W	VAC8	Transport	Phosphorylated vacuolar membrane protein (cytoplasm to vacuole targeting)
YGL212W	VAM7	Transport	Component of vacuole SNARE complex
YGR105W	VMA21	Other	Membrane protein required for vacuolar H ⁺ ATPase function
YML097C	VPS9	Transport	Guanine nucleotide exchange factor involved in vesicle mediated vacuolar protein transport
YLR337C	VRP1	Cytoskeleton assembly	Proline rich actin associated protein
YBR111C	YSA1	Other	Nudix hydrolase; ADP-ribose pyrophosphate
YJR099W	YUH1	Protein modification	Ubiquitin C-terminal hydrolase; generates monoubiquitin
YBR269C		Unknown	Putative protein of unknown function
YDR541C		Unknown	Putative dihydrokaempferol 4-reductase
YEL007W		Unknown	Putative protein; Poss. Gluconate transporter inducer
YGL081W		Unknown	Putative protein of unknown function
YGR122W		Unknown	Putative protein of unknown function
YJL160C		Unknown	Putative protein of unknown function
YKR016W		Unknown	Mitochondrial protein of unknown function
YLR346C		Unknown	Putative protein of unknown function
YPL041C		Unknown	Protein of unknown function

YPL066W		Unknown	Putative protein of unknown function
YPL272C		Unknown	Putative protein of unknown function

Table 4.3 *Cerivastatin* chemical genetic PE interactions, bold indicate MDR genes. GO process and annotations were retrieved from the Saccharomyces Genome Database

The chemical screens performed on 20 μ M *cerivastatin* yielded 78 PE interactions (Table 4.3) when analysed with SESA. GO analysis of PE genes showed 11/78 gene products (BEM2, BTS1, FCJ1, FMP21, HMG1, NDE1, OPI3, SPF1, SYH1, YLR346C and YSA1) are localised to the mitochondria, 8 genes (ARV1, ERV14, HMG1, MID1, OPI3, ORM1, SPF1 and VMA21) are localised to the ER, and 8 genes (ARV1, CHS5, DRS2, ERV14, GDA1, HOC1, MNN10 and RCY1) are localised to the Golgi apparatus. Some are localised to both organelles and are involved in vesicle transport between the Golgi and ER. Where VMA21 is required for the assembly of the V-ATPase complex (Graham and Stevens, 1999), ERV1 is an integral component of COPII vesicular transport (Otte, et al., 2001), ARV1 is involved in intracellular sterol distribution (Fei, et al., 2008) along with transport of glycosylphosphatidylinositol intermediates into the ER (Kajiwara, et al., 2008). Moreover, ARV1 is also involved with HOC1 and MNN10 which are localised to the Golgi and mediate the elongation of the polysaccharide mannan backbone (Jungmann, et al., 1999). The RCY1 protein is involved in the recycling of SNARE proteins from the plasma membrane via endocytosis. Thus, *cerivastatin* disrupts vesicular transport of proteins within the secretory pathway when compared to that of *atorvastatin* and *lovastatin*.

Seventeen genes (ARV1, ATG2, AVT5, CCH1, CHS5, DRS2, ERV14, MCH5, MID1, RCY1, RIM8, SLA1, SPF1, VAC8, VAM7, VPS9 and VRP1) are involved in intracellular vesicular transport.

Six lipid biosynthesis genes showed PE interactions with *cerivastatin*, namely ARV1, BTS1, HMG1, INO4, OPI3 and UPC2; and *atorvastatin* interacted with ARV1, BTS1, ERG6, HMG1, OPI3 and SUR2 showing commonality in the lipid synthesis and degradation genes, ARV1 and BST1. The others fall generally in lipid pathway genes and are likely to be significant in the mode of action of the drugs.

ERG3, INO4 and OPI3 genes are present in the *cerivastatin* screen, where OPI3 catalyses the last two steps in phosphatidylinositol choline biosynthesis (Nikoloff and Henry, 2003) and ERG3 catalyses the formation of episterol, a precursor in ergosterol biosynthesis (Lees, et al., 1995). In contrast, INO4 is involved in transcriptional regulation of expression of a large number of genes including a subset that are regulated by inositol and choline and involved in phospholipid, fatty acid and sterol biosynthesis (Santiago and Mamoun, 2003).

Table 4.4: *Cerivastatin* chemical genetic PS interactions

ORF	Gene	Process	Description
YLL006W	MMM1	Transport	Mitochondrial outer membrane; import and assembly of outer membrane β barrel proteins
YAL048C	GEM1	Transport	tail anchored outer mitochondrial membrane GTPase
YDL033C	SLM3	RNA Processing	tRNA-specific 2-thiouridylase; thiolation of wobble base of mitochondrial tRNAs
YLL009C	COX17	Other	Cu metallochaperone
YLR410W	VIP1	Other	Inositol hexakisphosphate and inositol heptakisphosphate kinase
YNL170W	YNL170W	Unknown	Dubious ORF unlikely to encode a functional protein
YKL157W	APE2	Other	Aminopeptidase ysII
YOR065W	CYT1	Metabolite Biosynthesis	Cyt c1, component of mitochondrial respiratory chain
YKL098W	YKL098W	Unknown	Protein of unknown function
YHR116W	COX23	Metabolite Biosynthesis	mitochondrial intermembrane space protein; Cu homeostasis
YLR038C	COX12	Other	Subunit Vib of cyc c oxidase
YEL033W	YEL033W	Unknown	Predicted metabolic role
YOR053W	YOR053W	Unknown	Dubious ORF unlikely to encode a protein
YBR132C	AGP2	Lipid Biosynthesis	Polyamide permease
YOR008C-A	YOR008C-A	Unknown	Putative protein of unknown function
YHR206W	SKN7	Other	Nuclear response regulator and transcription factor; induction of heat shock genes
YOR196C	LIP5	Metabolite Biosynthesis	biosynthesis of coenzyme lipoic acid
YMR256C	COX7	Metabolite Biosynthesis	Subunit VII of cyt c oxidase; electron transport
YBR266C	SLM6	Cytoskeleton assembly	Potential role in actin cytoskeleton organization
YDL136W	RPL35B	Translation	Component of 60s ribosomal subunit

YNL169C	PSD1	Lipid Biosynthesis	Phosphatidylserine decarboxylase of the inner mitochondrial membrane
YOR085W	OST3	Protein modification	g subunit of the oligosaccharyltransferase in ER; N-glycosylation
YJL131C	YJL131C	Unknown	Putative protein of unknown function
YKL037W	YKL037W	Unknown	Putative protein of unknown function
YEL007W	YEL007W	Unknown	Putative protein; Poss. Gluconate transporter inducer
YNR041C	COQ2	Metabolite Biosynthesis	Para hydroxybenzoate polyprenyl transferase; CoQ Synthesis
YKL109W	HAP4	Other	activator of global gene expression - heme activated
YLR114C	AVL9	Transport	Exocytic transport form golgi
YEL013W	VAC8	Transport	Phosphorylated vacuolar membrane protein (cytoplasm to vacuole targeting)
YDR512C	EMI1	Cell cycle	Transcriptional induction of early meiosis
YOR014W	RTS1	Translation	B-type regulatory subunit of PP2A
YKL168C	KKQ8	Unknown	Putative Ser/Thr kinase
YPR065W	ROX1	RNA Processing	Heme dependent repressor of hypoxic genes - contains an HMG domain
YDR393W	SHE9	Other	Mitochondrial inner membrane protein - morphology
YOL009C	MDM12	Protein modification	transmission of mitochondria to daughter cells
YDL182W	LYS20	Other	Homocitrate synthase isoenzyme
YLR061W	RPL22A	Translation	Component of 60s ribosomal subunit
YDL079C	MRK1	Protein modification	Glycogen synthase kinase 3; stress response/protein degradation
YHR181W	SVP26	Transport	Membrane protein Golgi/ER; COPII transport

YOR125C	CAT5	Metabolite Biosynthesis	CoQ synthesis
YOL008W	COQ10	Metabolite Biosynthesis	CoQ binding protein
YLR393W	ATP10	Other	mitochondrial inner membrane protein; F1F0 ATP synthase
YMR100W	MUB1	Protein modification	interacts with E2 and E3 enzymes; ubiquitylation and degradation
YBR076W	ECM8	Other	Unknown function
YOL032W	OPI10	Lipid Biosynthesis	Possible role in phospholipid biosynthesis
YKR016W	FMP13	Unknown	Mitochondrial protein of unknown function
YKR092C	SRP40	Transport	Nucleolar - ser rich; preribosome assembly or transport
YHR067W	HTD2	Lipid Biosynthesis	mitochondrial 3-hydroxyacyl-thioester dehydratase; fatty acid biosynthesis
YPL156C	PRM4	Other	Pheromone regulated protein
YNL180C	RHO5	Other	Small GTPase of Rho/Rac; PKC signaling
YNL111C	CYB5	Lipid Biosynthesis	Cyt b5 sterol and lipid biosynthesis
YKR074W	YKR074W	Unknown	Putative protein of unknown function
YHR009C	YHR009C	Unknown	Putative protein of unknown function
YPR084W	YPR084W	Unknown	Putative protein of unknown function
YDR486C	VPS60	Transport	Cytoplasmic and vacuolar membrane protein involved in endosome to vacuole transport
YKR007W	MEH1	Other	Component of EGO complex
YOL049W	GSH2	Metabolite Biosynthesis	Glutathione synthase
YER057C	HMF1	Other	p14.5 protein family
YJL105W	SET4	Unknown	Unknown function; contains a SET domain
YBR235W	YBR235W	Unknown	Putative Ion transporter
YLR368W	MDM30	Protein modification	F-Box protein, associates with mitochondria
YGL031C	RPL24A	Translation	Ribosomal protein L30 of 60s ribosomal subunit

YMR305C	SCW10	Other	Cell wall protein
YDL061C	RPS29B	Translation	Component of 40s ribosomal subunit
YKL010C	UFD4	Protein modification	E3 ligase; interacts with 26s proteasome
YOL081W	IRA2	Other	GTPase activating protein; negatively regulates RAS
YGL167C	PMR1	Transport	Ca ²⁺ /Mn ²⁺ P-type ATPase; Golgi transport

Table 4.4 *Cerivastatin* chemical genetic PS interactions, GO process and annotations were retrieved from the *Saccharomyces* Genome Database.

Table 4.4 shows the PS interactions that resulted from the three chemical screens performed utilising 20 μ M *cerivastatin*. There were 72 phenotypic suppression interactions (Table 4.4) evident when *cerivastatin* plates were compared to that of a DMSO control and assessed for growth. There were a large number of genes specific for *cerivastatin* not shared by the other statins for example 24 genes (AIM23, APE2, ATP10, CAT5, COQ10, COQ2, COX12, COX17, COX23, COX7, CYT1, FCJ1, GEM1, HTD2, IRA2, LIP5, LYS20, MDM12, MDM30, MMM1, PSD1, SHE9, SLM3 and UFD4) localised to the mitochondria, 4 of which are involved in cellular respiration/generation of precursor metabolites and energy (COQ10, COX23, COX7 and CYT1). Furthermore, 6 genes (AGP2, CYB5, MMM1, OST3, SCW10 and SVP26) were localised to the endoplasmic reticulum and 14 genes (AGP2, AVL9, COX17, GEM1, MDM12, MDM30, MMM1, PMR1, SLM6, SRP40, SVP26, VAC8, VPS60 and YBR235W) are involved intracellular vesicular transport. Besides this concentration of genes involving lipid and membrane biosynthesis there were many other epistatic genetic interactions with unrelated processes. *Cerivastatin* might show such an increased number of chemical genetic interactions consistent with its known propensity for side effects (Fuhrmans, et al.; Tuffs, 2001).

Table 4.5: *Lovastatin* chemical genetic PE interactions

ORF	Gene	Process	Description
YLR242C	ARV1	Lipid Biosynthesis	Transport of Glycosylphosphatidylinositol intermediates;
YNL242W	ATG2	Transport	Membrane protein, Vesicle formation
YJL095W	BCK1	Protein modification	MAP KKK; PKC signalling
YER155C	BEM2	Cytoskeleton assembly	Rho GTPase activating protein; cytoskeleton organisation
YNL271C	BNI1	Cell cycle	Formin linear actin filament formation
YNL233W	BNI4	Cell cycle	Targeting subunit for Glc7p protein phosphatase
YGL007W	BRP1	Unknown	Dubious ORF - deletion leads to polyamine resistance
YPL069C	BTS1	Lipid Biosynthesis	Geranylgeranyl diphosphate synthase
YGR217W	CCH1	Transport	Voltage gated Ca channel
YKL190W	CNB1	Other	Calcineurin B; stress response TF
YGL110C	CUE3	Protein modification	Protein of unknown function; Poss. intramolecular monoubiquitination
YGR092W	DBF2	Cell cycle	Ser/Thr kinase: transcription and stress response
YDR440W	DOT1	Protein modification	Nucleosomal Histone associated with transcriptionally active genes
YAL026C	DRS2	Transport	Aminophospholipid translocase (flippase); post golgi secretory vesicles
YGL043W	DST1	RNA Processing	Transcription elongation factor TFIIS
YCR089W	FIG2	Cell cycle	Cell wall adhesion; expressed during mating
YEL042W	GDA1	Transport	Guanosine diphosphate located in golgi
YPR160W	GPH1	Metabolite Biosynthesis	Glycogen phosphorylase
YFL031W	HAC1	Protein modification	Basic leucine zipper TF; UPR regulation

YML075C	HMG1	Lipid Biosynthesis	One of two isoenzymes encoding HMG-CoA reductase
YJR075W	HOC1	Other	α -1,6-mannosyltransferase- cell wall mannan biosynthesis
YNL291C	MID1	Transport	N-Glycosylated protein of ER membrane
YLR332W	MID2	Transport	O-Glycosylated PM protein, cell wall integrity sensor
YDR245W	MNN1	Protein modification	Golgi mannosyltransferase complex; elongation of mannan backbone
YMR224C	MRE11	Cell cycle	Repair of double stranded brakes; telomere stability
YBL024W	NCL1	RNA Processing	S-adenosyl-L-methionine-dependent tRNA; m5C-methyltransferase
YJR073C	OPI3	Lipid Biosynthesis	Phospholipid methyltransferase; phosphatidylcholine biosynthesis
YGR101W	PCP1	Protein modification	Mitochondrial serine protease
	RAM1	Protein modification	
YJL204C	RCY1	Transport	F-Box protein recycling PM proteins
YOR035C	SHE4	Cytoskeleton assembly	Regulates myosin function/endocytosis/actin polarization
YBL007C	SLA1	Cytoskeleton assembly	Cytoskeletal protein binding protein; assembly of cortical actin cytoskeleton
YHR030C	SLT2	Protein modification	Ser/Thr kinase MAP kinase; PKC1 signalling; cell cycle
YGL127C	SOH1	Cell cycle	Subunit of RNA pol II; meiosis
YEL031W	SPF1	Protein modification	P-type ATPase; ion transporter of the ER membrane; Ca ²⁺ homeostasis
YCR081W	SRB8	RNA Processing	Subunit of RNA pol II; glucose repression
YDR293C	SSD1	Other	Cell integrity; TOR pathway
YJL187C	SWE1	Cell cycle	Protein kinase; regulated G2/M transition
YPL105C	SYH1	Unknown	May interact with ribosome's
YJR099W	YUH1	Protein modification	Ubiquitin C-terminal hydrolase; generates monoubiquitin

YDR541C		Unknown	Putative dihydrokaempferol 4-reductase
YGL081W		Unknown	Putative protein of unknown function
YPL272C		Unknown	Putative protein of unknown function

Table 4.5 *Lovastatin* chemical genetic PE interactions, bold indicate MDR genes. GO process and annotations were retrieved from the Saccharomyces Genome Database

The chemical screens performed on 150 μ M *lovastatin* yielded 43 PE interactions (Table 4.5) when analysed with SESA, the *lovastatin* plates were compared to that of a DMSO (carrier) control and assessed for growth. There were 8 gene products (BEM2, BTS1, HMG1, MRE11, OPI3, PCP1, SPF1, and SYH1) localised to the mitochondria, these compared to those found with *cerivastatin* (BEM2, BTS1, FCJ1, FMP21, HMG1, NDE1, OPI3, SPF1, SYH1, YLR346C, YSA1). Six genes (ARV1, DRS2, GDA1, HOC1, MNN10 and RCY1) were localised to the Golgi apparatus compared to *cerivastatin* (ARV1, CHS5, DRS2, ERV14, GDA1, HOC1, MNN10 and RCY1) and 5 localised to the ER.

Moreover, there were also 9 genes (ARV1, ATG2, CCH1, DRS2, MID1, PCP1, RCY1, SLA1, and SPF1) involved in cellular transport and 5 genes (ARV1, BTS1, HAC1, HMG1 and OPI3) cf *atorvastatin* 6 genes (ARV1, BTS1, ERG6, HMG1, OPI3 and SUR2) involved in lipid biosynthesis. HAC1 is of particular interest as it is a known regulating element in the unfolded protein response (Welihinda, et al., 1997) which though non-essential appears to become essential in the presence of *lovastatin*.

Table 4.6 *Lovastatin* chemical genetic PS interactions

ORF	Gene	Process	Description
YLL006W	MMM1	Transport	Mitochondrial outer membrane; import and assembly of outer membrane β barrel proteins
YLL009C	COX17	Other	Cu metallochaperone
YNL322C	KRE1	Other	Cell wall glycoprotein; β -glucan assembly
YKR024C	DBP7	RNA Processing	Putative ATP-dependent RNA helicase of the DEAD box family
YBR132C	AGP2	Lipid Biosynthesis	Polyamine permease
YDR332W	IRC3	Unknown	Putative protein of unknown function
YCR028C-A	RIM1	Other	Single stranded DNA binding protein; mitochondrial genome maintenance
YNL199C	GCR2	Metabolite Biosynthesis	Transcriptional activator of genes involved in glycolysis
YLL040C	VPS13	Protein modification	Protein of unknown function; involved in sporulation, vacuolar sorting and golgi retention
YPL156C	PRM4	Other	Pheromone regulated protein
YOL032W	OPI10	Lipid Biosynthesis	Possible role in phospholipid biosynthesis
YDL033C	SLM3	RNA Processing	tRNA-specific 2-thiouridylase; thiolation of wobble base of mitochondrial tRNAs
YLL041C	SDH2	Metabolite Biosynthesis	Iron sulfur protein subunit of succinate dehydrogenase
YCR063W	BUD31	RNA Processing	Cell cycle/budding

Table 4.6 *Lovastatin* chemical genetic PS interactions, GO process and annotations were retrieved from the Saccharomyces Genome Database.

Table 4.6 shows the PS interactions that resulted from the three chemical screens performed on 150 μ M *lovastatin* which resulted in 15 PS interactions (Table 4.6) when analysed with SESA. These include 7 gene products (COX17, IRC3, MMM1, RIM1, SDH2, SLM3, and VPS13) localised to the mitochondria and 2 genes (AGP2 and MMM1) localised to the ER. There were also 4 genes (AGP2, COX17, MMM1, and VPS13) involved in cellular transport and 2 genes (GCR2 and SDH2) involved in the generation of precursor metabolites and energy.

4.3. Discussion

There are several significant points arising from the experiments described in this chapter. Though the epistatic interactions described do not attribute quantitative significance to the interactions shown, for example in Figure 4.2, focussing on interactions around the lipid pathways provide for some interesting observations.

Firstly, of the 32 overlapping PE genes in the *GO network* (Ashburner, et al., 2000) shared by all the statins, 4 genes, namely ARV1, BTS1, HMG1 and OPI3 are involved in lipid biosynthesis. Statins putatively act only on HMG-CoA-reductase, but the commonality of genetic interactions with these other genes forces consideration of statin action within a compensating network rather than as a single gene phenotype. Drugs, in general, like statins might be better understood in the context of genetic networks - a concept that has appeared in recent literature (Hopkins, 2008; Schadt, et al., 2009).

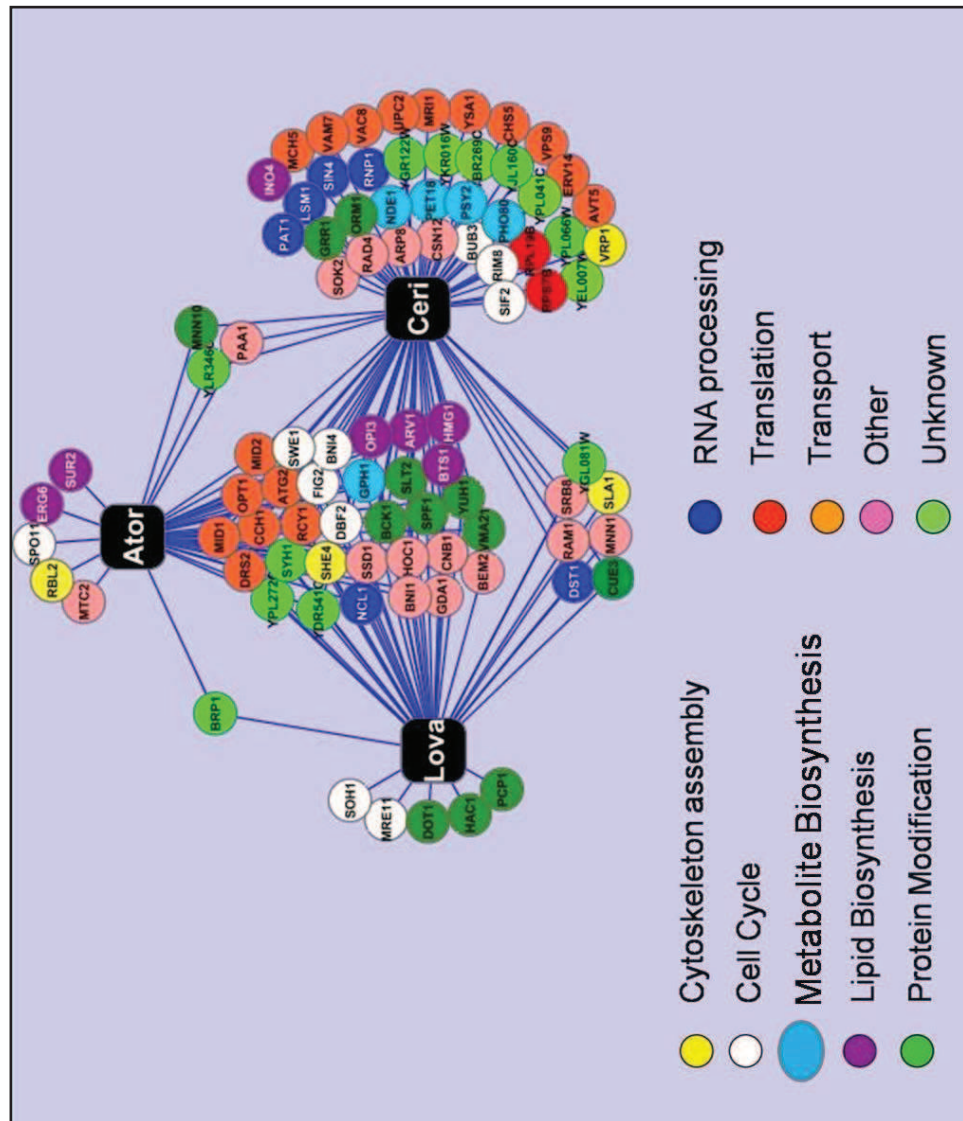


Figure 4.2 Cytoscape network graph showing the phenotypic enhancement interactions from the chemical genetic screens performed on *atorvastatin*, *cerivastatin* and *lovastatin*. The genes are grouped based on their GO terms (cellular process) generated with BiNGO (Maere, et al., 2005).

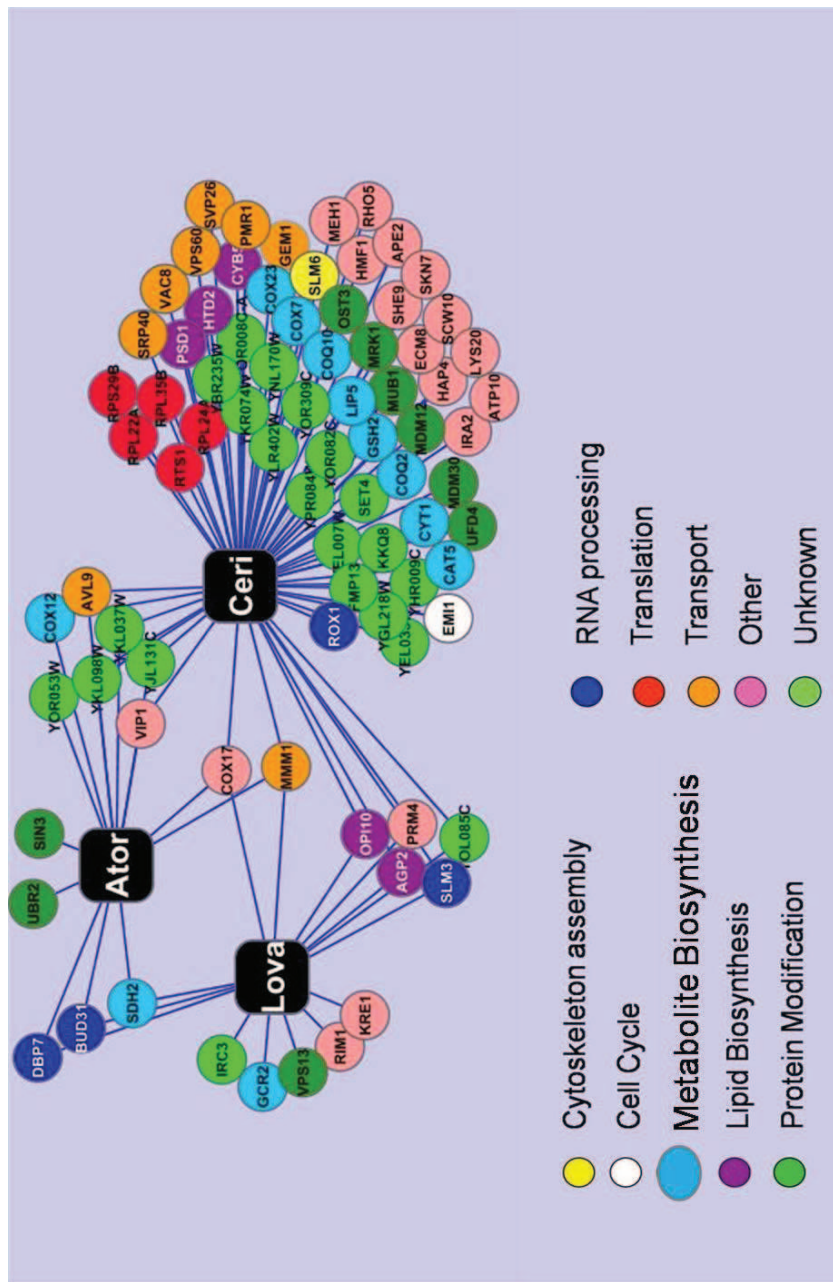


Figure 4.3 Cytoscape network graph showing the phenotypic suppression interactions from the chemical genetic screens performed on *atorvastatin*, *cerivastatin* and *lovastatin*. The genes are grouped based on their GO terms (cellular process).

Secondly, it has been reported that Hmg1p is stable (Federovitch, et al., 2008), whereas Hmg2p undergoes sterol pathway mediated degradation. The *BTS1* gene, a key regulator of Hmg2p (described in Chapter 3), can promote entry of Hmg2p into the HMG-CoA reductase degradation (HRD) pathway (Garza, et al., 2009b) after misfolding caused by statins. The unfolded protein probably induces the unfolded protein response (UPR), in which HAC1 is an integral member (Welihinda, et al., 1997). From the data presented in this chapter it can be suggested that *HMG2* has a more diverse role within the ER, via initiation of the UPR, and in agreement with the literature (Brown and Goldstein, 1980; Chun, et al., 1990; Cronin, et al., 2000; Federovitch, et al., 2008; Loertscher, et al., 2006), *HMG2* is regulated in a different manner to that of *HMG1*.

Thirdly, the PS results (i.e. instances in which drug-mutant combinations grew *better* than controls, Fig. 4.3) two genes namely *COX17* and *MMM1*, were common to all three statin drugs. *MMM1* is an ER membrane protein which links the ER to the mitochondria and promotes intra - organelle Ca^{2+} and phospholipid transport (Kornmann, et al., 2009). Therefore, the PS interaction of *MMM1* with statin drugs may be the outcome of decreased Ca^{2+} levels in the ER. Furthermore, the PE interactions of *MIDI/CCHI*, for which their main role consists of importing Ca^{2+} into the ER when secretory levels decrease (Locke, et al., 2000). Thus, it can be postulated that the cell is attempting to buffer the PE interactions by attempting to increase Ca^{2+} via an alternative route.

Fourthly, out of the combined 82 PE interactions seen in all statins, 28 are localised to or involved in mitochondrial function, refocusing our understanding of statin effects to include both ER and mitochondria. This point leads to the PS results in which genes involved in ubiquinone synthesis and distribution (CAT5, COQ10 and COQ2) are utilised to compensate for the decreased level of the isoprenoid precursor farnesyl pyrophosphate. A number of genes were also involved in the mitochondrial respiratory chain (COX12, COX17, COX23, COX7, CYT1, COX7 and SDH2). This suggests that alterations in the mitochondrial respiratory chain may compensate for another perturbed process. Moreover, there are genes involved in lipid biosynthesis (AGP2, CYB5, HTD2 and PSD1) that are also implicated in mitochondrial function.

Chapter 5. Double mutant chemical

genetic interactions of statin drugs with

their target genes

HMG-CoA reductase is encoded by duplicated reductase genes namely *HMG1* and *HMG2* but their genetic interactions (separately) are unknown as this requires testing epistatic interactions of one of the pair in the absence of the other. This question is technically difficult to resolve by genetic means alone since the combination of $\Delta hmg1$ and $\Delta hmg2$ in the same cell is lethal. Fortunately, chemical genetics provides a simplifying approach by utilising $\Delta hmg1$ and $\Delta hmg2$ SGA's (i.e. $\Delta hmg1$ in a genome-wide combination of deletion mutants, likewise $\Delta hmg2$) plus statins as inhibitors of the remaining intact gene to determine its genetic interactions. In this Chapter these experiments are called " $\Delta hmg1 \Delta xxx + statins$ " and " $\Delta hmg2 \Delta xxx + statins$ ". This approach has the potential to dissect out the individual genetic interactions of these HMG-CoA reductases providing information on the differing cellular roles played by HMG1 and HMG2.

The screens described in this chapter were designed to utilise the query gene strains $\Delta hmg1$ and $\Delta hmg2$ (separate SGAs) mated onto the deletion set. The haploid double mutants, $\Delta hmg1 \Delta xxx$, or $\Delta hmg2 \Delta xxx$, were then grown in the presence (separately) of each of the three statins in turn. These screens were performed as usual on agar plates with SC media minus histidine, arginine and lysine plus canavanine, thialysine, G418 and NAT. The double mutants were

replica pinned onto the drug containing selective media, grown for 48 h at 30⁰C, the resulting plates were imaged by COLONY HT and analysed with SESA using the appropriate control (DMSO for *atorvastatin* and *cerivastatin* or ethanol for *lovastatin*). After analysis with SESA any deletion strains (Δ xxx) that alone displayed epistatic interactions with Δ *hmg1*, Δ *hmg2*, *atorvastatin*, *cerivastatin* or *lovastatin* were removed from further consideration. As previously described deletion strains representing genes we have termed “frequent flyers” and Δ xxx deletion strains reported as *multidrug resistant* (Hillenmeyer, et al., 2008; Parsons, et al., 2004; Parsons, et al., 2006) were also noted.

5.1. Pilot Study: double mutant growth on statin drugs

Prior to application of the double mutant chemical genetic screen methodology just described, growth assays were performed to assess the growth inhibitory effects of *atorvastatin*, *cerivastatin* and *lovastatin* on solid medium in 1536 format as “controls” for the eventual Δ *hmg1* Δ xxx and Δ *hmg2* Δ xxx double mutant assays. These pilot studies used the SGA border strain growth as controls (see Methods) namely Δ *hmg1*::NatR Δ *his3*::KanR (Figs 5.1-5.3) and Δ *hmg2*::NatR Δ *his3*::KanR (Figs. 5.4-5.6) to determine the concentration of statin needed to observe effects in SGA format for the Δ *hmg1* Δ xxx + statins and Δ *hmg2* Δ xxx + statins experiments to be described later in this Chapter. Colonies were grown in 1536 format on SC media minus histidine, arginine and lysine plus canavanine, thialysine, G418 and Nat plates, which were then replica pinned onto

plates containing varying concentrations of *atorvastatin* (2-25 μ M), *cerivastatin* (2-25 μ M) and *lovastatin* (10-75 μ M) and grown for 48 h at 30⁰C. The plates were then photographed (Figs.5.1-5.6) and growth was evaluated via comparison to a no drug control (carrier, DMSO or ethanol).

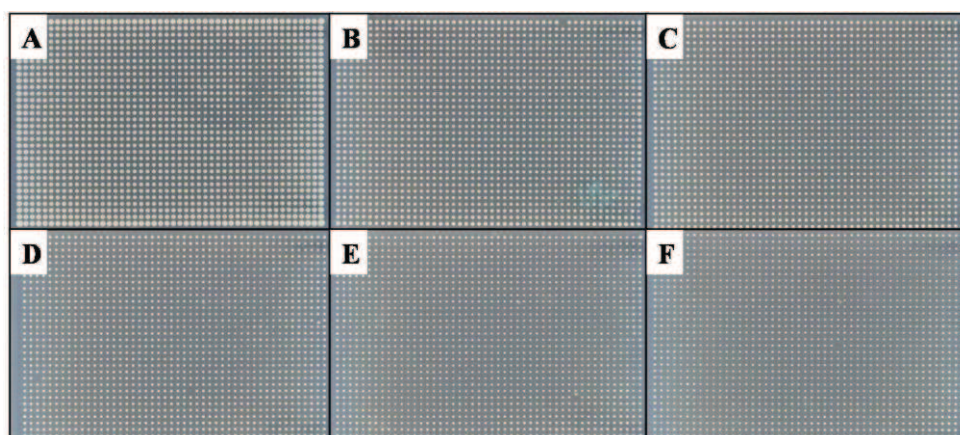


Figure 5.1 Double mutant chemical-genetic screen pilot for *atorvastatin* working concentrations in robotically pinned SGA formatted $\Delta hmg1 \Delta his3$. A DMSO control; B 2 μ M; C 5 μ M; 7 μ M; 10 μ M

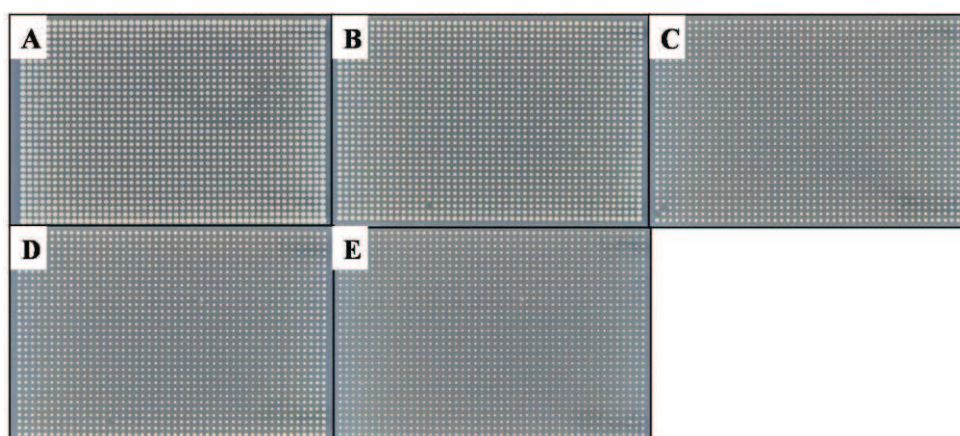


Figure 5.2 Double mutant chemical-genetic screen pilot for *cerivastatin* working concentrations in robotically pinned SGA formatted $\Delta hmg1 \Delta his3$. A DMSO; B 2 μ M; C 3 μ M; D 4 μ M; E 5 μ M; F 6 μ M

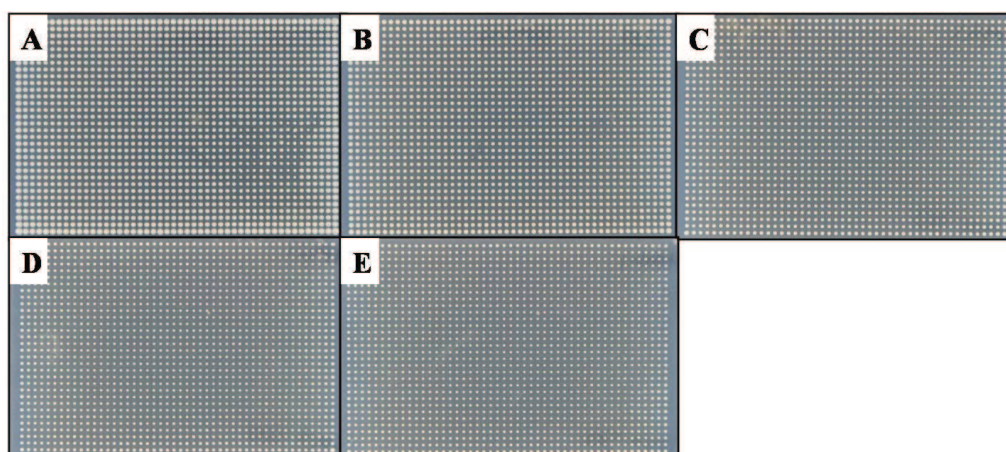


Figure 5.3 Double mutant chemical-genetic screen pilot for *lovastatin* working concentrations in robotically pinned SGA formatted $\Delta hmg1 \Delta his3$. A DMSO; B 20 μ M; C 30 μ M; D 40 μ M; E 50 μ M

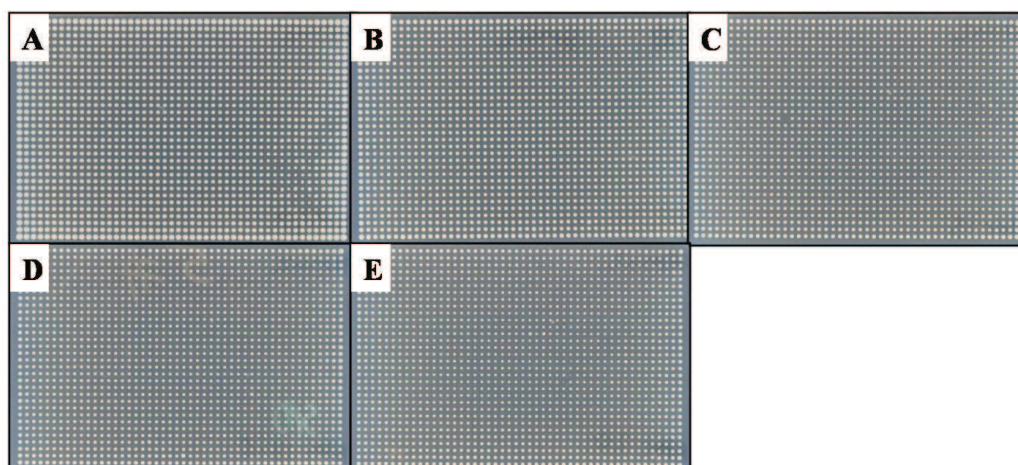


Figure 5.4 Double mutant chemical-genetic screen pilot for *atorvastatin* working concentrations in robotically pinned SGA formatted $\Delta hmg2 \Delta his3$. A DMSO; B 10 μ M; C 15 μ M; D 17.5 μ M; E 20 μ M

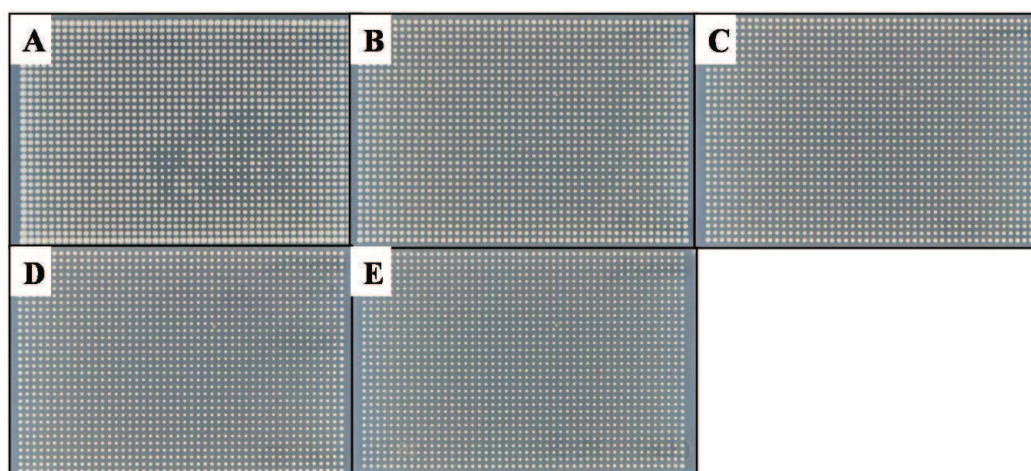


Figure 5.5 Double mutant chemical-genetic screen pilot for *cerivastatin* working concentrations in robotically pinned SGA formatted $\Delta hmg2 \Delta his3$. A DMSO; B 5 μ M; C 7.5 μ M; D 10 μ M; E 12.5 μ M

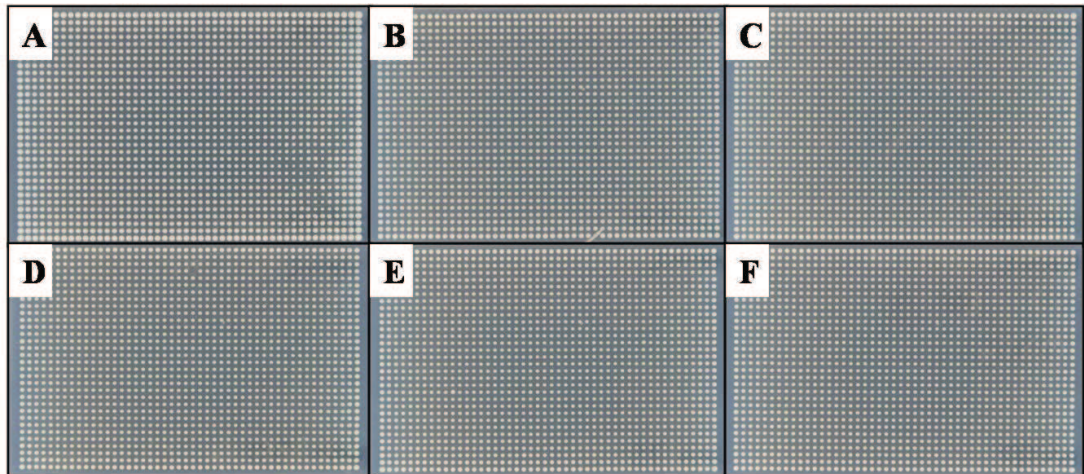


Figure 5.6 Double mutant chemical-genetic screen pilot for *lovastatin* working concentrations in robotically pinned SGA formatted $\Delta hmg2 \Delta his3$. A DMSO; B 60 μM ; C 65 μM ; D 70 μM ; E 75 μM ; F 80 μM

Figures 5.1 – 5.6 show the effect of *atorvastatin*, *cerivastatin* and *lovastatin* on the growth of $\Delta hmg1 \Delta his3$ and $\Delta hmg2 \Delta his3$ when maintained in 1536 format. The plates do not show differences readily discernable by eye but colony size differences with increasing statin were discernable by SESA for use as control information. Determining effective drug concentration in this way (rather than spot assays described in previous chapters) provides a more accurate drug concentration assessment in genome-wide SGA screening experiments performed on solid media. This is because the Singer RoToR colony printing robot used to replicate the plates transfers relatively large numbers of yeast cells by contrast to spot assays that start with relatively few cells per plate. Based on the pilot screens shown in figures 5.1-5.6 the following concentrations were used in the double mutant chemical genetic screens: $\Delta hmg1 + \Delta xxx$ *atorvastatin* 7 μM , *cerivastatin* 3 μM and *lovastatin* 30 μM ; $\Delta hmg2 + \Delta xxx$ *atorvastatin* 17.5 μM , *cerivastatin* 10 μM and *lovastatin* 80 μM . The original data for these screens are shown in Appendix 3 (Tables B1 – B6).

5.2. *Atorvastatin* + *Δhmg1* Δ xxx double mutant

chemical genetic screens

This experiment tests the *atorvastatin* chemical genetic epistatic interactions of *HMG2* in the absence of *HMG1*. Three *Δhmg1* double mutant chemical screens, i.e. *Δhmg1* Δ xxx + statins were performed on 7 μ M *atorvastatin* and analysed with SESA. These experiments resulted in 38 PE interactions, after adjusting the wider list of “gene hits” by discounting the DMSO controls, the genes that appeared as hits in the *Δhmg1* query gene SGA without statin and deletion strains that showed sensitivity to 25 μ M *atorvastatin* alone in the chemical genetic screen. The 38 genes were then analysed by gene ontology using the yeast GO Slim Mapper (SGD, 2009) and BiNGO (Maere, et al., 2005).

This analysis showed that 8 of 38 gene products (AIM34, COQ2, FAB1, GNP1, HMI1, IMG2, IRA2 and VPS21) were localised to the mitochondria (P-value = 0.42), 4/38 genes (IMG2, ITT1, RPL20B and TIF1) involved in translation (P-value = 0.035), 11 of 38 genes (EDE1, GNP1, SEC66, SLA1, VAM3, VPS21, VPS27, VPS4, VPS9, WHI2 and YDR387C) were involved in transport (P-value = 0.73), significantly including 8 of 11 transport genes (EDE1, SLA1, VAM3, VPS21, VPS27, VPS4, WHI2 and SEC66) that were involved in *vesicle mediated transport* (P-value = 0.0041). An interpretation of these interactions is that if *HMG1* and its epistatically interacting genes are shut off and *HMG2* is simultaneously inhibited with *atorvastatin*, the cells attempt to maintain membrane/lipid homeostasis by anterograde and retrograde transport

mechanisms. Five of 38 genes were involved in lipid biosynthesis namely COQ2, DGA1, FAB1, SUR1 and VPS4 (P-value = 0.016) with 4 of 39 genes (DGA1, KRE27, SEC66 and VPS4) showing localisation to the endoplasmic reticulum (P-value = 0.24).

The VPS21 gene in the mitochondria is a GTPase required for transport and sorting of vacuolar hydrolases. This gene requires geranylgeranylation for complete functionality, similar to that of IRA2. These results again (cf Chapter 4) implicate the importance of mitochondrial processes (inhibition of isoprenoid intermediates in the mevalonate pathway) in the mechanism of statins.

5.3. Atorvastatin + $\Delta hmg2$ Δxxx double mutant chemical genetic screens

This experiment tests the *atorvastatin* chemical genetic epistatic interactions of *HMG1* in the absence of *HMG2*. The three $\Delta hmg2$ double mutant chemical screens performed on 17.5 μ M *atorvastatin* resulted in 136 PE interactions (Appendix 3) when analysed with SESA (after a wider-list of hits was adjusted for the various controls as described above for $\Delta hmg1$). The 138 genes were then analysed based on gene ontology using the yeast GO Slim Mapper (SGD, 2009).

Gene ontology analysis of the 136 phenotypic enhancement interactions showed 24 of 136 gene products (ADH4, AIM34, CAT5, CHD1, COX14, ECM33, FAB1, GAS1, GET1, GNP1, HMI1, IRA2, ISC1, MRE11, PET122, PET8,

PFK2, QCR2, SNF1, SWS2, TAZ1, TPS2, VPS21 and YSA1) were localised to the mitochondria (P-value = 0.4), and 14 of 136 genes (CHO2, ERG2, FEN1, GET1, GET2, GUP1, ILM1, ISC1, LAS21, OST4, PMT2, SEC66, VPS4 and YTA7) were localised to the endoplasmic reticulum (P-value= 0.038). There were also 17/136 genes (CHO2, DEP1, DGA1, ERG2, FAB1, FEN1, GUP1, HST3, INP51, ISC1, LAS21, SUR1, TAZ1, TLG2, VAC14, VPS4 and YTA7) involved in lipid biosynthesis (P-value = 6.08×10^{-4}) and 38/136 genes (PMP3, WHI2, RVS161, GNP1, VRP1, VPS53, PEX5, PET8, VPS51, VPS74, CHS5, SEC66, GET2, GET1, EDE1, QCR2, GUP,1 ERD1, CCZ1, PEX10, FEN1, VPS9, VAM3, VAC14, SLA1, VAM7, VAM6, TLG2, VPS41, VPS4, MON1, VID22, SLM4, VPS24, RVS167, VPS21, VPS27 and RUD3) that were involved in cellular transport (P-value = 0.0029) including 24 of the 38 genes (CCZ1, CHS5, EDE1, FEN1, GET1, GET2, MON1, RIM8, RUD3, RVS161, RVS167, SLA1, TLG2, VAM3, VAM7, VPS21, VPS24, VPS27, VPS4, VPS51, VPS53, VPS74, VRP1 and WHI2) involved in vesicle mediated transport (P-value = 8.87×10^{-7}).

There were 7 of 33 transport genes (GET1, RUD3, SEC66, VPS27, VPS51, VPS53 and VPS74) that are involved in/with ER-golgi transport, *VPS51* and *VPS53* are 2 of 4 members of the Golgi-associated retrograde protein (GARP) complex which is required for the recycling of proteins from endosomes to the late Golgi (Siniossoglou and Pelham, 2002). Again an interim conclusion is that cells deprived of HMG Co- A reductase genes and their immediate enhancing epistatic interacting genes attempt to maintain lipid/membrane homeostasis by utilising otherwise cryptic membrane cycling genetic interactions.

5.4. *Cerivastatin* + *Δhmg1* Δ xxx double mutant

chemical genetic screens

This experiment tests the *cerivastatin* chemical genetic epistatic interactions of *HMG2* in the absence of *HMG1*. The three *Δhmg1* double mutant chemical screens performed on 3 μ M *cerivastatin* resulted in 31 PE interactions (Appendix 3) when the *cerivastatin* plates were analysed with SESA, and the wider list adjusted for controls as described above. The 31 genes were then analysed based on gene ontology using the yeast GO Slim Mapper (SGD, 2009) and BiNGO (Maere, et al., 2005).

Gene ontology analysis of the 31 PE interactions (Appendix 3) resulted in 6 of 36 gene products (AIM34, COQ2, ERG6, IRA2, SNF1 and YME1) localised to the mitochondria (P-value = 0.59), 4 of 36 genes (COQ2, ERG6, GET2 and VPS4) localised to the ER (P-value = 0.16) and were also involved in lipid biosynthesis (P-value = 0.036), 6 of 31 genes (GET2, DGA1, VPS27, VPS4, WHI2 and YDR387C) involved in cellular transport (P-value = 0.7), with 4 of 5 genes (WHI2, GET2, VPS4 and VPS27) involved in vesicle mediated transport (P-value = 0.09).

Similar to the result seen in the *Δhmg1 atorvastatin* screen, GET2, VPS27 and VPS4 are involved in ER/Golgi transport and retention. Moreover, there are 5 of 31 genes (ITT1, RPL20B, RPS21B, SNF1 and TIF1) involved in translation (P-

value = 0.459). Interestingly, *TIF1* (eukaryotic initiation factor 4a) is also a duplicate gene (*TIF1* and *TIF2*).

5.5. *Cerivastatin* + $\Delta hmg2$ Δ xxx double mutant

chemical genetic screens

This experiment tests the *cerivastatin* chemical genetic epistatic interactions of *HMG1* in the absence of *HMG2*. The three $\Delta hmg2$ double mutant chemical screens performed on 10 μ M *cerivastatin* resulted in 123 PE interactions (Appendix 3) when analysed with SESA and the wider list adjusted for controls as described above. The 123 PE genes were then analysed based on gene ontology using the yeast GO Slim Mapper (SGD, 2009) and BiNGO (Maere, et al., 2005).

Gene ontology analysis of the PE interactions (Appendix 3) resulted in 24 of 123 gene products (ADH4, AIM34, ARC18, CHD1, COX14, ECM33, ERG6, GAS1, GET1, GNP1, GPA2, IRA2, ISC1, MRE11, NEM1, NUT1, PET8, PFK2, SNF1, SWS2, VMR1, VPS1, VPS21 and YPT7) localised to the mitochondria (P-value = 0.07), 16 of 123 genes (ERG2, ERG3, ERG6, GET1, GET2, GUP1, ILM1, ISC1, LAS21, OST4, PMT2, RCE1, SEC66, SUR2, SWH1 and VPS4) localised to the endoplasmic reticulum (P-value = 1.24×10^{-3}) along with 10 genes (GET2, COG8, GET1, ISC1, TLG2, VPS53, VPS51, SWH1, MON2 and RUD3) that were localised to the Golgi (P-value = 6.29×10^{-3}).

Moreover, there are 12 genes (DGA1, ERG2, ERG3, ERG6, FAT1, GUP1, ISC1, LAS21, SUR1, SUR2, TLG2 and VPS4) involved in lipid biosynthesis (P-value =

4.6×10^{-4}) including ERG2, ERG3, ERG6 which are specifically involved in ergosterol production. The absence of these genes seriously perturbs ergosterol production in yeast (see Chapter 6: Ergosterol quantification) perhaps explaining that 37 of 123 genes (AGP1, ARN1, CCZ1, COG8, EDE1, ERG3, FAT1, GET1, GET2, GNP1, GUP1, MON1, MON2, PET8, PEX5, PMP3, RUD3, RVS161, RVS167, SEC66, SWH1, TLG2, TPM1, URE2, VAM3, VMR1, VPS1, VPS21, VPS24, VPS27, VPS4, VPS41, VPS51, VPS53, VPS8, WHI2 and YPT7) involved in cellular transport ($P\text{-value} = 1.5 \times 10^{-4}$) including 24 genes (CCZ1, COG8, EDE1, ERG3, GET1, GET2, MON1, MON2, RUD3, RVS161, RVS167, SWH1, TLG2, TPM1, VAM3, VPS21, VPS24, VPS27, VPS4, VPS51, VPS53, VPS8, WHI2, YPT7) specific to vesicle mediated transport ($P\text{-value} = 5.9 \times 10^{-9}$) now displayed genetic enhancements in compensation to decreased cellular sterol availability.

These results are consistent with those seen in the double mutant *Δhmg2 atorvastatin* chemical screen, in which they resulted in genes (COG8, GET1, GET2, MON2, RUD3, SEC66, TLG2, VPS1, VPS27, VPS41, VPS51 and VPS53) involved in ER/Golgi transport, including the retrograde transport GARP complex genes which are required for the recycling of proteins from endosomes to the late Golgi (Siniossoglou and Pelham, 2002).

5.6. ***Lovastatin + $\Delta hmg1$ Δ xxx double mutant*** **chemical genetic screens**

This experiment tests the *lovastatin* chemical genetic epistatic interactions of *HMG2* in the absence of *HMG1*. The three *Δhmg1* double mutant chemical screens performed on 30 μM *lovastatin* resulted in 86 PE interactions (Appendix 3) when analysed with SESA and the wider list adjusted for controls as described above. The 86 PE genes were then analysed based on gene ontology using the yeast GO Slim Mapper (SGD, 2009) and BiNGO (Maere, et al., 2005).

Upon GO slim term analysis, the *Δhmg1* 30μM *lovastatin* chemical genetic screen resulted in 3 of 22 gene products (IRA2, MDM12 and SNF1) localised to the mitochondria (P-value = 0.7) and ER (GET2, ORM2 and VMA21) P-value = 0.074), 5 of 22 genes (GET2, MDM12, RVS161, VPS27 and YDR387C) involved in cellular transport (P-value = 0.45) including GET2, RVS161 and VPS27 which were involved in vesicle mediated transport (P-value = 0.14).

Moreover, consistent with the *Δhmg1 atorvastatin* and *cerivastatin* double mutant chemical genetic screens there are 4 genes (ITT1, RPL20B, SNF1, and TIF1) involved in translation (P-value = 0.5). Conversely, there is only one gene (*DGA1*) involved in lipid homeostasis via triglyceride storage droplets. This may be due to the absence of *HMG1* whose main function is lipid biosynthesis, in contrast to that of *HMG2* whose role is thought to be more diverse (Basson, et al., 1988; Basson, et al., 1986; Federovitch, et al., 2008).

5.7. Lovastatin + *Δhmg2* Δ xxx double mutant

chemical genetic screens

This experiment tests the *lovastatin* chemical genetic epistatic interactions of *HMG1* in the absence of *HMG2*. The three *Δhmg2* double mutant chemical screens performed on 80 μ M *lovastatin* resulted in 111 PE interactions (Appendix 3) when analysed with SESA and the wider list adjusted for controls as described above. The 111 PE interactions were then analysed based on gene ontology using the yeast GO Slim Mapper (SGD, 2009) and BiNGO.

Of the 111 PE interactions 18 gene products (AEP2, AIM34, CHD1, CSF1, ECM33, ERG6, GAS1, GET1, GNP1, IMP2, IRA2, ISC1, MDM12, PET8, SNF1, VPS1, YPT7 and YSA1) localised to the mitochondria (P-value = 0.6), 15 of 111 genes (ERG2, ERG3, ERG6, GET1, GET2, GUP1, ILM1, ISC1, LAS21, OST4, PMT2, SEC66, SUR2, SVP26 and VPS4) localised to the ER (P-value = 339×10^{-4}) including 3 integral sterol biosynthesis genes *ERG2*, *ERG3* and *ERG6*.

Furthermore, there were 14 genes (CWH43, DEP1, DGA1, ERG2, ERG3, ERG6, FAT1, GUP1, INP51, ISC1, LAS21, SUR2, TLG2 and VPS4) involved in lipid biosynthesis (P-value = 8.5×10^{-4}) also with similarity to the other two screens of this type there were 31 of 111 genes (AGP1, CCZ1, ERG3, FAT1, GET1, GET2, GNP1, GUP1, IMP2, MDM12, MTH1, PET8, RUD3, RVS161, RVS167, SEC66, SVP26, TLG2, VAM3, VAM7, VPS1, VPS24, VPS27, VPS4, VPS41, VPS51, VPS53, VPS9, VRP1, WHI2 and YPT7) involved in cellular transport (4.5×10^{-4}) with 20 genes (WHI2, ERG3, RVS161, YPT7, VAM3, VRP1, VAM7, SVP26,

TLG2, VPS53, VPS41, VPS51, VPS4, GET2, GET1, VPS24, RVS167, CCZ1, VPS27 and RUD3) involved solely in vesicle mediated transport (P-value = 1.89×10^{-6}).

These results are consistent with those seen in the double mutant *Δhmg2* *atorvastatin* and *cerivastatin* chemical screens, in which GET1, GET2, MDM12, RUD3, SEC66, SVP26, TLG2, VPS1, VPS27, VPS41, VPS51 and VPS53 are involved in ER/Golgi transport. Of note are the retrograde transport GARP complex genes (VPS51 and VPS53) which are required for the recycling of proteins from endosomes to the late Golgi (Siniossoglou and Pelham, 2002).

5.8. Discussion: statins + *Δhmg1 Δxxx* double mutant chemical genetic screens

The three *Δhmg1* double mutant chemical genetic screens performed on 7 μM *atorvastatin*, 3 μM *cerivastatin* and 30 μM *lovastatin* resulted in 54 PE interactions (Appendix 3, Fig 5.7), 13 of which are shared by all three statins, 3 are shared between *lovastatin* and *cerivastatin* and 7 are shared between *atorvastatin* and *cerivastatin*. It is probable that genetic interactions shared by two out of the three statins are due to a dosage effect, i.e. the dose of the third statin may not have been high enough to exhibit that particular growth defect. If this is a correct interpretation of results, 23 genes could be said to be shared by the three statins, therefore comprising a list of the direct genetic interactions revealed by statin action in the absence of *HMGI*. In addition to the shared commonality of statin basic genetic interactions, *atorvastatin* shows 17 unique interactions as compared to 8 for *cerivastatin* and 5 for *lovastatin*. If these are “*off-target*” interactions as already noted they should be of interest in studies aimed at providing “*better statins*”.

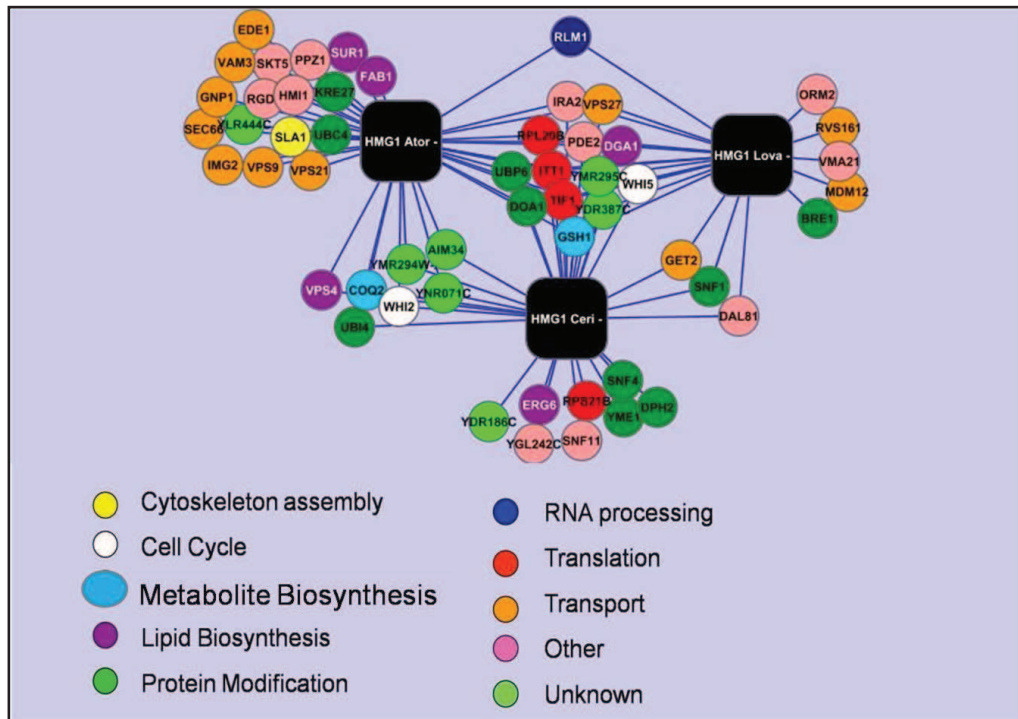


Figure 5.7 HMG1 based interactions. Cytoscape network graph showing the phenotypic enhancement interactions from the chemical genetic screens performed on *atorvastatin*, *cerivastatin* and *lovastatin*. The genes are grouped based on their GO terms (cellular process).

When the 13 genes that interacted with all three statins underwent GO analysis, there was only one gene involved in lipid synthesis (*DGA1*). *DGA1* is diacylglycerol acyltransferase, an integral enzyme in *de novo* synthesis and storage of triacylglycerols in lipid particles (Sorger and Daum, 2002). There are five lipid biosynthesis genes in the whole 54 PE interactions around *HMG2*, perhaps because *HMG2* has functions other than lipid biosynthesis.

Many of the genetic interactions described involve the ubiquitin – proteasome pathway, a pathway has been implicated in the cellular response to stress and oxidative damage. When cells are stressed they generate an increased number of misfolded proteins (a phenotype associated with *Δkre27*) which are a prime target for ubiquitin mediated degradation. This is mediated by *UBC4* (an E2 ubiquitin

conjugating enzyme) and *BRE1* (an E3 ubiquitin ligase), and can rapidly deplete free ubiquitin (Hanna, et al., 2003). If there is a shortage of free ubiquitin, it can be compensated for by the induction of *UBI4*, a polyubiquitination gene which can in turn, bind *VPS27*, required for the sorting of ubiquitinated proteins destined for degradation (Bilodeau, et al., 2002). In contrast to *UBI4*, *UBP6* (which interacts with all statins under these conditions) opposes polyubiquitination and releases free polyubiquitin chains and its resistance to oxidative stress is significantly decreased (Crosas, et al., 2006).

The inhibition of ubiquinone synthesis can lead to oxidative damage (ubiquinone is an antioxidant) and a decrease in ATP production via oxidative phosphorylation. In humans, disruption of the mitochondrial respiratory chain frequently causes mitochondrial encephalomyopathies, generally in organs with high energy requirements, such as muscle (Quinzii, et al., 2006). These studies reveal a dependence on *COQ2* in the respiratory chain. Its disruption leads to oxidative damage/stress, causing proteins to become unfolded/misfolded, therefore the need for ubiquitination of the damaged proteins to target them to the proteasome for degradation.

Genes involved with suppression of the translation (*TIF1*, *RPL20B* and *ITT1*) of constitutive mRNAs at the initiation step are known to synergise with an ER stress response (Brostrom, et al., 1997; Sheikh and Fornace, 1999). Furthermore, *DOA1* is required for recycling ubiquitin from proteasome-bound ubiquitinated proteins being transported to the vacuole/proteasome where it associates with

Vps4p, a protein involved with Vps27p in sorting of proteins in the multivesicular body (Amerik, et al., 2000; Ren, et al., 2008).

There is a possibility that the interactions described above are occurring under these experimental conditions as *COQ2*, which catalyses the second committed step in the ubiquinone synthesis pathway and interacts with *atorvastatin* and *Cerivastatin*. Furthermore the *YME1* gene product is responsible for degradation of unfolded/misfolded mitochondrial proteins (Leonhard, et al., 1999).

5.9. Discussion: statins + $\Delta hmg2$ Δxxx double mutant chemical genetic screens

The three $\Delta hmg2$ double mutant chemical genetic screens performed on 17.5 μ M *atorvastatin*, 10 μ M *cerivastatin* and 80 μ M *lovastatin* resulted in 197 PE interactions (Appendix 3, Fig 5.8), 62 of which are shared by all three statins, 15 are shared between *lovastatin* and *cerivastatin*, 16 are shared between *lovastatin* and *atorvastatin* and 21 are shared between *atorvastatin* and *cerivastatin*. As noted above, genes that share interactions affected by two out of the three statins may be due to a dosage effect, i.e. the dose of the third statin may not have been high enough to exhibit that particular growth defect. Accepting this proviso, 114 genes could be said to be shared by the three statins, therefore comprising the most direct mechanism of statin action on *HMG1* in the absence of *HMG2*. The genes not shared by *HMG1* and *HMG2* are of interest in their own right, and may

also be of importance in statin side effects. *Atorvastatin* shows 37 unique interactions as compared to 27 for *cerivastatin* and 19 for *lovastatin*.

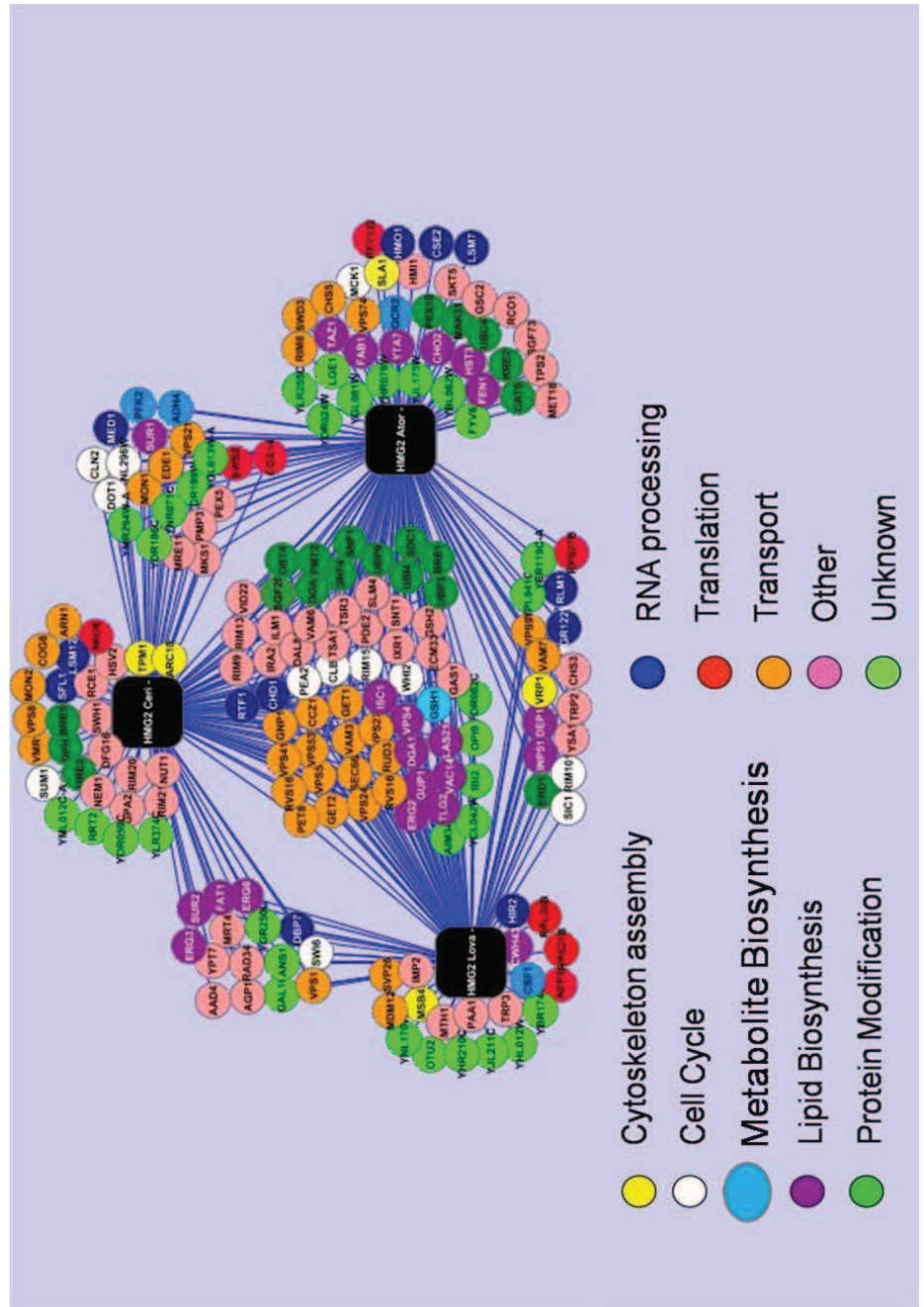


Figure 5.8 HMG2 based interactions. Cytoscape network graph showing the phenotypic enhancement interactions from the chemical genetic screens performed on *atorvastatin*, *cerivastatin* and *lovastatin*. The genes are grouped based on their GO terms (cellular process).

When the 62 genes of the null *HMG2* set which are common to all statins are analysed based on GO slim – process (SGD, 2009), there were 8 genes involved in lipid biosynthesis. However, when added to those that interact with two statins and the individual hits there are 22 lipid biosynthesis genes that show genetic interactions with *HMG1* in the absence of *HMG2*.

The lipid biosynthesis genes represented (22 genes) have diverse cellular roles, including sterol biosynthesis, sphingolipid biosynthesis, triacylglycerol (TAG) biosynthesis and phospholipid biosynthesis. There are three genes (*ERG3*, *ERG6* and *ERG2*) directly involved in ergosterol biosynthesis (Veen and Lang, 2005), and are downstream from HMG – CoA reductase in the mevalonate pathway (Fig1.4). *DGA1* is of particular interest since it also shows up in all the *HMG2*-based screens (see below). It is involved with triglyceride synthesis/utilisation possibly reflecting that when all other avenues are shut off for lipid homeostasis, the cells resort to triglyceride (lipid) storage (Petschnigg, et al., 2009).

It is clear that many more genes involved in lipid synthesis and membrane cycling processes appeared in the *statins* + $\Delta hmg2$ Δxxx double mutant chemical genetic screens than the *statins* + $\Delta hmg1$ Δxxx counterparts leading to the conclusion that the *HMG1* isoenzyme is the more important enzyme in these processes pointing to a more specific role of *HMG1* in sterol biosynthesis and its compensating membrane recycling processes. Another valid conclusion could be that *HMG2* is more redundant in these processes than *HMG1*, therefore resulting in less extensive genetic interaction networks.

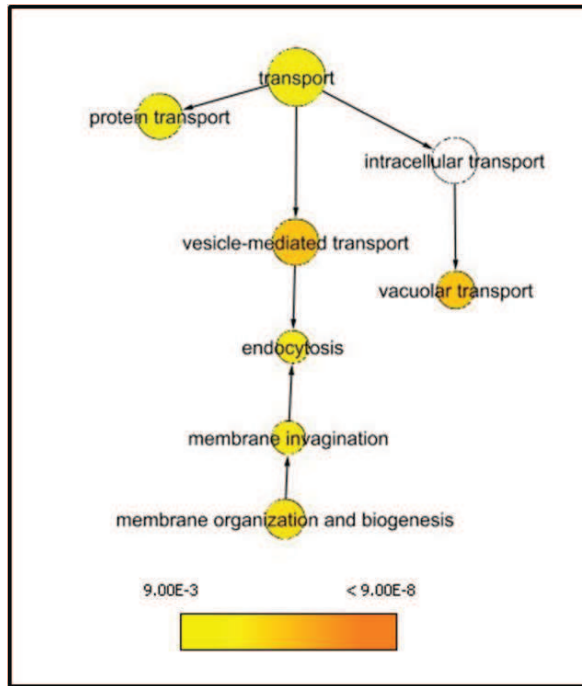


Figure 5.9 Graph of GO processes involving HMG1 showing enrichment for vesicle mediated transport genetic interactions.

GO term analysis by BiNGO (Fig.5.9) shows that the processes and the secretory pathway organelles enriched in the statins + *Δhmg2 Δxxx* double mutant chemical genetic screen are statistically significant (P-value <0.05) especially that of vesicle mediated and vacuolar transport including anterograde and retrograde transport (GET1, GET2, VPS1, VPS53 and UBP3) and protein sorting to the multivesicular body (VPS24, VPS27, VPS4 and DOA1). This situation is unlike the majority of those mentioned in the *HMG1* double mutant chemical genetic screen.

However, the data also support the idea that *HMG2* has different roles than that of its ‘duplicate’. For example, Hmg2p may be involved in the HRD-ubiquitin mediated degradation pathway which is not associated with Hmg1p. This explanation coincides with the increase in ubiquitin related genes in the statins + *Δhmg1 Δxxx* screen, where ubiquitin is an essential mediator for Hmg2p

degradation. It is concluded that inhibition of Hmg2p rather than Hmg1p leads to a severe disruption of the ubiquitin/proteasome pathway.

A recent study performed by Petschnigg, et al., 2009 suggested that diacylglycerol (DAG), a potent signalling molecule, may involve the mitochondria and be associated with the generation of reactive oxygen species when overproduced. Furthermore, there is a distinct relationship between with lipid droplets (mainly containing TAG) and peroxisomes, where degradation of fatty acid occurs. Thus, disruption of the relationship between lipid droplets and peroxisome leads to a disruption of membrane homeostasis. This coupled with a depletion of sterol esters as a result of perturbed sterol synthesis may in turn lead to the inhibition of membranous vesicular transport of lipid droplets among other cargoes (Petschnigg, et al., 2009).

A relationship has been described by Fei, et al., 2009 that closely links conditions of ER stress which leads to an increase in lipid droplets possibly as a self protective mechanism employed by a range of eukaryotic cells. Moreover, lipid trafficking from other cellular compartments to the ER is also enhanced under stress conditions possibly providing increased substrate availability for the synthesis *de novo* of TAG (via *DGAT*) and sterol esters (Fei, et al., 2008; Fei, et al., 2009). This explanation is supported by the data presented in this and the previous chapter showing that when sterol ester synthesis is inhibited the cell mobilises the use of lipid storage droplets.

Chapter 6. Ergosterol quantification

In order to associate a quantitative phenotype with specific genotypes, a biochemical assay for ergosterol was applied and optimised as part of this dissertation. The assay development is reported here (with an example of its use) as a separate chapter, as existing methods (previously described in the literature) were unsuitable, requiring too much starting material and were insufficiently reproducible. The assay involves a saponification reaction with potassium hydroxide, followed by a liquid: liquid extraction of non-saponifiable lipids with diethyl ether. The resulting lipids are then dried and quantified with HPLC. Initially this assay required a large amount of lyophilised yeast (approximately 3g i.e. ~800 mL culture) but improved experimental design enabled a reduction of the required amount of yeast to about ~400 mL of cells achieving reproducible results.

The assay was optimised using two haploid and one diploid strain (BY4741, BY7092 and BY4743 respectively). In another assay reported in the literature (Eisenkolb, et al., 2002; Schulz and Prinz, 2007) the deletion mutants *Δerg3* and *Δerg6* were found to have decreased ergosterol levels by comparison to an ergosterol standard.

The optimised assay was applied to two *molliside* (Yibmantasisri, Northcote, Bellows, unpublished data) yeast strains (in BY7092 MAT α background) generated by Ploi Yibmantasisri (PhD candidate, Chemical Genetics, VUW) that

confer resistance to this marine natural product (isolated from the sponge *Australostichopus mollis*). The putative target of this drug has been identified (Yibmantasiri and Bellows, unpublished) via linkage mapping of the resistant strain to be NCP1 gene. NCP1 regulates ERG11, an essential gene that catalyzes the C-14 demethylation of lanosterol in the ergosterol pathway (Daum, et al., 1999; Turi and Loper, 1992). Utilising the assay developed as part of this dissertation, the *Molliside* resistant mutant was found to have decreased ergosterol levels providing strong supporting evidence that the target of *Molliside* in *Saccharomyces cerevisiae* is NCP1.

6.1. Ergosterol standard

In order to quantify ergosterol, a standard curve was generated using purified ergosterol (Sigma), at half log dilutions (0.001 – 1.0 mg/mL) injected into the chromatograph (see Chapter 2), and absorbance was measured at 282nm (Lamacka and Sajbidor, 1997) after which the area under the peak was calculated (mAU²) as a reference to generate a standard curve (Fig 6.1 and 6.2). When calculated and plotted the resulting r value was 0.9998 (P value < 0.005).

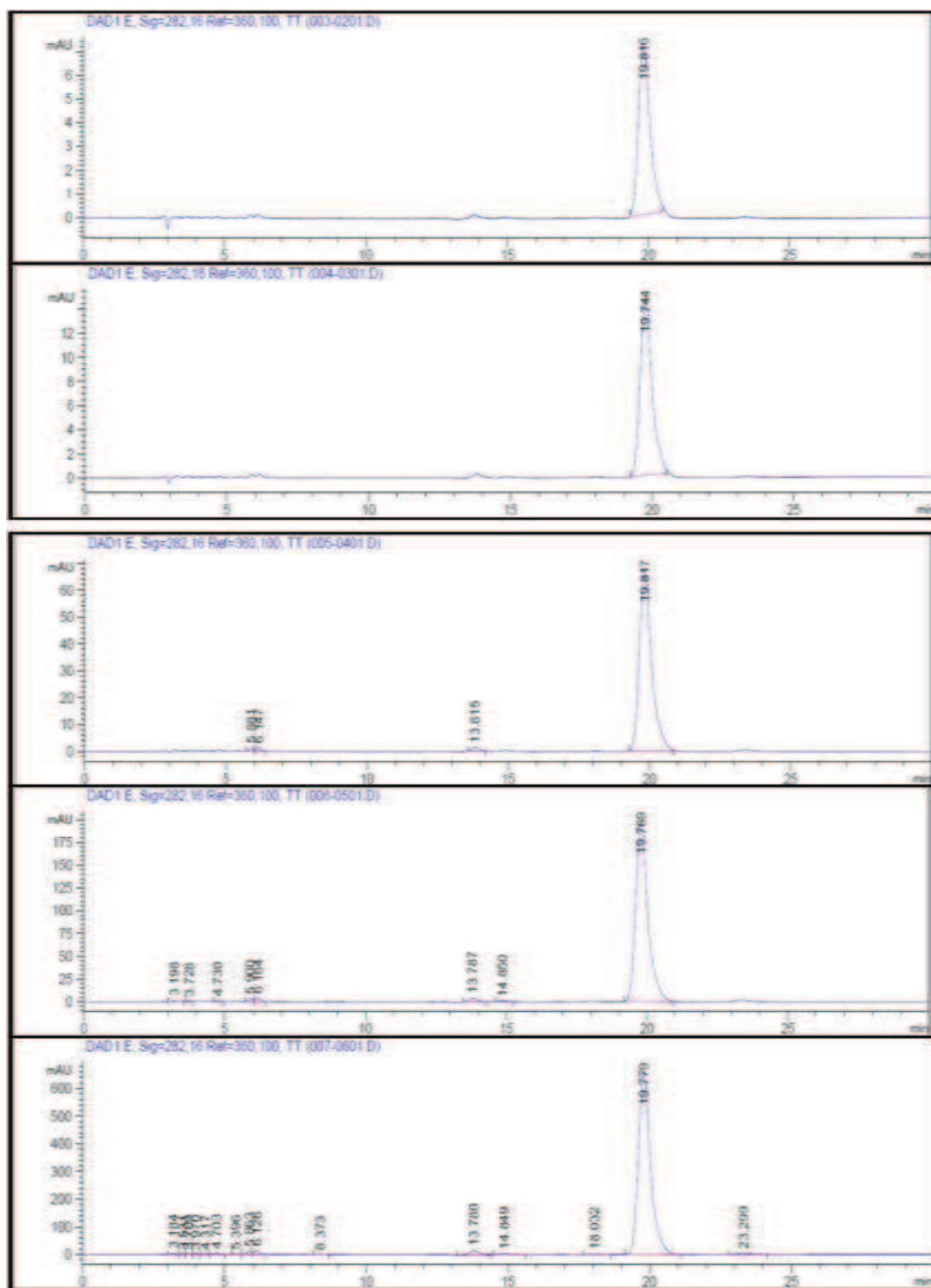


Figure 6.1 Ergosterol standard HPLC chromatographs. Top - Bottom 0.001 mg/mL, 0.0316 mg/mL, 0.1 mg/mL, 0.316 mg/mL and 1.0 mg/mL, with the retention time (shown at the top of peaks) of approximately 19.8 min.

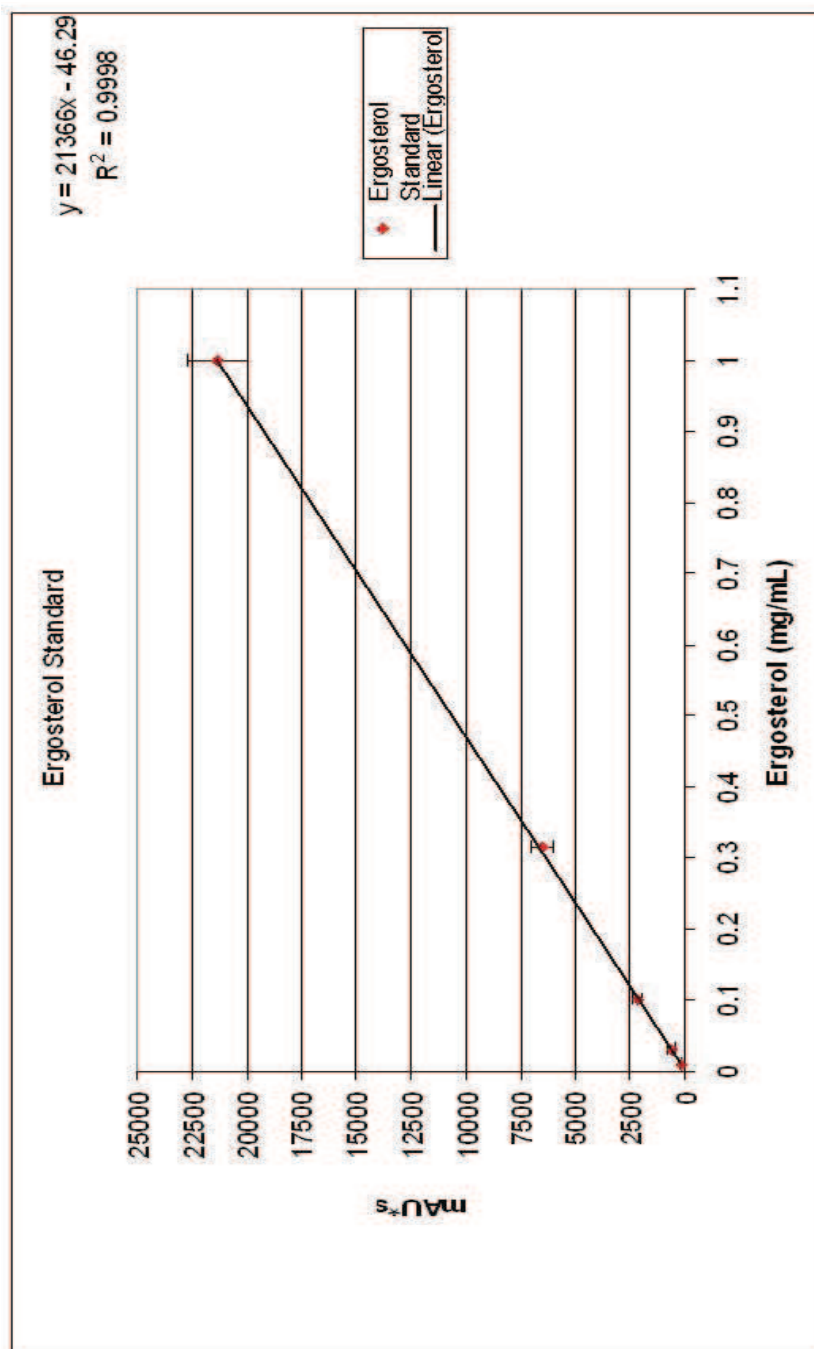


Figure 6.2 Ergosterol Concentration Standardisation. Half log dilutions from 1 mg/mL – 0.001 mg/mL.

6.2. Method optimisation

Initially 800mL yeast cultures (BY4743, BY4741 and *Δerg3*) were grown to saturation, for ergosterol quantification. These cultures gave a 2.4-3 gm yeast pellet (lyophilised). The ergosterol was then extracted, dried and stored at -20°C. The ergosterol was then resuspended in either 10 or 20 mL methanol (HPLC grade, Scharlau) dependent on solubility and filtered through a 0.22 μm filter. In light of the sensitivity of the HPLC and as can be observed from Fig 6.2 the error bars increase as the ergosterol concentration increases, therefore samples were diluted at 1:10 – 1:30. It was found that ergosterol extracted from an 800 mL wild-type culture far exceeded levels required to detect it in HPLC. In contrast, the *Δerg3* mutant strain showed no measurable ergosterol (<0.001 mg/mL) and its use was discontinued in the optimisation of this assay. It was however replaced with the *Δerg6* strain, which has been reported to produce a decreased amount of ergosterol (Eisenkolb, et al., 2002).

Strain	4741 10mL	4741 100mL	4741 400mL	4741 800mL	4743 800mL	<i>Δerg6</i> 10mL	<i>Δerg6</i> 100mL
Ergosterol content mg/gm (Avg.)	1.179	0.688	0.808	0.799	0.799	0.359	0.492
Std dev	0.425	0.214	0.074	0.088	0.113	0.141	0.112

Table 6.1 Ergosterol content of wild-type and mutant strains

Improvements in the assay were made to reduce the culture size required whilst continuing to obtain reproducible results. This was carried out using 400 mL, 100 mL, 50 mL and 10 mL culture sizes (Table 6.1 and Fig 6.3). The results showed (Figure 6.3; raw data see Appendix 2) that as the culture size decreases, the variation (standard deviation) increases. Based on the optimisation experiments 400mL is the minimum culture size required to achieve reproducible quantification of ergosterol from yeast by the assay described in this dissertation.

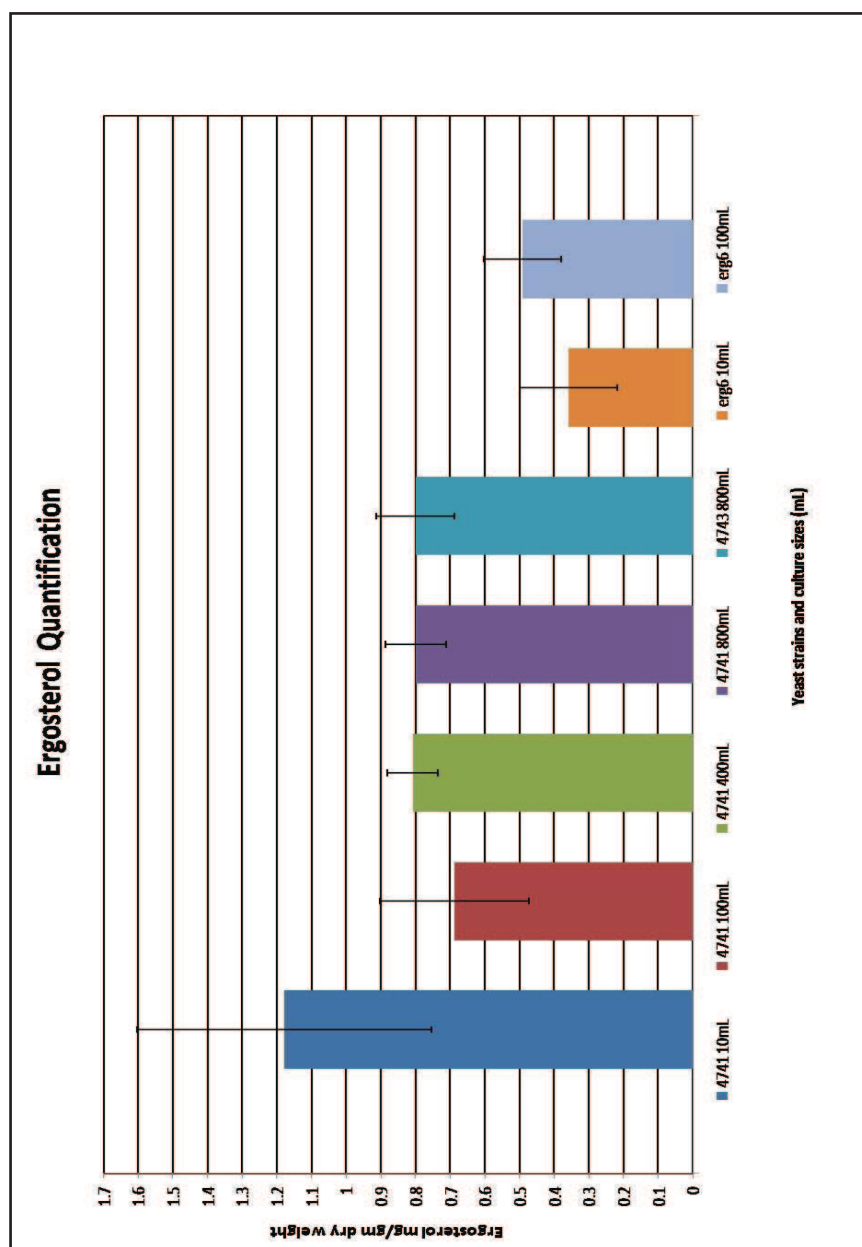


Figure 6.3 Ergosterol quantification results in different sample sizes. 800 mL cultures BY4741, BY4743; 400mL 4741, 100mL, 50 mL and 10 mL cultures of BY4741, $\Delta erg6$.

6.3. *Molliside* resistant mutants

The ergosterol content of two individual strains that show resistance to a SMP, *molliside*, was compared to that of wild type (BY7092). The graph shown in Figure 6.4 shows the resistant *molr1* and *molr2* strains show 50% and 60% reduced ergosterol respectively (Table 6.2 and Fig6.4, Appendix 2) providing supporting evidence that NCP1 is the target gene of *Molliside*.

Strain	BY7092	<i>molr1</i>	<i>molr2</i>
Ergosterol content Avg. mg/gm dry weight	1.009	0.615	0.489
Std dev	0.0614	0.012	0.051

Table 6.2 Ergosterol content of *molr1* and *molr2* mutants

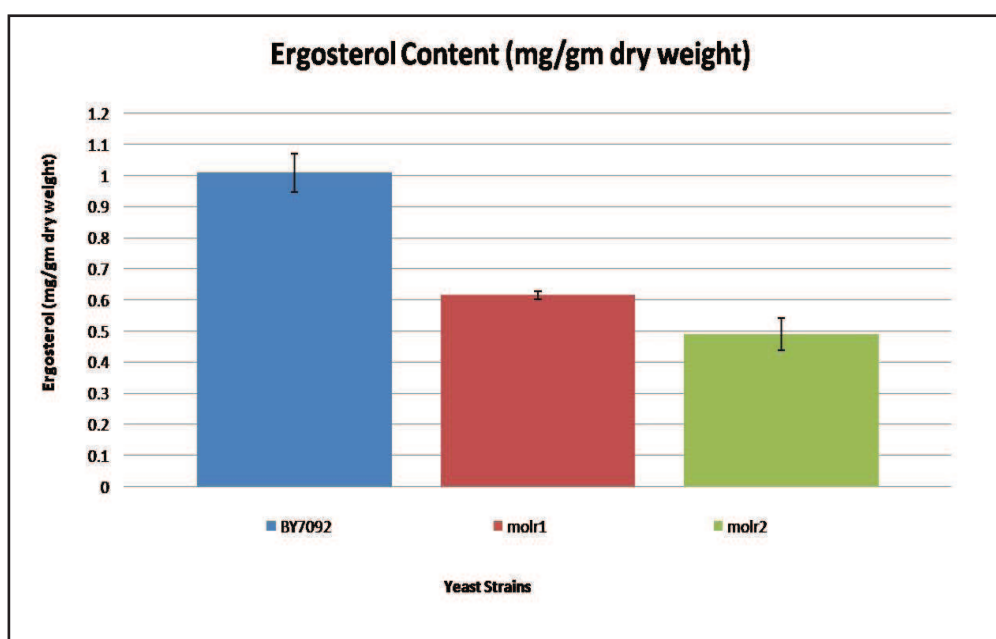


Figure 6.4 Ergosterol quantification *molliside* resistant mutants *molr1* and *molr2* compared to wild type (BY7092).

6.4. Discussion

The observed results in this chapter present a method that has been applied to yeast with the ability to extract and quantify ergosterol on a smaller scale than reported in the literature. However, the size of the assay will limit future experiments based on the required culture size if SMP's to be assayed are available in limited quantities.

Nonetheless, the assay has proved very useful. Evidence has been provided to support independent evidence (Yibmantasiri and Bellows, unpublished) of the putative target of *mollisoside* in *Saccharomyces cerevisiae*, which in turn can be applied to strains that show sensitivity to the statin drugs. In future work, this assay may be used with chemical or genetic perturbations, thereby providing phenotypic data that can be compared to that of data from the chemical genetic and genetic screens discussed in this thesis. Future improvements may make 100 mL cultures a feasible starting point for obtaining such ergosterol phenotypes, but in the interim, as the *mollisoside* results show, the assay was able to provide critical confirmatory phenotypic data.

Chapter 7. General Discussion,

Conclusions and Future Directions

Researching gene function has taken a new dimension with the ability to apply genome-wide analysis of epistasis between gene pairs that indicate functional connections between the double mutant components. Chemical genomics is part of this new approach in which a well-chosen SMP may substitute for a mutation, particularly in the ablation of gene function mimicking deletion mutations (Hillenmeyer, et al., 2008; Parsons, et al., 2004; Parsons, et al., 2006; Schuldiner, et al., 2005). Thus the combination of deletion mutant analysis and SMPs provides a powerful approach to such systematic epistasis measurements which has been applied in investigation of statin drug mechanisms.

7.1. Epistasis

Epistasis is '*an interaction between non-allelic genes where a combination of their effects exceeds the sum (multiplication) of the expected effects of the individual genes*'. Masking epistasis as described by Bateson (1909, cited in Phillips, 1998), is a particular case in which a gene masks the effects of another where the locus being masked is said to be *hypostatic* to that of the other locus (Phillips, 1998) an example being *BTS1* mutations that leads to growth defect interactions surrounding HMG2 and genes further downstream of the *BTS1* gene. Fisher (1918, cited in Phillips, 1998) describes a more generalised mechanism of

epistasis, where the phenotype of a given double mutant exceeds the summed or multiplicative combined effects of its components. *Synthetic lethality* in this (Fisher) definition is an extreme case of an aggravating interaction and can be observed in the interactions of particular $\Delta hmg1 \Delta xxx$ and $\Delta hmg2 \Delta xxx$ combinations where *xxx* might for example be *DGAI*. In explanation, the cell can tolerate loss in sterol synthesis and triacylglycerol synthesis alone, but when combined as in $\Delta hmg1 \Delta dgal$ or $\Delta hmg2 \Delta dgal$ the result is synthetic lethality. This dissertation has mostly focussed on *synthetic lethal* phenotypes and its less drastic growth reducing form, *phenotypic enhancement (PE)* though particularly pronounced examples of *phenotypic suppression (PS)* i.e. growth enhanced phenotypes are also discussed in the following sections.

7.2. Isoprenoid compensatory pathways

within the mitochondria

Though statin action has long been thought of as inhibition of HMG CoA-reductase it is clear from this dissertation that such inhibition must be considered in context of several other major intermediary pathways. The isoprenoid pathways, Chapters 3 & 4, describe genes downstream of mevalonate (Figs. 1.4 and 1.6) involved with isoprenylation that include the depletion of intracellular pools of geranylgeranyl pyrophosphate which in turn decreases the isoprenylation of the Rho GTPases RhoA and Rac1 (Zhong, et al., 2005). The present work observed that there are three Rho GTPases (*BEMI*, *GRR1* and *SSD1*) that interact with the statins. *BEMI* and *SSD1* deletion mutants are sensitive to all three statins.

Significantly, these genes regulate the kinase/phosphatase activity for which *BCK1* (mitogen-activated protein (MAP) kinase kinase kinase signalling pathway), and *SLT2* (PKC1-mediated signalling pathway) which also show a PE interaction with the statins (Chapter 4). These five PE interactions play an important role in cell growth where inhibition of Rho GTPases by statins, via decreased isoprenylation, leads to a significant enrichment in phenotypic suppression interactions via *GEM1*, *RHO5* consistent with previous studies (Kim, et al., 1994). These interactions highlight Rho activation via geranylgeranylation, suggesting that the inhibitory effects of statins have important interactions additional to inhibition of ergosterol synthesis (cholesterol in mammals).

7.3. Statin compensating genes

Along with *HMGI*, three other lipid biosynthesis genes interacted with all the statin drugs namely *ARV1*, *BTS1* and *OPI3*. *BTS1* as discussed in Chapters 3 & 4 is involved with the regulation of Hmg2p; *ARV1* is an important factor contributing to sterol storage and transport within the cell where *Δarv1* null mutants accumulate abnormal internalised unesterified sterols (Fei, et al., 2008) and *OPI3* catalyzes the last two steps in *de novo* phosphatidylcholine biosynthesis within the ER (Daum, et al., 1998). A recent study has proposed that in addition to sterol transport, *ARV1* may be involved in glycosylphosphatidylinositol biosynthesis (Morihisa and Taroh, 2009). Defects in phosphatidylcholine synthesis generally lead to disruptions in membrane structure and can cause structural as well as chemical imbalances in the membrane bilayers. This, coupled

with altered sterol levels as a result of statin treatment, can cause unwanted hydrophilic substances to enter the cell most of which would be excluded under normal conditions (McMaster, 2001). Thus, continuing the conclusion of the previous discussion section, statins in inhibiting primary sterol synthesis through HMG-CoA-reductases cause changes to the compensatory functions of *OPI3* (phospholipid synthesis) to *BTS1* with its effect on geranylgeranylation and to *ARV1* with its involvement in sterol/lipid transport. These three genes are good projects for further investigation as other cellular and environmental variables affecting them (e.g. individual gene expression differences or contraindicating drugs) could result in side effects.

7.4. Vesicular transport

The theme of compensating genes in statins action can be extended when considering membrane recycling processes. A strong pattern of gene-usage involving anterograde and retrograde vesicular transport emerges in response to eliminating *HMG1* and its genetic/chemical genetic interactions. It is likely such pathways are always part of a cellular homeostasis and become emphasised when stress such as gene deletion (or effective gene ablation by SMPs) is affected. Chapter 5 describes a number of genes that interact solely with statins + $\Delta hmg2$ Δxxx , which are involved in vesicular transport, including 2 out of 3 members (*GET1* and *GET2*) of the Golgi – ER trafficking (GET) complex. This complex mediates the insertion of tail anchored proteins into the ER membrane (Schuldiner, et al., 2005). These characteristic transmembrane proteins are found

throughout the secretory pathway, the nuclear envelope, peroxisomes and mitochondria (Wattenberg and Lithgow, 2001). They play important roles within the secretory pathway such as enabling vesicular traffic including many of the small peripheral membrane anchored proteins (SNAREs) that mediate fusion of secretory vesicles in secretory pathway events (Schuldiner, et al., 2008). Absence of *GET1/GET2* causes secretion of proteins with the HDEL ER retention marker instead of being returned by retrograde Golgi to ER transport (Schuldiner, et al., 2005). Though noted (Schuldiner, et al., 2005; Schuldiner, et al., 2008) deletion of any genes of the GET complex leads to a secretion phenotype similar to that seen in a *Kar2p* strain lacking the HDEL receptor, these authors did not specify a role in anterograde transport. The current results (Chapter 5) show that in the absence of *HMG2* coupled with inhibition of *Hmg1p* by statins, retrograde transport is also disrupted.

The genes *VPS51* and *VPS53* described as showing epistatic interactions with statins + *Δhmg2 Δxxx* in Ch 5, are integral components of the four-member Golgi associated retrograde protein (GARP) complex which is involved in retrograde transport from early endosomes to the late Golgi. Moreover, *TLG2*, a SNARE protein (described above) interacts with the GARP complex, which in turn facilitates vesicle fusion within the Trans Golgi Network (TGN). However, it has been described that these and other protein facilitators interact with specific Rab proteins (Conibear, et al., 2003), coupling membrane recognition with the activation of Rab GTPase which are inhibited by geranylgeranylation (Garza, et al., 2009b). These results extend the notion that genes involved in membrane recycling beyond the ER-Golgi step of the secretory pathway are also affected by

statins, as might be expected if cells are compensating for loss of viable membrane by recycling.

7.5. Other lipid synthesis genes

A lipid biosynthesis gene that showed interaction under all conditions described in Chapter 5 is *DGAT1*, an integral component in the *de novo* synthesis of TAG lipid droplet formation, a pool that also affects membrane trafficking within the cell (Petschnigg, et al., 2009). Relatedly, when the ER becomes stressed (such as the conditions presented in Chapters 4 & 5) lipid droplet formation increases. It is of interest that changes in lipid droplet dynamics have been associated with a number of pathological conditions including obesity, type 2 diabetes, fatty liver and atherosclerosis (Fei, et al., 2009).

7.6. The HRD – ubiquitin pathway

Although Hmg1p and Hmg2p are both structurally and enzymatically similar, differences exist in the way cells respond to these proteins and their cellular distribution and structure within the ER (Federovitch, et al., 2008). Furthermore, the Hmg1p protein is stable, whereas Hmg2p undergoes rapid HRD-mediated degradation via the ubiquitinone – proteasome pathway (Garza, et al., 2009a) pointing to dissimilar roles (with respect to the ubiquitinone – proteasome degradation pathway) requiring further analysis.

All the statins show interactions with *SPF1*, whose gene product is responsible for Ca^{2+} ion homeostasis in the ER and for the regulation of Hmg2p degradation in the ER (Cronin, et al., 2000). The interactions described in Chapter 4 also suggest *MID1* (and *CCH1* a voltage gated Ca^{2+} channel) regulates Hmg2p degradation functioning as a Ca^{2+} cation channel in the ER. These data are consistent with the observations of Cronin et al 2000 and suggest that Hmg2p degradation via the HRD – ubiquitin mediated pathway is regulated by Ca^{2+} signalling.

The ERAD pathway is tightly coupled with the HRD pathway responsible for the degradation on Hmg2p (Garza, et al., 2009a). If Hmg2p is perturbed by statins then it may become misfolded presenting as a target for this pathway. A summary of results discussed thus far is that when under *chemical genetic* perturbation, the sterol/lipid ratio alters the fluidity properties of the membrane initiating the unfolded protein response (Ron and Walter, 2007) for proteins like Hmh2p. In the UPR, the recognition of misfolded proteins by the transmembrane sensor Ire1p activates the transcription factor Hac1p which then in turn activates a distinct set of genes involved in UPR, ERAD and proteasome processes (Cox and Walter, 1996; Jonikas, et al., 2009). The involvement of UPR, hence ERAD and the proteasome, may be evidenced by *lovastatin* showing a PE interaction with *HAC1*. An investigation of the other statins at higher concentrations might also show involvement of *HAC1*.

7.7. Statins and quantitative traits

Most traits are complex made up of partial quantitative contributions of a number of genes as the QTL literature (e.g. Schadt and Lum, 2006) has shown.

Individuals show variation in the quantitative contributions of the component genes making up a trait. This perspective is useful in accounting for observations in Ch 3, 4, and 5 that detail enhancing or suppressing effects of genes in relation to statins, a perspective, that combined with the concept of *network drug effects* (Hopkins, 2008) allows an explanation of statin pleiotropy.

For example, in relation to the results of this thesis, an individual might have decreased or repressed *ARV1*, *BTS1* or *OPI3* expression as a heritable genetic trait (Schadt and Lum, 2006; Steinmetz, et al., 2002). Were this the case, therapeutic intervention with statins might cause symptoms of a deficiency because of these gene functions being unable to compensate for statins, even if these underlying traits were asymptomatic. Such an individual would most likely experience unwanted side effects should they take a statin drug. A number of specific hypotheses could follow from these suppositions just discussed that should provide fruitful avenues to follow in further investigation into the pleiotropic effects of statin drugs.

7.8. Overall conclusions

The aim of this thesis was to study the genetic networks surrounding important enzymes of sterol synthesis, regulation and inhibition by use of statin drugs in cells. This thesis elucidates the involvement of numerous genes pointing to key genes and processes which could not otherwise have been discerned.

A number of important points emerge from this work. Firstly, genetic interaction networks have been elucidated that are not necessarily an obvious consequence of statin effects and in fact are cryptic until “unmasking” as described in Chapter 5, such as in membrane retrograde transport that appears when *HMG1* enzyme is inhibited by statins in the absence of compensating *HMG2* enzyme.

Secondly, SGA analysis of the isoenzymes *HMG1* and *HMG2* showed some, but surprisingly little overlap in their genetic interactions supporting a view of independent roles of the two genes in addition to their known commonality in HMG-CoA reductase. The results of this dissertation strongly suggest that statin use targeting HMG CoA-reductase requires genes in multiple pathways acting as a network to maintain cellular homeostasis. From this point of view, statins would fit the description of “*network acting drugs*” as is now being discussed (Hopkins, 2008; Schadt, et al., 2009; Schadt and Lum, 2006).

\

Thirdly, strong evidence is presented showing involvement of genes acting within the ubiquitin – proteasome pathway. This coupled with the known mechanism of HRD degradation of Hmg2p leads to the suggestion of a role for Hmg2p in the initiation of the UPR.

Fourthly, when *HMG1* and its epistatically interacting genes are shut off (with null mutation) and *HMG2* is simultaneously shut off with a statin, it is apparent that the cell attempts to maintain membrane/lipid homeostasis via anterograde and retrograde transport mechanisms, including the mobilisation of lipid storage droplets.

7.9. Future directions

A number of possibilities are raised by this work which could be usefully further investigated. A potentially fruitful line of enquiry relates to the unknown genes showing similar GO enrichments to the known genes variously discussed.

Enrichment of ER/lipid synthesis genes in statin chemical genetic interactions suggests that genes displaying *unknown* functions, namely YGL081W, YDR541C, YLR346C and YPL272C belong to the same functional category. The genetic interaction function of these genes could be elucidated by SGA analysis, possibly leading to similar results as those described in Chapter 3, after which, the double mutants could be applied to statin drugs or even other drugs that are known to effect ergosterol synthesis in by different mechanisms (e.g. Nystatin).

This experiment could place any or all of YGL081W, YDR541C, YLR346C and YPL272C in ergosterol pathways or to others if they belong elsewhere.

The genes that show *phenotypic enhancement* interactions with all the statins (BTS1, ARV1, OPI3) along with those that show *phenotypic suppression* interactions (COX17 and MMM1) may underlie a complex phenotype of statin effects because they do not lie in any one specific biochemical pathway. Could they relate to side effects experienced by those taking statins because of known variations in the expression of these genes relating to known human genetic/metabolic defects or contraindicated drugs?

One way to resolve this question could involve searching relevant databases for homology of these genes with ones that are annotated as being involved in human diseases or for being the primary targets of other therapeutic drugs. One could also analyse complex traits by investigating whether the mRNAs for the specific genes above behave as a heritable quantitative traits (Mackay, et al., 2009; Steinmetz, et al., 2002). It is possible these genes could be responding variably in statin treated individuals. In a third approach, cells could be treated with statin and screened against drug libraries with the possibility of uncovering epistatically interacting drugs, which in turn may lead to lower dose and increased efficacy with respect to minimising side effects and a greater reduction in sterol levels. This concept could be extended to testing the United States Food and Drug Administration library of approved drugs for contraindications affecting expression of *BTS1*, *ARV1*, *OPI3*, *COX17* and *MMM1*.

As described in Chapter 5, when cells are deprived of sterol biosynthesis they appear to maintain sterol/lipid homeostasis by utilisation of the lipid storage droplets and membrane recycling. A compelling line of research would be to investigate mechanisms with high-throughput automated confocal microscopy (available in this laboratory), following a DGA1-GFP reporter gene. Subcellular location phenotypes are likely to be more sensitive and revealing than the simple growth assays described in most of this dissertation.

References

- Amerik, A. Y., Nowak, J., Swaminathan, S. and Hochstrasser, M. (2000). The Doa4 Deubiquitinating Enzyme Is Functionally Linked to the Vacuolar Protein-sorting and Endocytic Pathways. *Mol. Biol. Cell* **11**, 3365-3380.
- Ashburner, M., Ball, C. A., Blake, J. A., Botstein, D., Butler, H., Cherry, J. M., Davis, A. P., Dolinski, K., Dwight, S. S., Eppig, J. T., Harris, M. A., Hill, D. P., Issel-Tarver, L., Kasarskis, A., Lewis, S., Matese, J. C., Richardson, J. E., Ringwald, M., Rubin, G. M. and Sherlock, G. (2000). Gene Ontology: tool for the unification of biology. *Nat Genet* **25**, 25-29.
- Austin, M. A., Hutter, C. M., Zimmern, R. L. and Humphries, S. E. (2004). Familial Hypercholesterolemia and Coronary Heart Disease: A HuGE Association Review. *Am. J. Epidemiol.* **160**, 421-429.
- Bassett, D. E., Boguski, M. S., Spencer, F., Reeves, R., Kim, S.-h., Weaver, T. and Hieter, P. (1997). Genome cross-referencing and XREFdb: Implications for the identification and analysis of genes mutated in human disease. *Nat Genet* **15**, 339-344.
- Basson, M. E., Moore, R. L., O'Rear, J. and Rine, J. (1987). Identifying Mutations in Duplicated Functions in *Saccharomyces cerevisiae*: Recessive Mutations in HMG-CoA Reductase Genes. *Genetics* **117**, 645-655.

Basson, M. E., Thorsness, M., Finer-Moore, J., Stroud, R. M. and Rine, J. (1988).

Structural and functional conservation between yeast and human 3-hydroxy-3-methylglutaryl coenzyme A reductases, the rate-limiting enzyme of sterol biosynthesis. *Mol. Cell. Biol.* **8**, 3797-3808.

Basson, M. E., Thorsness, M. and Rine, J. (1986). *Saccharomyces cerevisiae*

contains two functional genes encoding 3-hydroxy-3-methylglutaryl-coenzyme A reductase. *Proceedings of the National Academy of Sciences of the United States of America* **83**, 5563-5567.

Bilodeau, P. S., Urbanowski, J. L., Winistorfer, S. C. and Piper, R. C. (2002). The

Vps27p-Hse1p complex binds ubiquitin and mediates endosomal protein sorting. *Nat Cell Biol* **4**, 534-539.

Blank, L., Kuepfer, L. and Sauer, U. (2005). Large-scale ¹³C-flux analysis

reveals mechanistic principles of metabolic network robustness to null mutations in yeast. *Genome Biology* **6**, R49.

Blank, N., Schiller, M., Krienke, S., Busse, F., Schatz, B., Ho, A. D., Kalden, J.

R. and Lorenz, H.-M. (2007). Atorvastatin Inhibits T Cell Activation through 3-Hydroxy-3-Methylglutaryl Coenzyme A Reductase without Decreasing Cholesterol Synthesis. *J Immunol* **179**, 3613-3621.

Bocking, T., Barrow, K. D., Netting, A. G., Chilcott, T. C., Coster, H. G. L. and

Hofer M (2000). Effects of a singlet oxygen on membrane sterols in the yeast *Saccharomyces cerevisiae*. *Eur. J. Biochem* **267**, 1607-1618.

- Boone, C., Bussey, H. and Andrews, B. J. (2007). Exploring genetic interactions and networks with yeast. *Nat Rev Genet* **8**, 437-449.
- Broome, S. (1991). Risk of fatal coronary heart disease in familial hypercholesterolaemia. Scientific Steering Committee on behalf of the Simon Broome Register Group. *BMJ* **303**, 893-896.
- Brostrom, C. O., Brostrom, M. A. and Kivie, M. (1997). Regulation of Translational Initiation during Cellular Responses to Stress, *Progress in Nucleic Acid Research and Molecular Biology*, Academic Press, pp. 79-125.
- Brown, M. and Goldstein, J. (1980). Multivalent feedback regulation of HMG CoA reductase, a control mechanism coordinating isoprenoid synthesis and cell growth. *J. Lipid Res.* **21**, 505-517.
- Chun, K. T., Bar-Nun, S. and Simoni, R. D. (1990). The regulated degradation of 3-hydroxy-3-methylglutaryl-CoA reductase requires a short-lived protein and occurs in the endoplasmic reticulum. *Journal of Biological Chemistry* **265**, 22004-22010.

Cline, M. S., Smoot, M., Cerami, E., Kuchinsky, A., Landys, N., Workman, C., Christmas, R., Avila-Campilo, I., Creech, M., Gross, B., Hanspers, K., Isserlin, R., Kelley, R., Killcoyne, S., Lotia, S., Maere, S., Morris, J., Ono, K., Pavlovic, V., Pico, A. R., Vailaya, A., Wang, P.-L., Adler, A., Conklin, B. R., Hood, L., Kuiper, M., Sander, C., Schmulevich, I., Schwikowski, B., Warner, G. J., Ideker, T. and Bader, G. D. (2007). Integration of biological networks and gene expression data using Cytoscape. *Nat. Protocols* **2**, 2366-2382.

Collins, S., Schuldiner, M., Krogan, N. and Weissman, J. (2006). A strategy for extracting and analyzing large-scale quantitative epistatic interaction data. *Genome Biology* **7**, R63.

Collins, S. R. HT Colony Grid Analyzer.

Conibear, E., Cleck, J. N. and Stevens, T. H. (2003). Vps51p Mediates the Association of the GARP (Vps52/53/54) Complex with the Late Golgi t-SNARE Tlg1p. *Mol. Biol. Cell* **14**, 1610-1623.

Cox, J. S. and Walter, P. (1996). A Novel Mechanism for Regulating Activity of a Transcription Factor That Controls the Unfolded Protein Response. *Cell* **87**, 391-404.

Cronin, S. R., Khoury, A., Ferry, D. K. and Hampton, R. Y. (2000). Regulation of Hmg-CoA Reductase Degradation Requires the P-Type Atpase Cod1p/Spflp. *J. Cell Biol.* **148**, 915-924.

- Crosas, B., Hanna, J., Kirkpatrick, D. S., Zhang, D. P., Tone, Y., Hathaway, Nathaniel A., Buecker, C., Leggett, D. S., Schmidt, M., King, R. W., Gygi, Steven P. and Finley, D. (2006). Ubiquitin Chains Are Remodeled at the Proteasome by Opposing Ubiquitin Ligase and Deubiquitinating Activities. *Cell* **127**, 1401-1413.
- Daum, G., Lees, N. D., Bard, M. and Dickson, R. (1998). Biochemistry, cell biology and molecular biology of lipids of *Saccharomyces cerevisiae*. *Yeast* **14**, 1471-1510.
- Daum, G., Tuller, G., Nemec, T., Hrastnik, C., Balliano, G., Cattell, L., Milla, P., Rocco, F., Conzelmann, A., Vionnet, C., Kelly, D. E., Kelly, S., Schweizer, E., Schüller, H.-J., Hojad, U., Greiner, E. and Finger, K. (1999). Systematic analysis of yeast strains with possible defects in lipid metabolism. *Yeast* **15**, 601-614.
- Dimster-Denk, D., Rine, J., Phillips, J., Scherer, S., Cundiff, P., DeBord, K., Gilliland, D., Hickman, S., Jarvis, A., Tong, L. and Ashby, M. (1999). Comprehensive evaluation of isoprenoid biosynthesis regulation in *Saccharomyces cerevisiae* utilizing the Genome Reporter Matrix(TM). *J. Lipid Res.* **40**, 850-860.
- Dykens, J. A. and Will, Y. (2007). The significance of mitochondrial toxicity testing in drug development. *Drug Discovery Today* **12**, 777-785.

- Eisenkolb, M., Zenzmaier, C., Leitner, E. and Schneider, R. (2002). A Specific Structural Requirement for Ergosterol in Long-chain Fatty Acid Synthesis Mutants Important for Maintaining Raft Domains in Yeast. *Mol. Biol. Cell* **13**, 4414-4428.
- Federovitch, C. M., Jones, Y. Z., Tong, A. H., Boone, C., Prinz, W. A. and Hampton, R. Y. (2008). Genetic and Structural Analysis of Hmg2p-induced Endoplasmic Reticulum Remodeling in *Saccharomyces cerevisiae*. *Mol. Biol. Cell* **19**, 4506-4520.
- Fei, W., Alfaro, G., Muthusamy, B. P., Klaassen, Z., Graham, T. R., Yang, H. and Beh, C. T. (2008). Genome-Wide analysis of sterol-lipid storage and trafficking in *Saccharomyces cerevisiae*. *Eukaryotic Cell* **7**, 401-414.
- Fei, W., Wang, H., Fu, X., Bielby, C. and Yang, H. (2009). Conditions of endoplasmic reticulum stress stimulate lipid droplet formation in *Saccharomyces cerevisiae*. *Biochemical Journal* **424**, 61-67.
- Foury, F. (1997). Human genetic diseases: a cross-talk between man and yeast. *Gene* **195**, 1-10.
- Fuhrmans, V., Winslow, R. and Harris, G. Bayer recall spurs Europe to wide review. *Wall Street Journal*, August 10, 2001, A3.
- Furberg, C. and Pitt, B. (2001). Withdrawal of cerivastatin from the world market. *Current Controlled Trials in Cardiovascular Medicine* **2**, 205 - 207.

- Garza, R. M., Sato, B. K. and Hampton, R. Y. (2009a). In Vitro Analysis of Hrd1p-mediated Retrotranslocation of Its Multispanning Membrane Substrate 3-Hydroxy-3-methylglutaryl (HMG)-CoA Reductase. *Journal of Biological Chemistry* **284**, 14710-14722.
- Garza, R. M., Tran, P. N. and Hampton, R. Y. (2009b). Geranylgeranyl Pyrophosphate Is a Potent Regulator of HRD-dependent 3-Hydroxy-3-methylglutaryl-CoA Reductase Degradation in Yeast. *Journal of Biological Chemistry* **284**, 35368-35380.
- Gene Ontology Consortium (2004). The Gene Ontology (GO) database and informatics resource. *Nucl. Acids Res.* **32**, D258-261.
- Gessner, M. and Schmitt, A. (1996). Use of Solid-Phase Extraction To Determine Ergosterol Concentrations in Plant Tissue Colonized by Fungi. *Applied Environmental Microbiology* **62**, 415-419.
- Gietz, R. D. and Schiestl, R. H. (2007). Quick and easy yeast transformation using the LiAc/SS carrier DNA/PEG method. *Nat. Protocols* **2**, 35-37.
- Gilles Labbe, D. P. B. F. (2008). Drug-induced liver injury through mitochondrial dysfunction: mechanisms and detection during preclinical safety studies. *Fundamental & Clinical Pharmacology* **22**, 335-353.
- Goldstein, J. L. and Brown, M. S. (1990). Regulation of the mevalonate pathway. *Nature* **343**, 425-430.

- Gosalakkal, J. A. and Kamoji, V. (2008). Reye Syndrome and Reye-Like Syndrome. *Pediatric Neurology* **39**, 198-200.
- Graham, L. A. and Stevens, T. H. (1999). Assembly of the Yeast Vacuolar Proton-Translocating ATPase. *Journal of Bioenergetics and Biomembranes* **31**, 39-47.
- Hampton, R. Y. and Rine, J. (1994). Regulated degradation of HMG-CoA reductase, an integral membrane protein of the endoplasmic reticulum, in yeast. *J. Cell Biol.* **125**, 299-312.
- Hanna, J., Leggett, D. S. and Finley, D. (2003). Ubiquitin Depletion as a Key Mediator of Toxicity by Translational Inhibitors. *Mol. Cell. Biol.* **23**, 9251-9261.
- Henneberry, A. L. and Sturley, S. L. (2005). Sterol homeostasis in the budding yeast, *Saccharomyces cerevisiae*. *Seminars in Cell & Developmental Biology* **16**, 155-161.
- Hillenmeyer, M. E., Fung, E., Wildenhain, J., Pierce, S. E., Hoon, S., Lee, W., Proctor, M., St.Onge, R. P., Tyers, M., Koller, D., Altman, R. B., Davis, R. W., Nislow, C. and Giaever, G. (2008). The Chemical Genomic Portrait of Yeast: Uncovering a Phenotype for All Genes. *Science* **320**, 362-365.
- Hopkins, A. L. (2008). Network pharmacology: the next paradigm in drug discovery. *Nat Chem Biol* **4**, 682-690.

- Huang, S. (2002). Rational drug discovery: what can we learn from regulatory networks? *Drug Discovery Today* **7**, s163-s169.
- Istvan, E. S. and Deisenhofer, J. (2001). Structural Mechanism for Statin Inhibition of HMG-CoA Reductase. *Science* **292**, 1160-1164.
- Jedlickova, L., Gadas, D., Havlově, P. and Havel, J. (2008). Determination of Ergosterol Levels in Barley and Malt Varieties in the Czech Republic via HPLC. *Journal of Agricultural and Food Chemistry* **56**, 4092-4095.
- Jiang, Y., Proteau, P., Poulter, D. and Ferro-Novick, S. (1995). BTS1 Encodes a Geranylgeranyl Diphosphate Synthase in *Saccharomyces cerevisiae*. *Journal of Biological Chemistry* **270**, 21793-21799.
- Jonikas, M. C., Collins, S. R., Denic, V., Oh, E., Quan, E. M., Schmid, V., Weibezahn, J., Schwappach, B., Walter, P., Weissman, J. S. and Schuldiner, M. (2009). Comprehensive Characterization of Genes Required for Protein Folding in the Endoplasmic Reticulum. *Science* **323**, 1693-1697.
- Jungmann, J., Rayner, J. C. and Munro, S. (1999). The *Saccharomyces cerevisiae* Protein Mnn10p/Bed1p Is a Subunit of a Golgi Mannosyltransferase Complex. *Journal of Biological Chemistry* **274**, 6579-6585.

- Kajiwara, K., Watanabe, R., Pichler, H., Ihara, K., Murakami, S., Riezman, H. and Funato, K. (2008). Yeast ARV1 Is Required for Efficient Delivery of an Early GPI Intermediate to the First Mannosyltransferase during GPI Assembly and Controls Lipid Flow from the Endoplasmic Reticulum. *Mol. Biol. Cell* **19**, 2069-2082.
- Kaufmann, P., Török, M., Zahno, A., Waldhauser, K., Brecht, K. and Krähenbühl, S. (2006). Toxicity of statins on rat skeletal muscle mitochondria. *Cellular and Molecular Life Sciences (CMLS)* **63**, 2415-2425.
- Kim, Y., Francisco, L., Chen, G., Marcotte, E. and Chan, C. (1994). Control of cellular morphogenesis by the Ip12/Bem2 GTPase-activating protein: possible role of protein phosphorylation. *J. Cell Biol.* **127**, 1381-1394.
- Kornmann, B., Currie, E., Collins, S. R., Schuldiner, M., Nunnari, J., Weissman, J. S. and Walter, P. (2009). An ER-Mitochondria Tethering Complex Revealed by a Synthetic Biology Screen. *Science* **325**, 477-481.
- Kromer, A. and Moosmann, B. (2009). Statin-induced liver injury involves cross-talk between cholesterol and selenoprotein biosynthetic pathways. *Mol Pharmacol*, mol.108.053678.
- Lamacka, M. and Sajbidor, J. (1997). Ergosterol determination in *Saccharomyces cerevisiae*. Comparison of different methods. *Biotechnology Techniques* **11**, 723-725.

- Laufs, U., La Fata, V., Plutzky, J. and Liao, J. K. (1998). Upregulation of Endothelial Nitric Oxide Synthase by HMG CoA Reductase Inhibitors. *Circulation* **97**, 1129-1135.
- Lees, N., Skaggs, B., Kirsch, D. and Bard, M. (1995). Cloning of the late genes in the ergosterol biosynthetic pathway of *Saccharomyces cerevisiae*—A review. *Lipids* **30**, 221-226.
- Leonhard, K., Stiegler, A., Neupert, W. and Langer, T. (1999). Chaperone-like activity of the AAA domain of the yeast Yme1 AAA protease. *Nature* **398**, 348-351.
- Liao, J. K. and Laufs, U. (2005). Pleiotropic effects of statins. *Annual Review of Pharmacology and Toxicology* **45**, 89-118.
- Locke, E. G., Bonilla, M., Liang, L., Takita, Y. and Cunningham, K. W. (2000). A Homolog of Voltage-Gated Ca²⁺ Channels Stimulated by Depletion of Secretory Ca²⁺ in Yeast. *Mol. Cell. Biol.* **20**, 6686-6694.
- Loertscher, J., Larson, L. L., Matson, C. K., Parrish, M. L., Felthouser, A., Sturm, A., Tachibana, C., Bard, M. and Wright, R. (2006). Endoplasmic Reticulum-Associated Degradation Is Required for Cold Adaptation and Regulation of Sterol Biosynthesis in the Yeast *Saccharomyces cerevisiae*. *Eukaryotic Cell* **5**, 712-722.

- Lorenz, R. T. and Parks, L. W. (1990). Effects of lovastatin (mevinolin) on sterol levels and on activity of azoles in *Saccharomyces cerevisiae*. *Antimicrob. Agents Chemother.* **34**, 1660-1665.
- Maass, K., Fischer, M. A., Seiler, M., Temmerman, K., Nickel, W. and Seedorf, M. (2009). A signal comprising a basic cluster and an amphipathic {alpha}-helix interacts with lipids and is required for the transport of Ist2 to the yeast cortical ER. *J Cell Sci* **122**, 625-635.
- Mackay, T. F. C., Stone, E. A. and Ayroles, J. F. (2009). The genetics of quantitative traits: challenges and prospects. *Nat Rev Genet* **10**, 565-577.
- Maere, S., Heymans, K. and Kuiper, M. (2005). BiNGO: a Cytoscape plugin to assess overrepresentation of Gene Ontology categories in Biological Networks. *Bioinformatics* **21**, 3448-3449.
- McMaster, C. R. (2001). Lipid metabolism and vesicle trafficking: More than just greasing the transport machinery. *Biochemistry and Cell Biology* **79**, 681-692.
- MOH (2003). NZ health stratigy - Cardiovascular Disease.
- Morihisa, F. and Taroh, K. (2009). Structural remodeling of GPI anchors during biosynthesis and after attachment to proteins. *FEBS letters*.

- Musso, G., Costanzo, M., Huangfu, M., Smith, A. M., Paw, J., San Luis, B.-J., Boone, C., Giaever, G., Nislow, C., Emili, A. and Zhang, Z. (2008). The extensive and condition-dependent nature of epistasis among whole-genome duplicates in yeast. *Genome Research* **18**, 1092-1099.
- Nikoloff, D. M. and Henry, S. A. (2003). Genetic Analysis of Yeast Phospholipid Biosynthesis. *Annual Review of Genetics* **25**, 559-559.
- Otte, S., Belden, W. J., Heidtman, M., Liu, J., Jensen, O. N. and Barlowe, C. (2001). Erv41p and Erv46p: New Components of Copii Vesicles Involved in Transport between the ER and Golgi Complex. *J. Cell Biol.* **152**, 503-518.
- Parsons, A. B., Brost, R. L., Ding, H., Li, Z., Zhang, C., Sheikh, B., Brown, G. W., Kane, P. M., Hughes, T. R. and Boone, C. (2004). Integration of chemical-genetic and genetic interaction data links bioactive compounds to cellular target pathways. *Nat Biotech* **22**, 62-69.
- Parsons, A. B., Lopez, A., Givoni, I. E., Williams, D. E., Gray, C. A., Porter, J., Chua, G., Sopko, R., Brost, R. L., Ho, C.-H., Wang, J., Ketela, T., Brenner, C., Brill, J. A., Fernandez, G. E., Lorenz, T. C., Payne, G. S., Ishihara, S., Ohya, Y., Andrews, B., Hughes, T. R., Frey, B. J., Graham, T. R., Andersen, R. J. and Boone, C. (2006). Exploring the Mode-of-Action of Bioactive Compounds by Chemical-Genetic Profiling in Yeast. *Cell* **126**, 611-625.

- Petschnigg, J., Wolinski, H., Kolb, D., Zellnig, G. n., Kurat, C. F., Natter, K. and Kohlwein, S. D. (2009). Good Fat, Essential Cellular Requirements for Triacylglycerol Synthesis to Maintain Membrane Homeostasis in Yeast. *Journal of Biological Chemistry* **284**, 30981-30993.
- Phillips, P. C. (1998). The Language of Gene Interaction. *Genetics* **149**, 1167-1171.
- Quinzii, C., Naini, A., Salviati, L., Trevisson, E., Navas, P., DiMauro, S. and Hirano, M. (2006). A Mutation in Para-Hydroxybenzoate-Polyprenyl Transferase (COQ2) Causes Primary Coenzyme Q10 Deficiency. *The American Journal of Human Genetics* **78**, 345-349.
- Rauniyar, J. T. and Atkinson, P. H. (2007, unpublished). Statin chemical genetic interactions in *Saccharomyces cerevisiae* School of Biological Sciences, Victoria University of Wellington.
- Ren, J., Pashkova, N., Winistorfer, S. and Piper, R. C. (2008). DOA1/UFD3 Plays a Role in Sorting Ubiquitinated Membrane Proteins into Multivesicular Bodies. *Journal of Biological Chemistry* **283**, 21599-21611.
- Ron, D. and Walter, P. (2007). Signal integration in the endoplasmic reticulum unfolded protein response. *Nat Rev Mol Cell Biol* **8**, 519-529.

- Santiago, T. C. and Mamoun, C. B. (2003). Genome Expression Analysis in Yeast Reveals Novel Transcriptional Regulation by Inositol and Choline and New Regulatory Functions for Opi1p, Ino2p, and Ino4p. *Journal of Biological Chemistry* **278**, 38723-38730.
- Scannell, D. R., Frank, A. C., Conant, G. C., Byrne, K. P., Woolfit, M. and Wolfe, K. H. (2007). Independent sorting-out of thousands of duplicated gene pairs in two yeast species descended from a whole-genome duplication. *Proceedings of the National Academy of Sciences of the United States of America* **104**, 8397-8402.
- Schachter, M. (2005). Chemical, pharmacokinetic and pharmacodynamic properties of statins: an update. *Fundamental & Clinical Pharmacology* **19**, 117-125.
- Schadt, E. E., Friend, S. H. and Shaywitz, D. A. (2009). A network view of disease and compound screening. *Nat Rev Drug Discov* **8**, 286-295.
- Schadt, E. E. and Lum, P. Y. (2006). Thematic review series: Systems Biology Approaches to Metabolic and Cardiovascular Disorders. Reverse engineering gene networks to identify key drivers of complex disease phenotypes. *J. Lipid Res.* **47**, 2601-2613.
- Schekman, R. (2002). SEC mutants and the secretory apparatus. *Nat Med* **8**, 1055-1058.

- Schenker, N., and Gentleman, J. F. (2001). On Judging the Significance of Differences by Examining the Overlap between Confidence Intervals, . *The American Statistician* **55**, 182-186.
- Schuldiner, M., Collins, S., Thompson, N., Denic, V., Bhamidipati, A., Punna, T., Ihmels, J., Andrews, B., Boone, C. and Greenblatt, J. (2005). Exploration of the function and organization of the yeast early secretory pathway through an epistatic miniarray profile. *Cell* **123**, 507 - 519.
- Schuldiner, M., Metz, J., Schmid, V., Denic, V., Rakwalska, M., Schmitt, H. D., Schwappach, B. and Weissman, J. S. (2008). The GET Complex Mediates Insertion of Tail-Anchored Proteins into the ER Membrane. *Cell* **134**, 634-645.
- Schulz, T. A. and Prinz, W. A. (2007). Sterol transport in yeast and the oxysterol binding protein homologue (OSH) family. *Biochimica et Biophysica Acta (BBA) - Molecular and Cell Biology of Lipids* **1771**, 769-780.
- SGD (2009). *Saccharomyces* Genome Database.
- Sheikh, M. S. and Fornace, A. J. (1999). Regulation of translation initiation following stress
Nature Oncogene **18**, 6121-6128.
- Silverman, D. W. (1990). Density Estimation of for statistics and Data Analysis, Chapman and Hall.

- Siniosoglou, S. and Pelham, H. R. B. (2002). Vps51p Links the VFT Complex to the SNARE Tlg1p. *Journal of Biological Chemistry* **277**, 48318-48324.
- Smith, S. J., Crowley, J. H. and Parks, L. W. (1996). Transcriptional regulation by ergosterol in the yeast *Saccharomyces cerevisiae*. *Mol. Cell. Biol.* **16**, 5427-5432.
- Sorger, D. and Daum, G. (2002). Synthesis of Triacylglycerols by the Acyl-Coenzyme A:Diacyl-Glycerol Acyltransferase Dga1p in Lipid Particles of the Yeast *Saccharomyces cerevisiae*. *J. Bacteriol.* **184**, 519-524.
- Steinmetz, L. M., Sinha, H., Richards, D. R., Spiegelman, J. I., Oefner, P. J., McCusker, J. H. and Davis, R. W. (2002). Dissecting the architecture of a quantitative trait locus in yeast. *Nature* **416**, 326-330.
- Sturley, S. L. (2000). Conservation of eukaryotic sterol homeostasis: new insights from studies in budding yeast. *Biochimica et Biophysica Acta (BBA) - Molecular and Cell Biology of Lipids* **1529**, 155-163.
- Tong, A. H. and Boone, C. (2005). Synthetic Genetic Array Analysis in *Saccharomyces cerevisiae*, *Yeast Protocols*, Humana Press, pp. 171-191.
- Tong, A. H. Y., Evangelista, M., Parsons, A. B., Xu, H., Bader, G. D., Page, N., Robinson, M., Raghizadeh, S., Hogue, C. W. V., Bussey, H., Andrews, B., Tyers, M. and Boone, C. (2001). Systematic Genetic Analysis with Ordered Arrays of Yeast Deletion Mutants. *Science* **294**, 2364-2368.

Tong, A. H. Y., Lesage, G., Bader, G. D., Ding, H., Xu, H., Xin, X., Young, J., Berriz, G. F., Brost, R. L., Chang, M., Chen, Y., Cheng, X., Chua, G., Friesen, H., Goldberg, D. S., Haynes, J., Humphries, C., He, G., Hussein, S., Ke, L., Krogan, N., Li, Z., Levinson, J. N., Lu, H., Menard, P., Munyana, C., Parsons, A. B., Ryan, O., Tonikian, R., Roberts, T., Sdicu, A.-M., Shapiro, J., Sheikh, B., Suter, B., Wong, S. L., Zhang, L. V., Zhu, H., Burd, C. G., Munro, S., Sander, C., Rine, J., Greenblatt, J., Peter, M., Bretscher, A., Bell, G., Roth, F. P., Brown, G. W., Andrews, B., Bussey, H. and Boone, C. (2004). Global Mapping of the Yeast Genetic Interaction Network. *Science* **303**, 808-813.

Tuffs, A. (2001). Bayer faces potential fine over cholesterol lowering drug. *BMJ* **323**, 415.

Turi, T. G. and Loper, J. C. (1992). Multiple regulatory elements control expression of the gene encoding the *Saccharomyces cerevisiae* cytochrome P450, lanosterol 14 alpha-demethylase (ERG11). *Journal of Biological Chemistry* **267**, 2046-2056.

Van Aelst, L. and Dae Souza-Schorey, C. (1997). Rho GTPases and signaling networks. *Genes & Development* **11**, 2295-2322.

Veen, M. and Lang, C. (2005). Interactions of the ergosterol biosynthetic pathway with other lipid pathways. *Biochem. Soc. Trans.* **33**, 1178-1181.

Wattenberg, B. and Lithgow, T. (2001). Targeting of C-Terminal (Tail)-Anchored Proteins: Understanding how Cytoplasmic Activities are Anchored to Intracellular Membranes. *Traffic* **2**, 66-71.

Weitz-Schmidt, G., Welzenbach, K., Brinkmann, V., Kamata, T., Kallen, J., Bruns, C., Cottens, S., Takada, Y. and Hommel, U. (2001). Statins selectively inhibit leukocyte function antigen-1 by binding to a novel regulatory integrin site. *Nat Med* **7**, 687-692.

Welihinda, A. A., Tirasophon, W., Green, S. R. and Kaufman, R. J. (1997). Gene induction in response to unfolded protein in the endoplasmic reticulum is mediated through Ire1p kinase interaction with a transcriptional coactivator complex containing Ada5p. *Proceedings of the National Academy of Sciences of the United States of America* **94**, 4289-4294.

White, L. W. (1972). Feedback Regulation of Cholesterol Biosynthesis: Studies With Cholestyramine. *Circ Res* **31**, 899-907.

WHO (2001). World Health Organisation, major causes of death, World Health organisation.

Winzeler, E. A., Shoemaker, D. D., Astromoff, A., Liang, H., Anderson, K., Andre, B., Bangham, R., Benito, R., Boeke, J. D., Bussey, H., Chu, A. M., Connelly, C., Davis, K., Dietrich, F., Dow, S. W., El Bakkoury, M., Foury, F., ccedil, oise, Friend, S. H., Gentalen, E., Giaever, G., Hegemann, J. H., Jones, T., Laub, M., Liao, H., Liebundguth, N., Lockhart, D. J., Lucau-Danila, A., Lussier, M., M'Rabet, N., Menard, P., Mittmann, M., Pai, C., Rebischung, C., Revuelta, J. L., Riles, L., Roberts, C. J., Ross-MacDonald, P., Scherens, B., Snyder, M., Sookhai-Mahadeo, S., Storms, R. K., eacute, ronneau, S., Voet, M., Volckaert, G., Ward, T. R., Wysocki, R., Yen, G. S., Yu, K., Zimmermann, K., Philippsen, P., Johnston, M. and Davis, R. W. (1999). Functional Characterization of the *S. cerevisiae* Genome by Gene Deletion and Parallel Analysis. *Science* **285**, 901-906.

Yoshida, M., Sawada, T., Ishii, H., Gerszten, R. E., Rosenzweig, A., Gimbrone, M. A., Jr, Yasukochi, Y. and Numano, F. (2001). HMG-CoA Reductase Inhibitor Modulates Monocyte-Endothelial Cell Interaction Under Physiological Flow Conditions In Vitro : Involvement of Rho GTPase-Dependent Mechanism. *Arterioscler Thromb Vasc Biol* **21**, 1165-1171.

Yuan, J.-P., Kuang, H.-C., Wang, J.-H. and Liu, X. (2008). Evaluation of ergosterol and its esters in the pileus, gill, and stipe tissues of agaric fungi and their relative changes in the comminuted fungal tissues. *Applied Microbiology and Biotechnology* **80**, 459-465.

- Yusuf, S., Reddy, S., Ounpuu, S. and Anand, S. (2001). Global Burden of Cardiovascular Diseases: Part II: Variations in Cardiovascular Disease by Specific Ethnic Groups and Geographic Regions and Prevention Strategies. *Circulation* **104**, 2855-2864.
- Zehmer, J. K., Bartz, R., Liu, P. and Anderson, R. G. W. (2008). Identification of a novel N-terminal hydrophobic sequence that targets proteins to lipid droplets. *J Cell Sci* **121**, 1852-1860.
- Zhong, W. B., Liang, Y. C., Wang, C. Y., Chang, T. C. and Lee, W. S. (2005). Lovastatin suppresses invasiveness of anaplastic thyroid cancer cells by inhibiting Rho geranylgeranylation and RhoA/ROCK signaling. *Endocr Relat Cancer* **12**, 615-629.
- Zhou, Q., Zhang, L., Fu, X.-Q. and Chen, G.-Q. (2002). Quantitation of yeast ceramides using high-performance liquid chromatography-evaporative light-scattering detection. *Journal of Chromatography B* **780**, 161-169.

Appendix 1 Media and components

YPD (Agar)

Distilled Water	1000mL
Yeast extract (BD)	10g
Peptone (BD)	20g
Adenine (sigma)	0.12g
Agar (Invitrogen)	20g
40% Glucose (sigma)	50mL

Autoclave (121°C for 22 minutes) and cool to 65°C, before adding glucose and antibiotics (YPD broth is prepared as above without the addition of agar).

SD complete (Agar)

Distilled Water	1000mL
Yeast nitrogen base (BD)	1.7g
w/o amino acids or ammonium sulphate	
MSG (BDH)	1g
Amino acid (sigma) mixture to suit	2g
Agar (BD)	20g
40% Glucose (Sigma)	50mL

Autoclave and cool to 65°C, add glucose and antibiotics if needed

Enriched Sporulation (Agar)

Potassium Acetate	10g
Yeast extract	1g
Glucose	0.5g
Amino acid supplement (His/Leu/Lys/Ura)	0.1g
Agar	20g

Antibiotics Stock Working

ClonNat	100mg/mL in H ₂ O	100µg/mL
G418	200mg/mL in H ₂ O	200µg/mL
Canavanine	50mg/mL in H ₂ O	50µg/mL
Thialysine	50mg/mL in H ₂ O	50µg/mL

Appendix 2: Ergosterol quantification

data

Strain/dilution	Units mAU* (raw)	adjusted mAU*	Ergosterol content ng/mL	Dry weight (g/m)	ergosterol (mg)/gram dry yeast
BY4741					
10 in 5ml	1326	1326	0.012874	0.04	1.609203875
10 in 10ml	186.34	186.34	0.00395	0.026	0.759600084
10 in 10ml	337.054	337.054	0.006771	0.029	1.167497829
50 in 10ml	2027	2027	0.019435	0.21	0.462749005
100 in 10ml	1189.44	1189.44	0.022729	0.24	0.473526865
100 in 10ml	6604	6604	0.061356	0.34	0.902300797
400 in 10ml	902.6	18052	0.16944	1.12	0.75642919
400 in 10ml	342.33	20539.8	0.192728	1.12	0.860391092
800 in 20ml	1887.1	37742	0.353752	2.4	0.736982628
800 in 20ml	735.4	44124	0.413491	2.4	0.86144049
ERG6					
10 in 10ml	303	303	0.003298	0.06	0.274805766
10 in 10ml	86.92	86.92	0.002089	0.02	0.522161378
10 in 10ml	50.46	50.46	0.001406	0.025	0.281213142
50 in 10ml	1128	1128	0.01102	0.17	0.324124089
100 in 10ml	4090	4090	0.038747	0.34	0.569801664
100 in 10ml	1100.89	1100.89	0.021072	0.29	0.363301991
100 in 10ml	1594.97	1594.97	0.030321	0.28	0.541452709
800 in 10ml 1:10	3401	34010	0.318818	2.52	0.632574711

Strain/dilution	Units mAU* (raw)	adjusted mAU*	Ergosterol content mg/mL	Dry weight (gm)	ergosterol (mg)/gram dry yeast
BY4743					
400 in 10ml 1:10	1101.2	22024	0.206621	1.43	0.72245002
800 in 10ml 1:30	402.6	24156	0.226578	1.43	0.792229534
800 in 10ml 1:10	2712.4	54248	0.508259	2.63	0.966271526
800 in 20ml 1:10	1058.5	42340	0.396792	2.97	0.66800001
800 in 200ml 1:30	408	48960	0.45876	2.97	0.772322589
BY7092					
400 in 20 mL 1:5	2112	21120	0.198159	0.94	1.054035443
400 in 20 ml 1:5	1065.61	21312.2	0.199958	1.065	0.938768936
400 in 20 ml 1:5	1321.79	26435.8	0.247918	1.2	1.032992059
mel1					
400 in 20 mL 1:5	1861	18610	0.174663	1.61	0.54243289
400 in 20 ml 1:5	1300.16	26003.2	0.243869	1.45	0.840956448
400 in 20 ml 1:5	469.8	9396	0.088414	1.18	0.374636481
mel2r					
400 in 10 mL 1:5	860	8600	0.080963	1.59	0.254601003
400 in 20 ml 1:5	934.5	18690	0.175412	1.64	0.534793426
400 in 20 ml 1:5	878.06	17561.2	0.164846	1.65	0.499533101

Table A.1 Ergosterol quantification data analysis

Table B.1: Atorvastatin + Δ hmg1 Δ xxx PE interactions

YMR003W	AIM34	Protein of unknown function; GFP-fusion protein localizes to the mitochondria; null mutant is viable and displays reduced frequency of mitochondrial genome loss
YNR041C	COQ2	Para hydroxybenzoate: polyprenyl transferase, catalyzes the second step in ubiquinone (coenzyme Q) biosynthesis
YOR245C	DGA1	Diacylglycerol acyltransferase, catalyzes the terminal step of triacylglycerol (TAG) formation, acylates diacylglycerol using acyl-CoA as an acyl donor, localized to lipid particles
YKL213C	DOA1	WD repeat protein required for ubiquitin-mediated protein degradation, forms complex with Cdc48p, plays a role in controlling cellular ubiquitin concentration; also promotes efficient NHEJ in postdiauxic/stationary phase
YBL047C	EDE1	Key endocytic protein involved in a network of interactions with other endocytic proteins, binds membranes in a ubiquitin-dependent manner, may also bind ubiquitinated membrane-associated proteins
YFR019W	FAB1	1-phosphatidylinositol-3-phosphate 5-kinase; vacuolar membrane kinase that generates phosphatidylinositol (3,5)P ₂ , which is involved in vacuolar sorting and homeostasis
YDR508C	GNP1	High-affinity glutamine permease, also transports Leu, Ser, Thr, Cys, Met and Asn; expression is fully dependent on Grr1p and modulated by the Ssy1p-Ptr3p-Ssy5p (SPS) sensor of extracellular amino acids
YJL101C	GSH1	Gamma glutamylcysteine synthetase catalyzes the first step in glutathione (GSH) biosynthesis; expression induced by oxidants, cadmium, and mercury
YOL095C	HMI1	Mitochondrial inner membrane localized ATP-dependent DNA helicase, required for the maintenance of the mitochondrial genome; not required for mitochondrial transcription; has homology to E. coli helicase uvrD
YCR071C	IMG2	Mitochondrial ribosomal protein of the small subunit
YOL081W	IRA2	GTPase-activating protein that negatively regulates RAS by converting it from the GTP- to the GDP-bound inactive form, required for reducing cAMP levels under nutrient limiting conditions, has similarity to Ira1p and human neurofibromin
YML068W	ITT1	Protein that modulates the efficiency of translation termination, interacts with translation release factors eRF1 (Sup45p) and eRF3 (Sup35p) in vitro, contains a zinc finger domain characteristic of the TRIAD class of proteins
YIL027C	KRE27	Member of a transmembrane complex required for efficient folding of proteins in the ER; null mutant displays induction of the unfolded protein response, and also shows K1 killer toxin resistance
YOR360C	PDE2	High-affinity cyclic AMP phosphodiesterase, component of the cAMP-dependent protein kinase signaling system, protects the cell from extracellular cAMP, contains readthrough motif surrounding termination codon
YML016C	PPZ1	Serine/threonine protein phosphatase Z, isoform of Ppz2p; involved in regulation of potassium transport, which affects osmotic stability, cell cycle progression, and halotolerance

YBR260C	RGD1	GTPase-activating protein (RhoGAP) for Rho3p and Rho4p, possibly involved in control of actin cytoskeleton organization
YPL089C	RLM1	MADS-box transcription factor, component of the protein kinase C-mediated MAP kinase pathway involved in the maintenance of cell integrity; phosphorylated and activated by the MAP-kinase Slt2p
YOR312C	RPL20B	Protein component of the large (60S) ribosomal subunit, nearly identical to Rpl20Ap and has similarity to rat L18a ribosomal protein
YBR171W	SEC66	Non-essential subunit of Sec63 complex (Sec63p, Sec62p, Sec66p and Sec72p); with Sec61 complex, Kar2p/BiP and Lhs1p forms a channel competent for SRP-dependent and post-translational SRP-independent protein targeting and import into the ER
YBL061C	SKT5	Activator of Chs3p (chitin synthase III), recruits Chs3p to the bud neck via interaction with Bni4p; has similarity to Shc1p, which activates Chs3p during sporulation
YBL007C	SLA1	Cytoskeletal protein binding protein required for assembly of the cortical actin cytoskeleton; interacts with proteins regulating actin dynamics and proteins required for endocytosis; found in the nucleus and cell cortex; has 3 SH3 domains
YPL057C	SUR1	Probable catalytic subunit of a mannosylinositol phosphorylceramide (MIPC) synthase, forms a complex with probable regulatory subunit Csg2p; function in sphingolipid biosynthesis is overlapping with that of Csh1p
YKR059W	TIF1	Translation initiation factor eIF4A, identical to Tif2p; DEA(D/H)-box RNA helicase that couples ATPase activity to RNA binding and unwinding; forms a dumbbell structure of two compact domains connected by a linker; interacts with eIF4G
YBR082C	UBC4	Ubiquitin-conjugating enzyme (E2), mediates degradation of abnormal or excess proteins, including calmodulin and histone H3; interacts with many SCF ubiquitin protein ligases; component of the cellular stress response
YLL039C	UBI4	Ubiquitin, becomes conjugated to proteins, marking them for selective degradation via the ubiquitin-26S proteasome system; essential for the cellular stress response; encoded as a polyubiquitin precursor comprised of 5 head-to-tail repeats
YFR010W	UBP6	Ubiquitin-specific protease situated in the base subcomplex of the 26S proteasome, releases free ubiquitin from branched polyubiquitin chains; works in opposition to polyubiquitin elongation activity of Hul5p
YOR106W	VAM3	Syntaxin-related protein required for vacuolar assembly; functions with Vam7p in vacuolar protein trafficking; member of the syntaxin family of proteins
YOR089C	VPS21	GTPase required for transport during endocytosis and for correct sorting of vacuolar hydrolases; localized in endocytic intermediates; detected in mitochondria; geranylgeranylation required for membrane association; mammalian Rab5 homolog
YNR006W	VPS27	Endosomal protein that forms a complex with Hse1p; required for recycling Golgi proteins, forming luminal membranes and sorting ubiquitinated proteins destined for degradation; has Ubiquitin Interaction Motifs which bind ubiquitin (Ubi4p)

YPR173C	VPS4	AAA-ATPase involved in multivesicular body (MVB) protein sorting, ATP-bound Vps4p localizes to endosomes and catalyzes ESCRT-III disassembly and membrane release; ATPase activity is activated by Vta1p; regulates cellular sterol metabolism
YML097C	VPS9	A guanine nucleotide exchange factor involved in vesicle-mediated vacuolar protein transport; specifically stimulates the intrinsic guanine nucleotide exchange activity of Vps21p/Rab5: similar to mammalian ras inhibitors; binds ubiquitin
YOR043W	WHI2	Protein required, with binding partner Psr1p, for full activation of the general stress response, possibly through Msn2p dephosphorylation; regulates growth during the diauxic shift; negative regulator of G1 cyclin expression
YOR083W	WHI5	Repressor of G1 transcription that binds to SCB binding factor (SBF) at SCB target promoters in early G1; phosphorylation of Whi5p by the CDK, Cln3p/Cdc28p relieves repression and promoter binding by Whi5; periodically expressed in G1
YMR294W-A		Dubious open reading frame unlikely to encode a functional protein, substantially overlaps YMR295C; deletion causes sensitivity to unfolded protein response-inducing agents
YDR387C		Putative transporter, member of the sugar porter family; YDR387C is not an essential gene
YLR444C		Dubious open reading frame unlikely to encode a functional protein, based on available experimental and comparative sequence data
YMR295C		Protein of unknown function that associates with ribosomes; green fluorescent protein (GFP)-fusion protein localizes to the cell periphery and bud; YMR295C is not an essential gene
YNR071C		Putative protein of unknown function

Table B.2: Cerivastatin + Δ hmg1 Δ xxx PE interactions

YMR003W	AIM34	Protein of unknown function; GFP-fusion protein localizes to the mitochondria; null mutant is viable and displays reduced frequency of mitochondrial genome loss
YNR041C	COQ2	Para hydroxybenzoate: polyprenyl transferase, catalyzes the second step in ubiquinone (coenzyme Q) biosynthesis
YIR023W	DAL81	Positive regulator of genes in multiple nitrogen degradation pathways; contains DNA binding domain but does not appear to bind the dodecanucleotide sequence present in the promoter region of many genes involved in allantoin catabolism
YOR245C	DGA1	Diacylglycerol acyltransferase, catalyzes the terminal step of triacylglycerol (TAG) formation, acylates diacylglycerol using acyl-CoA as an acyl donor, localized to lipid particles
YKL213C	DOA1	WD repeat protein required for ubiquitin-mediated protein degradation, forms complex with Cdc48p, plays a role in controlling cellular ubiquitin concentration; also promotes efficient NHEJ in postdiauxic/stationary phase
YKL191W	DPH2	Protein required, along with Dph1p, Kti11p, Jjj3p, and Dph5p, for synthesis of diphthamide, which is a modified histidine residue of translation elongation factor 2 (Eft1p or Eft2p); may act in a complex with Dph1p and Kti11p
YML008C	ERG6	Delta(24)-sterol C-methyltransferase, converts zymosterol to fecosterol in the ergosterol biosynthetic pathway by methylating position C-24; localized to both lipid particles and mitochondrial outer membrane
YER083C	GET2	Subunit of the GET complex; involved in insertion of proteins into the ER membrane; required for the retrieval of HDEL proteins from the Golgi to the ER in an ERD2 dependent fashion and for meiotic nuclear division
YJL101C	GSH1	Gamma glutamylcysteine synthetase catalyzes the first step in glutathione (GSH) biosynthesis; expression induced by oxidants, cadmium, and mercury
YOL081W	IRA2	GTPase-activating protein that negatively regulates RAS by converting it from the GTP- to the GDP-bound inactive form, required for reducing cAMP levels under nutrient limiting conditions, has similarity to Ira1p and human neurofibromin
YML068W	ITT1	Protein that modulates the efficiency of translation termination, interacts with translation release factors eRF1 (Sup45p) and eRF3 (Sup35p) in vitro, contains a zinc finger domain characteristic of the TRIAD class of proteins
YOR360C	PDE2	High-affinity cyclic AMP phosphodiesterase, component of the cAMP-dependent protein kinase signaling system, protects the cell from extracellular cAMP, contains readthrough motif surrounding termination codon
YOR312C	RPL20B	Protein component of the large (60S) ribosomal subunit, nearly identical to Rpl20Ap and has similarity to rat L18a ribosomal protein
YJL136C	RPS21B	Protein component of the small (40S) ribosomal subunit; nearly identical to Rps21Ap and has similarity to rat S21 ribosomal protein

YDR477W	SNF1	AMP-activated serine/threonine protein kinase found in a complex containing Snf4p and members of the Sip1p/Sip2p/Gal83p family; required for transcription of glucose-repressed genes, thermotolerance, sporulation, and peroxisome biogenesis
YDR073W	SNF11	Subunit of the SWI/SNF chromatin remodeling complex involved in transcriptional regulation; interacts with a highly conserved 40-residue sequence of Snf2p
YGL115W	SNF4	Activating gamma subunit of the AMP-activated Snf1p kinase complex (contains Snf1p and a Sip1p/Sip2p/Gal83p family member); activates glucose-repressed genes, represses glucose-induced genes; role in sporulation, and peroxisome biogenesis
YKR059W	TIF1	Translation initiation factor eIF4A, identical to Tif2p; DEA(D/H)-box RNA helicase that couples ATPase activity to RNA binding and unwinding; forms a dumbbell structure of two compact domains connected by a linker; interacts with eIF4G
YLL039C	UBI4	Ubiquitin, becomes conjugated to proteins, marking them for selective degradation via the ubiquitin-26S proteasome system; essential for the cellular stress response; encoded as a polyubiquitin precursor comprised of 5 head-to-tail repeats
YFR010W	UBP6	Ubiquitin-specific protease situated in the base subcomplex of the 26S proteasome, releases free ubiquitin from branched polyubiquitin chains; works in opposition to polyubiquitin elongation activity of Hul5p
YNR006W	VPS27	Endosomal protein that forms a complex with Hse1p; required for recycling Golgi proteins, forming luminal membranes and sorting ubiquitinated proteins destined for degradation; has Ubiquitin Interaction Motifs which bind ubiquitin (Ubi4p)
YPR173C	VPS4	AAA-ATPase involved in multivesicular body (MVB) protein sorting, ATP-bound Vps4p localizes to endosomes and catalyzes ESCRT-III disassembly and membrane release; ATPase activity is activated by Vta1p; regulates cellular sterol metabolism
YOR043W	WHI2	Protein required, with binding partner Psr1p, for full activation of the general stress response, possibly through Msn2p dephosphorylation; regulates growth during the diauxic shift; negative regulator of G1 cyclin expression
YOR083W	WHI5	Repressor of G1 transcription that binds to SCB binding factor (SBF) at SCB target promoters in early G1; phosphorylation of Whi5p by the CDK, Cln3p/Cdc28p relieves repression and promoter binding by Whi5; periodically expressed in G1
YPR024W	YME1	Catalytic subunit of the mitochondrial inner membrane i-AAA protease complex, which is responsible for degradation of unfolded or misfolded mitochondrial gene products; mutation causes an elevated rate of mitochondrial turnover
YMR294W-A		Dubious open reading frame unlikely to encode a functional protein, substantially overlaps YMR295C; deletion causes sensitivity to unfolded protein response-inducing agents
YDR387C		Putative transporter, member of the sugar porter family; YDR387C is not an essential gene

YMR295C		Protein of unknown function that associates with ribosomes; green fluorescent protein (GFP)-fusion protein localizes to the cell periphery and bud; YMR295C is not an essential gene
YDR186C		Putative protein of unknown function; may interact with ribosomes, based on co-purification experiments; green fluorescent protein (GFP)-fusion protein localizes to the cytoplasm
YGL242C		Putative protein of unknown function; deletion mutant is viable
YNR071C		Putative protein of unknown function

Table B.3: Lovastatin + Δ hmg1 Δ xxx PE interactions

YDL074C	BRE1	E3 ubiquitin ligase, forms heterodimer with Rad6p to monoubiquitinate histone H2B-K123, which is required for the subsequent methylation of histone H3-K4 and H3-K79; required for DSBR, transcription, silencing, and checkpoint control
YIR023W	DAL81	Positive regulator of genes in multiple nitrogen degradation pathways; contains DNA binding domain but does not appear to bind the dodecanucleotide sequence present in the promoter region of many genes involved in allantoin catabolism
YOR245C	DGA1	Diacylglycerol acyltransferase, catalyzes the terminal step of triacylglycerol (TAG) formation, acylates diacylglycerol using acyl-CoA as an acyl donor, localized to lipid particles
YKL213C	DOA1	WD repeat protein required for ubiquitin-mediated protein degradation, forms complex with Cdc48p, plays a role in controlling cellular ubiquitin concentration; also promotes efficient NHEJ in postdiauxic/stationary phase
YER083C	GET2	Subunit of the GET complex; involved in insertion of proteins into the ER membrane; required for the retrieval of HDEL proteins from the Golgi to the ER in an ERD2 dependent fashion and for meiotic nuclear division
YJL101C	GSH1	Gamma glutamylcysteine synthetase catalyzes the first step in glutathione (GSH) biosynthesis; expression induced by oxidants, cadmium, and mercury
YOL081W	IRA2	GTPase-activating protein that negatively regulates RAS by converting it from the GTP- to the GDP-bound inactive form, required for reducing cAMP levels under nutrient limiting conditions, has similarity to Ira1p and human neurofibromin
YML068W	ITT1	Protein that modulates the efficiency of translation termination, interacts with translation release factors eRF1 (Sup45p) and eRF3 (Sup35p) in vitro, contains a zinc finger domain characteristic of the TRIAD class of proteins
YOL009C	MDM12	Mitochondrial outer membrane protein, required for transmission of mitochondria to daughter cells; component of the ERMES complex that links the ER to mitochondria; may influence import and assembly of outer membrane beta-barrel proteins
YLR350W	ORM2	Evolutionarily conserved protein with similarity to Orm1p, required for resistance to agents that induce the unfolded protein response; human ortholog is located in the endoplasmic reticulum
YOR360C	PDE2	High-affinity cyclic AMP phosphodiesterase, component of the cAMP-dependent protein kinase signaling system, protects the cell from extracellular cAMP, contains readthrough motif surrounding termination codon
YOR153W	PDR5	Plasma membrane ATP-binding cassette (ABC) transporter, multidrug transporter actively regulated by Pdr1p; also involved in steroid transport, cation resistance, and cellular detoxification during exponential growth

YPL089C	RLM1	MADS-box transcription factor, component of the protein kinase C-mediated MAP kinase pathway involved in the maintenance of cell integrity; phosphorylated and activated by the MAP-kinase Slt2p
YOR312C	RPL20B	Protein component of the large (60S) ribosomal subunit, nearly identical to Rpl20Ap and has similarity to rat L18a ribosomal protein
YCR009C	RVS161	Amphiphysin-like lipid raft protein; interacts with Rvs167p and regulates polarization of the actin cytoskeleton, endocytosis, cell polarity, cell fusion and viability following starvation or osmotic stress
YDR477W	SNF1	AMP-activated serine/threonine protein kinase found in a complex containing Snf4p and members of the Sip1p/Sip2p/Gal83p family; required for transcription of glucose-repressed genes, thermotolerance, sporulation, and peroxisome biogenesis
YKR059W	TIF1	Translation initiation factor eIF4A, identical to Tif2p; DEA(D/H)-box RNA helicase that couples ATPase activity to RNA binding and unwinding; forms a dumbbell structure of two compact domains connected by a linker; interacts with eIF4G
YFR010W	UBP6	Ubiquitin-specific protease situated in the base subcomplex of the 26S proteasome, releases free ubiquitin from branched polyubiquitin chains; works in opposition to polyubiquitin elongation activity of Hul5p
YGR105W	VMA21	Integral membrane protein that is required for vacuolar H ⁺ -ATPase (V-ATPase) function, although not an actual component of the V-ATPase complex; functions in the assembly of the V-ATPase; localized to the yeast endoplasmic reticulum (ER)
YNR006W	VPS27	Endosomal protein that forms a complex with Hse1p; required for recycling Golgi proteins, forming luminal membranes and sorting ubiquitinated proteins destined for degradation; has Ubiquitin Interaction Motifs which bind ubiquitin (Ubi4p)
YOR083W	WHI5	Repressor of G1 transcription that binds to SCB binding factor (SBF) at SCB target promoters in early G1; phosphorylation of Whi5p by the CDK, Cln3p/Cdc28p relieves repression and promoter binding by Whi5; periodically expressed in G1
YDR387C		Putative transporter, member of the sugar porter family; YDR387C is not an essential gene
YMR295C		Protein of unknown function that associates with ribosomes; green fluorescent protein (GFP)-fusion protein localizes to the cell periphery and bud; YMR295C is not an essential gene

Table B.4: Atorvastatin + Δ hmg2 Δ xxx PE interactions

YGL256W	ADH4	Alcohol dehydrogenase isoenzyme type IV, dimeric enzyme demonstrated to be zinc-dependent despite sequence similarity to iron-activated alcohol dehydrogenases; transcription is induced in response to zinc deficiency
YMR003W	AIM34	Protein of unknown function; GFP-fusion protein localizes to the mitochondria; null mutant is viable and displays reduced frequency of mitochondrial genome loss
YDL074C	BRE1	E3 ubiquitin ligase, forms heterodimer with Rad6p to monoubiquitinate histone H2B-K123, which is required for the subsequent methylation of histone H3-K4 and H3-K79; required for DSBR, transcription, silencing, and checkpoint control
YOR125C	CAT5	Protein required for ubiquinone (Coenzyme Q) biosynthesis; localizes to the matrix face of the mitochondrial inner membrane in a large complex with ubiquinone biosynthetic enzymes; required for gluconeogenic gene activation
YBR131W	CCZ1	Protein involved in vacuolar assembly, essential for autophagy and the cytoplasm-to-vacuole pathway
YER164W	CHD1	Nucleosome remodeling factor that functions in regulation of transcription elongation; contains a chromo domain, a helicase domain and a DNA-binding domain; component of both the SAGA and SLIK complexes
YGR157W	CHO2	Phosphatidylethanolamine methyltransferase (PEMT), catalyzes the first step in the conversion of phosphatidylethanolamine to phosphatidylcholine during the methylation pathway of phosphatidylcholine biosynthesis
YBR023C	CHS3	Chitin synthase III, catalyzes the transfer of N-acetylglucosamine (GlcNAc) to chitin; required for synthesis of the majority of cell wall chitin, the chitin ring during bud emergence, and spore wall chitosan
YLR330W	CHS5	Component of the exomer complex, which also contains Csh6p, Bch1p, Bch2p, and Bud7p and is involved in export of selected proteins, such as chitin synthase Chs3p, from the Golgi to the plasma membrane
YDL155W	CLB3	B-type cyclin involved in cell cycle progression; activates Cdc28p to promote the G2/M transition; may be involved in DNA replication and spindle assembly; accumulates during S phase and G2, then targeted for ubiquitin-mediated degradation
YPL256C	CLN2	G1 cyclin involved in regulation of the cell cycle; activates Cdc28p kinase to promote the G1 to S phase transition; late G1 specific expression depends on transcription factor complexes, MBF (Swi6p-Mbp1p) and SBF (Swi6p-Swi4p)
YML129C	COX14	Mitochondrial membrane protein, involved in translational regulation of Cox1p and assembly of cytochrome c oxidase (complex IV); associates with complex IV assembly intermediates and complex III/complex IV supercomplexes
YNR010W	CSE2	Subunit of the RNA polymerase II mediator complex; associates with core polymerase subunits to form the RNA polymerase II holoenzyme; component of the Med9/10 module; required for regulation of RNA polymerase II activity
YIR023W	DAL81	Positive regulator of genes in multiple nitrogen degradation pathways; contains DNA binding domain but does not appear to bind the dodecanucleotide sequence present in the promoter region of many genes involved in allantoin catabolism

YAL013W	DEP1	Transcriptional modulator involved in regulation of structural phospholipid biosynthesis genes and metabolically unrelated genes, as well as maintenance of telomeres, mating efficiency, and sporulation
YOR245C	DGA1	Diacylglycerol acyltransferase, catalyzes the terminal step of triacylglycerol (TAG) formation, acylates diacylglycerol using acyl-CoA as an acyl donor, localized to lipid particles
YKL213C	DOA1	WD repeat protein required for ubiquitin-mediated protein degradation, forms complex with Cdc48p, plays a role in controlling cellular ubiquitin concentration; also promotes efficient NHEJ in postdiauxic/stationary phase
YDR440W	DOT1	Nucleosomal histone H3-Lys79 methylase; methylation is required for telomeric silencing, meiotic checkpoint control, and DNA damage response
YBR078W	ECM33	GPI-anchored protein of unknown function, has a possible role in apical bud growth; GPI-anchoring on the plasma membrane crucial to function; phosphorylated in mitochondria; similar to Sps2p and Pst1p
YBL047C	EDE1	Key endocytic protein involved in a network of interactions with other endocytic proteins, binds membranes in a ubiquitin-dependent manner, may also bind ubiquitinated membrane-associated proteins
YDR414C	ERD1	Predicted membrane protein required for the retention of luminal endoplasmic reticulum proteins; mutants secrete the endogenous ER protein, BiP (Kar2p)
YMR202W	ERG2	C-8 sterol isomerase, catalyzes the isomerization of the delta-8 double bond to the delta-7 position at an intermediate step in ergosterol biosynthesis
YFR019W	FAB1	1-phosphatidylinositol-3-phosphate 5-kinase; vacuolar membrane kinase that generates phosphatidylinositol (3,5)P ₂ , which is involved in vacuolar sorting and homeostasis
YCR034W	FEN1	Fatty acid elongase, involved in sphingolipid biosynthesis; acts on fatty acids of up to 24 carbons in length; mutations have regulatory effects on 1,3-beta-glucan synthase, vacuolar ATPase, and the secretory pathway
YGR196C	FYV8	Protein of unknown function, required for survival upon exposure to K1 killer toxin
YMR307W	GAS1	Beta-1,3-glucanosyltransferase, required for cell wall assembly and also has a role in transcriptional silencing; localizes to the cell surface via a glycosylphosphatidylinositol (GPI) anchor; also found at the nuclear periphery
YGL020C	GET1	Subunit of the GET complex; involved in insertion of proteins into the ER membrane; required for the retrieval of HDEL proteins from the Golgi to the ER in an ERD2 dependent fashion and for normal mitochondrial morphology and inheritance
YER083C	GET2	Subunit of the GET complex; involved in insertion of proteins into the ER membrane; required for the retrieval of HDEL proteins from the Golgi to the ER in an ERD2 dependent fashion and for meiotic nuclear division
YDR508C	GNP1	High-affinity glutamine permease, also transports Leu, Ser, Thr, Cys, Met and Asn; expression is fully dependent on Grr1p and modulated by the Ssy1p-Ptr3p-Ssy5p (SPS) sensor of extracellular amino acids
YGR032W	GSC2	Catalytic subunit of 1,3-beta-glucan synthase, involved in formation of the inner layer of the spore wall; activity positively regulated by Rho1p and negatively by Smk1p; has similarity to an alternate catalytic subunit, Fks1p (Gsc1p)

YJL101C	GSH1	Gamma glutamylcysteine synthetase catalyzes the first step in glutathione (GSH) biosynthesis; expression induced by oxidants, cadmium, and mercury
YOL049W	GSH2	Glutathione synthetase, catalyzes the ATP-dependent synthesis of glutathione (GSH) from gamma-glutamylcysteine and glycine; induced by oxidative stress and heat shock
YGL084C	GUP1	Plasma membrane protein involved in remodeling GPI anchors; member of the MBOAT family of putative membrane-bound O-acyltransferases; proposed to be involved in glycerol transport
YOL095C	HMI1	Mitochondrial inner membrane localized ATP-dependent DNA helicase, required for the maintenance of the mitochondrial genome; not required for mitochondrial transcription; has homology to E. coli helicase uvrD
YDR174W	HMO1	Chromatin associated high mobility group (HMG) family member involved in genome maintenance; rDNA-binding component of the Pol I transcription system; associates with a 5'-3' DNA helicase and Fpr1p, a prolyl isomerase
YOR025W	HST3	Member of the Sir2 family of NAD(+)-dependent protein deacetylases; involved along with Hst4p in telomeric silencing, cell cycle progression, radiation resistance, genomic stability and short-chain fatty acid metabolism
YJR118C	ILM1	Protein of unknown function; may be involved in mitochondrial DNA maintenance; required for slowed DNA synthesis-induced filamentous growth
YIL002C	INP51	Phosphatidylinositol 4,5-bisphosphate 5-phosphatase, synaptojanin-like protein with an N-terminal Sac1 domain, plays a role in phosphatidylinositol 4,5-bisphosphate homeostasis and in endocytosis; null mutation confers cold-tolerant growth
YOL081W	IRA2	GTPase-activating protein that negatively regulates RAS by converting it from the GTP- to the GDP-bound inactive form, required for reducing cAMP levels under nutrient limiting conditions, has similarity to Ira1p and human neurofibromin
YER019W	ISC1	Mitochondrial membrane localized inositol phosphosphingolipid phospholipase C, hydrolyzes complex sphingolipids to produce ceramide; activated by phosphatidylserine, cardiolipin, and phosphatidylglycerol; mediates Na ⁺ and Li ⁺ halotolerance
YKL032C	IXR1	Protein that binds DNA containing intrastrand cross-links formed by cisplatin, contains two HMG (high mobility group box) domains, which confer the ability to bend cisplatin-modified DNA; mediates aerobic transcriptional repression of COX5b
YDR483W	KRE2	Alpha1,2-mannosyltransferase of the Golgi involved in protein mannosylation
YJL062W	LAS21	Integral plasma membrane protein involved in the synthesis of the glycosylphosphatidylinositol (GPI) core structure; mutations affect cell wall integrity
YPL055C	LGE1	Protein of unknown function; null mutant forms abnormally large cells, and homozygous diploid null mutant displays delayed premeiotic DNA synthesis and reduced efficiency of meiotic nuclear division
YNL147W	LSM7	Lsm (Like Sm) protein; part of heteroheptameric complexes (Lsm2p-7p and either Lsm1p or 8p): cytoplasmic Lsm1p complex involved in mRNA decay; nuclear Lsm8p complex part of U6 snRNP and possibly involved in processing tRNA, snoRNA, and rRNA

YCR020C-A	MAK31	Non-catalytic subunit of N-terminal acetyltransferase of the NatC type; required for replication of dsRNA virus; member of the Sm protein family
YNL307C	MCK1	Protein serine/threonine/tyrosine (dual-specificity) kinase involved in control of chromosome segregation and in regulating entry into meiosis; related to mammalian glycogen synthase kinases of the GSK-3 family
YPR070W	MED1	Subunit of the RNA polymerase II mediator complex; associates with core polymerase subunits to form the RNA polymerase II holoenzyme; essential for transcriptional regulation
YIL128W	MET18	DNA repair and TFIIH regulator, required for both nucleotide excision repair (NER) and RNA polymerase II (RNAP II) transcription; involved in telomere maintenance
YNL076W	MKS1	Pleiotropic negative transcriptional regulator involved in Ras-CAMP and lysine biosynthetic pathways and nitrogen regulation; involved in retrograde (RTG) mitochondria-to-nucleus signaling
YGL124C	MON1	Protein required for fusion of cvt-vesicles and autophagosomes with the vacuole; associates, as a complex with Ccz1p, with a perivacuolar compartment; potential Cdc28p substrate
YMR224C	MRE11	Subunit of a complex with Rad50p and Xrs2p (MRX complex) that functions in repair of DNA double-strand breaks and in telomere stability, exhibits nuclease activity that appears to be required for MRX function; widely conserved
YLR338W	OPI9	Dubious open reading frame unlikely to encode a protein, based on available experimental and comparative sequence data; partially overlaps the verified ORF VRP1/YLR337C
YDL232W	OST4	Subunit of the oligosaccharyltransferase complex of the ER lumen, which catalyzes protein asparagine-linked glycosylation; type I membrane protein required for incorporation of Ost3p or Ost6p into the OST complex
YOR360C	PDE2	High-affinity cyclic AMP phosphodiesterase, component of the cAMP-dependent protein kinase signaling system, protects the cell from extracellular cAMP, contains readthrough motif surrounding termination codon
YGL013C	PDR1	Zinc cluster protein that is a master regulator involved in recruiting other zinc cluster proteins to pleiotropic drug response elements (PDREs) to fine tune the regulation of multidrug resistance genes
YER149C	PEA2	Coiled-coil polarisome protein required for polarized morphogenesis, cell fusion, and low affinity Ca ²⁺ influx; forms polarisome complex with Bni1p, Bud6p, and Spa2p; localizes to sites of polarized growth
YER153C	PET122	Mitochondrial translational activator specific for the COX3 mRNA, acts together with Pet54p and Pet494p; located in the mitochondrial inner membrane
YNL003C	PET8	S-adenosylmethionine transporter of the mitochondrial inner membrane, member of the mitochondrial carrier family; required for biotin biosynthesis and respiratory growth
YDR265W	PEX10	Peroxisomal membrane E3 ubiquitin ligase required for for Ubc4p-dependent Pex5p ubiquitination and peroxisomal matrix protein import; contains zinc-binding RING domain; mutations in human homolog cause various peroxisomal disorders
YDR244W	PEX5	Peroxisomal membrane signal receptor for the C-terminal tripeptide signal sequence (PTS1) of peroxisomal matrix proteins, required for peroxisomal matrix protein import; also proposed to have PTS1-receptor independent functions

YMR205C	PFK2	Beta subunit of heterooctameric phosphofructokinase involved in glycolysis, indispensable for anaerobic growth, activated by fructose-2,6-bisphosphate and AMP, mutation inhibits glucose induction of cell cycle-related genes
YDR276C	PMP3	Small plasma membrane protein related to a family of plant polypeptides that are overexpressed under high salt concentration or low temperature, not essential for viability, deletion causes hyperpolarization of the plasma membrane potential
YAL023C	PMT2	Protein O-mannosyltransferase, transfers mannose residues from dolichyl phosphate-D-mannose to protein serine/threonine residues; acts in a complex with Pmt1p, can instead interact with Pmt5p in some conditions; target for new antifungals
YPR191W	QCR2	Subunit 2 of the ubiquinol cytochrome-c reductase complex, which is a component of the mitochondrial inner membrane electron transport chain; phosphorylated; transcription is regulated by Hap1p, Hap2p/Hap3p, and heme
YMR075W	RCO1	Essential subunit of the histone deacetylase Rpd3S complex; interacts with Eaf3p
YHL027W	RIM101	Transcriptional repressor involved in response to pH and in cell wall construction; required for alkaline pH-stimulated haploid invasive growth and sporulation; activated by proteolytic processing; similar to A. nidulans PacC
YMR154C	RIM13	Calpain-like cysteine protease involved in proteolytic activation of Rim101p in response to alkaline pH; has similarity to A. nidulans palB
YFL033C	RIM15	Glucose-repressible protein kinase involved in signal transduction during cell proliferation in response to nutrients, specifically the establishment of stationary phase; identified as a regulator of IME2; substrate of Pho80p-Pho85p kinase
YGL045W	RIM8	Protein involved in proteolytic activation of Rim101p in response to alkaline pH; similar to A. nidulans PalF; essential for anaerobic growth; member of the arrestin-related trafficking adaptor family
YMR063W	RIM9	Protein of unknown function, involved in the proteolytic activation of Rim101p in response to alkaline pH; has similarity to A. nidulans PalI; putative membrane protein
YPL089C	RLM1	MADS-box transcription factor, component of the protein kinase C-mediated MAP kinase pathway involved in the maintenance of cell integrity; phosphorylated and activated by the MAP-kinase Slt2p
YHR021C	RPS27B	Protein component of the small (40S) ribosomal subunit; nearly identical to Rps27Ap and has similarity to rat S27 ribosomal protein
YGL244W	RTF1	Subunit of the RNA polymerase II-associated Paf1 complex; directly or indirectly regulates DNA-binding properties of Spt15p and relative activities of different TATA elements; involved in telomere maintenance
YOR216C	RUD3	Golgi matrix protein involved in the structural organization of the cis-Golgi; interacts genetically with COG3 and USO1
YCR009C	RVS161	Amphiphysin-like lipid raft protein; interacts with Rvs167p and regulates polarization of the actin cytoskeleton, endocytosis, cell polarity, cell fusion and viability following starvation or osmotic stress
YDR388W	RVS167	Actin-associated protein, interacts with Rvs161p to regulate actin cytoskeleton, endocytosis, and viability following starvation or osmotic stress; homolog of mammalian amphiphysin

YDR469W	SDC1	Subunit of the COMPASS (Set1C) complex, which methylates lysine 4 of histone H3 and is required in chromatin silencing at telomeres; contains a Dpy-30 domain that mediates interaction with Bre2p; similar to C. elegans and human DPY-30
YBR171W	SEC66	Non-essential subunit of Sec63 complex (Sec63p, Sec62p, Sec66p and Sec72p); with Sec61 complex, Kar2p/BiP and Lhs1p forms a channel competent for SRP-dependent and post-translational SRP-independent protein targeting and import into the ER
YCL010C	SGF29	Probable subunit of SAGA histone acetyltransferase complex
YGL066W	SGF73	Subunit of SAGA histone acetyltransferase complex; involved in formation of the preinitiation complex assembly at promoters; null mutant displays defects in premeiotic DNA synthesis
YLR079W	SIC1	Inhibitor of Cdc28-Clb kinase complexes that controls G1/S phase transition, preventing premature S phase and ensuring genomic integrity; phosphorylation targets Sic1p for SCF(CDC4)-dependent turnover; functional homolog of mammalian Kip1
YBL061C	SKT5	Activator of Chs3p (chitin synthase III), recruits Chs3p to the bud neck via interaction with Bni4p; has similarity to Shc1p, which activates Chs3p during sporulation
YBL007C	SLA1	Cytoskeletal protein binding protein required for assembly of the cortical actin cytoskeleton; interacts with proteins regulating actin dynamics and proteins required for endocytosis; found in the nucleus and cell cortex; has 3 SH3 domains
YBR077C	SLM4	Component of the EGO complex, which is involved in the regulation of microautophagy, and of the GSE complex, which is required for proper sorting of amino acid permease Gap1p; gene exhibits synthetic genetic interaction with MSS4
YDR477W	SNF1	AMP-activated serine/threonine protein kinase found in a complex containing Snf4p and members of the Sip1p/Sip2p/Gal83p family; required for transcription of glucose-repressed genes, thermotolerance, sporulation, and peroxisome biogenesis
YGL115W	SNF4	Activating gamma subunit of the AMP-activated Snf1p kinase complex (contains Snf1p and a Sip1p/Sip2p/Gal83p family member); activates glucose-repressed genes, represses glucose-induced genes; role in sporulation, and peroxisome biogenesis
YCR033W	SNT1	Subunit of the Set3C deacetylase complex that interacts directly with the Set3C subunit, Sif2p; putative DNA-binding protein
YPL057C	SUR1	Probable catalytic subunit of a mannosylinositol phosphorylceramide (MIPC) synthase, forms a complex with probable regulatory subunit Csg2p; function in sphingolipid biosynthesis is overlapping with that of Csh1p
YBR175W	SWD3	Essential subunit of the COMPASS (Set1C) complex, which methylates histone H3 on lysine 4 and is required in transcriptional silencing near telomeres; WD40 beta propeller superfamily member and ortholog of mammalian WDR5
YNL081C	SWS2	Putative mitochondrial ribosomal protein of the small subunit, has similarity to E. coli S13 ribosomal protein; participates in controlling sporulation efficiency
YPR140W	TAZ1	Lyso-phosphatidylcholine acyltransferase, required for normal phospholipid content of mitochondrial membranes; may remodel acyl groups of cardiolipin in the inner membrane; human ortholog tafazzin is implicated in Barth syndrome

YOL018C	TLG2	Syntaxin-like t-SNARE that forms a complex with Tlg1p and Vti1p and mediates fusion of endosome-derived vesicles with the late Golgi; binds Vps45p, which prevents Tlg2p degradation and also facilitates t-SNARE complex formation
YDR074W	TPS2	Phosphatase subunit of the trehalose-6-phosphate synthase/phosphatase complex, which synthesizes the storage carbohydrate trehalose; expression is induced by stress conditions and repressed by the Ras-cAMP pathway
YER090W	TRP2	Anthranilate synthase, catalyzes the initial step of tryptophan biosynthesis, forms multifunctional hetero-oligomeric anthranilate synthase:indole-3-glycerol phosphate synthase enzyme complex with Trp3p
YML028W	TSA1	Thioredoxin peroxidase, acts as both a ribosome-associated and free cytoplasmic antioxidant; self-associates to form a high-molecular weight chaperone complex under oxidative stress; deletion results in mutator phenotype
YOR006C	TSR3	Putative protein of unknown function; green fluorescent protein (GFP)-fusion protein localizes to both the cytoplasm and the nucleus
YBR082C	UBC4	Ubiquitin-conjugating enzyme (E2), mediates degradation of abnormal or excess proteins, including calmodulin and histone H3; interacts with many SCF ubiquitin protein ligases; component of the cellular stress response
YLL039C	UBI4	Ubiquitin, becomes conjugated to proteins, marking them for selective degradation via the ubiquitin-26S proteasome system; essential for the cellular stress response; encoded as a polyubiquitin precursor comprised of 5 head-to-tail repeats
YER151C	UBP3	Ubiquitin-specific protease that interacts with Bre5p to co-regulate anterograde and retrograde transport between endoplasmic reticulum and Golgi compartments; inhibitor of gene silencing; cleaves ubiquitin fusions but not polyubiquitin
YFR010W	UBP6	Ubiquitin-specific protease situated in the base subcomplex of the 26S proteasome, releases free ubiquitin from branched polyubiquitin chains; works in opposition to polyubiquitin elongation activity of Hul5p
YLR386W	VAC14	Protein involved in regulated synthesis of PtdIns(3,5)P(2), in control of trafficking of some proteins to the vacuole lumen via the MVB, and in maintenance of vacuole size and acidity; interacts with Fig4p; activator of Fab1p
YOR106W	VAM3	Syntaxin-related protein required for vacuolar assembly; functions with Vam7p in vacuolar protein trafficking; member of the syntaxin family of proteins
YDL077C	VAM6	Vacuolar protein that plays a critical role in the tethering steps of vacuolar membrane fusion by facilitating guanine nucleotide exchange on small guanosine triphosphatase Ypt7p
YGL212W	VAM7	Component of the vacuole SNARE complex involved in vacuolar morphogenesis; SNAP-25 homolog; functions with a syntaxin homolog Vam3p in vacuolar protein trafficking
YLR373C	VID22	Glycosylated integral membrane protein localized to the plasma membrane; plays a role in fructose-1,6-bisphosphatase (FBPase) degradation; involved in FBPase transport from the cytosol to Vid (vacuole import and degradation) vesicles

YOR089C	VPS21	GTPase required for transport during endocytosis and for correct sorting of vacuolar hydrolases; localized in endocytic intermediates; detected in mitochondria; geranylgeranylation required for membrane association; mammalian Rab5 homolog
YKL041W	VPS24	One of four subunits of the endosomal sorting complex required for transport III (ESCRT-III); forms an ESCRT-III subcomplex with Did4p; involved in the sorting of transmembrane proteins into the multivesicular body (MVB) pathway
YNR006W	VPS27	Endosomal protein that forms a complex with Hse1p; required for recycling Golgi proteins, forming luminal membranes and sorting ubiquitinated proteins destined for degradation; has Ubiquitin Interaction Motifs which bind ubiquitin (Ubi4p)
YPR173C	VPS4	AAA-ATPase involved in multivesicular body (MVB) protein sorting, ATP-bound Vps4p localizes to endosomes and catalyzes ESCRT-III disassembly and membrane release; ATPase activity is activated by Vta1p; regulates cellular sterol metabolism
YDR080W	VPS41	Vacuolar membrane protein that is a subunit of the homotypic vacuole fusion and vacuole protein sorting (HOPS) complex; essential for membrane docking and fusion at the Golgi-to-endosome and endosome-to-vacuole stages of protein transport
YKR020W	VPS51	Component of the GARP (Golgi-associated retrograde protein) complex, Vps51p-Vps52p-Vps53p-Vps54p, which is required for the recycling of proteins from endosomes to the late Golgi; links the (VFT/GARP) complex to the SNARE Tlg1p
YJL029C	VPS53	Component of the GARP (Golgi-associated retrograde protein) complex, Vps51p-Vps52p-Vps53p-Vps54p, which is required for the recycling of proteins from endosomes to the late Golgi; required for vacuolar protein sorting
YDR372C	VPS74	Protein required for Golgi localization of glycosyltransferases; binds the cytosolic domains of Golgi glycosyltransferases; functions as a heterotetramer
YML097C	VPS9	A guanine nucleotide exchange factor involved in vesicle-mediated vacuolar protein transport; specifically stimulates the intrinsic guanine nucleotide exchange activity of Vps21p/Rab5: similar to mammalian ras inhibitors; binds ubiquitin
YLR337C	VRP1	Proline-rich actin-associated protein involved in cytoskeletal organization and cytokinesis; related to mammalian Wiskott-Aldrich syndrome protein (WASP)-interacting protein (WIP)
YOR043W	WHI2	Protein required, with binding partner Psr1p, for full activation of the general stress response, possibly through Msn2p dephosphorylation; regulates growth during the diauxic shift; negative regulator of G1 cyclin expression
YGR281W	YOR1	Plasma membrane ATP-binding cassette (ABC) transporter, multidrug transporter mediates export of many different organic anions including oligomycin; similar to human cystic fibrosis transmembrane receptor (CFTR)
YBR111C	YSA1	Nudix hydrolase family member with ADP-ribose pyrophosphatase activity; shown to metabolize O-acetyl-ADP-ribose to AMP and acetylated ribose 5'-phosphate
YGR270W	YTA7	Protein that localizes to chromatin and has a role in regulation of histone gene expression; has a bromodomain-like region that interacts with the N-terminal tail of histone H3, and an ATPase domain; potentially phosphorylated by Cdc28p

YMR294W-A		Dubious open reading frame unlikely to encode a functional protein, substantially overlaps YMR295C; deletion causes sensitivity to unfolded protein response-inducing agents
YOR062C		Protein of unknown function; similar to YKR075Cp and Reg1p; expression regulated by glucose and Rgt1p; GFP-fusion protein is induced in response to the DNA-damaging agent MMS
YHR078W		High osmolarity-regulated gene of unknown function
YNL296W		Dubious open reading frame unlikely to encode a functional protein; deletion adversely affects sporulation; deletion mutant exhibits synthetic phenotype under expression of mutant huntingtin fragment, but gene does not have human ortholog
YPL041C		Protein of unknown function involved in maintenance of proper telomere length
YOR024W		Dubious open reading frame unlikely to encode a protein, based on available experimental and comparative sequence data
YGL081W		Putative protein of unknown function; non-essential gene; interacts genetically with CHS5, a gene involved in chitin biosynthesis
YJL175W		Dubious open reading frame unlikely to encode a functional protein; deletion confers resistance to cisplatin, hypersensitivity to 5-fluorouracil, and growth defect at high pH with high calcium; overlaps gene for SWI3 transcription factor
YMR295C		Protein of unknown function that associates with ribosomes; green fluorescent protein (GFP)-fusion protein localizes to the cell periphery and bud; YMR295C is not an essential gene
YGR122W		Probable ortholog of <i>A. nidulans</i> PalC, which is involved in pH regulation and binds to the ESCRT-III complex; null mutant does not properly process Rim101p and has decreased resistance to rapamycin; GFP-fusion protein is cytoplasmic
YDR186C		Putative protein of unknown function; may interact with ribosomes, based on co-purification experiments; green fluorescent protein (GFP)-fusion protein localizes to the cytoplasm
YLR255C		Dubious ORF unlikely to encode a functional protein, based on available experimental and comparative sequence data
YDR199W		Dubious open reading frame unlikely to encode a protein, based on available experimental and comparative sequence data; partially overlaps the verified gene VPS64; computationally predicted to have thiol-disulfide oxidoreductase activity
YER119C-A		Dubious open reading frame, not conserved in closely related <i>Saccharomyces</i> species; deletion mutation blocks replication of Brome mosaic virus in <i>S. cerevisiae</i> , but this is likely due to effects on the overlapping gene SCS2
YNR071C		Putative protein of unknown function
YBL062W		Dubious open reading frame unlikely to encode a protein, based on available experimental and comparative sequence data
YCL042W		Putative protein of unknown function; epitope-tagged protein localizes to the cytoplasm
YOL013W-A		Putative protein of unknown function; identified by SAGE

Table B.5: Cerivastatin + Δ hmg2 Δ xxx PE interactions

YDL243C	AAD4	Putative aryl-alcohol dehydrogenase with similarity to <i>P. chrysosporium</i> aryl-alcohol dehydrogenase, involved in the oxidative stress response; expression induced in cells treated with the mycotoxin patulin
YGL256W	ADH4	Alcohol dehydrogenase isoenzyme type IV, dimeric enzyme demonstrated to be zinc-dependent despite sequence similarity to iron-activated alcohol dehydrogenases; transcription is induced in response to zinc deficiency
YCL025C	AGP1	Low-affinity amino acid permease with broad substrate range, involved in uptake of asparagine, glutamine, and other amino acids; expression is regulated by the SPS plasma membrane amino acid sensor system (Ssy1p-Ptr3p-Ssy5p)
YMR003W	AIM34	Protein of unknown function; GFP-fusion protein localizes to the mitochondria; null mutant is viable and displays reduced frequency of mitochondrial genome loss
YHR126C	ANS1	Putative protein of unknown function; transcription dependent upon Azf1p
YLR370C	ARC18	Subunit of the ARP2/3 complex, which is required for the motility and integrity of cortical actin patches
YHL040C	ARN1	Transporter, member of the ARN family of transporters that specifically recognize siderophore-iron chelates; responsible for uptake of iron bound to ferrirubin, ferrirhodin, and related siderophores
YDL074C	BRE1	E3 ubiquitin ligase, forms heterodimer with Rad6p to monoubiquitinate histone H2B-K123, which is required for the subsequent methylation of histone H3-K4 and H3-K79; required for DSBR, transcription, silencing, and checkpoint control
YNR051C	BRE5	Ubiquitin protease cofactor, forms deubiquitination complex with Ubp3p that coregulates anterograde and retrograde transport between the endoplasmic reticulum and Golgi compartments; null is sensitive to brefeldin A
YBR131W	CCZ1	Protein involved in vacuolar assembly, essential for autophagy and the cytoplasm-to-vacuole pathway
YER164W	CHD1	Nucleosome remodeling factor that functions in regulation of transcription elongation; contains a chromo domain, a helicase domain and a DNA-binding domain; component of both the SAGA and SLIK complexes
YDL155W	CLB3	B-type cyclin involved in cell cycle progression; activates Cdc28p to promote the G2/M transition; may be involved in DNA replication and spindle assembly; accumulates during S phase and G2, then targeted for ubiquitin-mediated degradation
YPL256C	CLN2	G1 cyclin involved in regulation of the cell cycle; activates Cdc28p kinase to promote the G1 to S phase transition; late G1 specific expression depends on transcription factor complexes, MBF (Swi6p-Mbp1p) and SBF (Swi6p-Swi4p)
YML071C	COG8	Component of the conserved oligomeric Golgi complex (Cog1p through Cog8p), a cytosolic tethering complex that functions in protein trafficking to mediate fusion of transport vesicles to Golgi compartments
YML129C	COX14	Mitochondrial membrane protein, involved in translational regulation of Cox1p and assembly of cytochrome c oxidase (complex IV); associates with complex IV assembly intermediates and complex III/complex IV supercomplexes

YIR023W	DAL81	Positive regulator of genes in multiple nitrogen degradation pathways; contains DNA binding domain but does not appear to bind the dodecanucleotide sequence present in the promoter region of many genes involved in allantoin catabolism
YKR024C	DBP7	Putative ATP-dependent RNA helicase of the DEAD-box family involved in ribosomal biogenesis; essential for growth under anaerobic conditions
YOR030W	DFG16	Probable multiple transmembrane protein, involved in diploid invasive and pseudohyphal growth upon nitrogen starvation; required for accumulation of processed Rim101p
YOR245C	DGA1	Diacylglycerol acyltransferase, catalyzes the terminal step of triacylglycerol (TAG) formation, acylates diacylglycerol using acyl-CoA as an acyl donor, localized to lipid particles
YKL213C	DOA1	WD repeat protein required for ubiquitin-mediated protein degradation, forms complex with Cdc48p, plays a role in controlling cellular ubiquitin concentration; also promotes efficient NHEJ in postdiauxic/stationary phase
YDR440W	DOT1	Nucleosomal histone H3-Lys79 methylase; methylation is required for telomeric silencing, meiotic checkpoint control, and DNA damage response
YKL191W	DPH2	Protein required, along with Dph1p, Kti11p, Jjj3p, and Dph5p, for synthesis of diphthamide, which is a modified histidine residue of translation elongation factor 2 (Eft1p or Eft2p); may act in a complex with Dph1p and Kti11p
YBR078W	ECM33	GPI-anchored protein of unknown function, has a possible role in apical bud growth; GPI-anchoring on the plasma membrane crucial to function; phosphorylated in mitochondria; similar to Sps2p and Pst1p
YBL047C	EDE1	Key endocytic protein involved in a network of interactions with other endocytic proteins, binds membranes in a ubiquitin-dependent manner, may also bind ubiquitinated membrane-associated proteins
YMR202W	ERG2	C-8 sterol isomerase, catalyzes the isomerization of the delta-8 double bond to the delta-7 position at an intermediate step in ergosterol biosynthesis
YLR056W	ERG3	C-5 sterol desaturase, catalyzes the introduction of a C-5(6) double bond into episterol, a precursor in ergosterol biosynthesis; mutants are viable, but cannot grow on non-fermentable carbon sources
YML008C	ERG6	Delta(24)-sterol C-methyltransferase, converts zymosterol to fecosterol in the ergosterol biosynthetic pathway by methylating position C-24; localized to both lipid particles and mitochondrial outer membrane
YBR041W	FAT1	Fatty acid transporter and very long-chain fatty acyl-CoA synthetase, may form a complex with Faa1p or Faa4p that imports and activates exogenous fatty acids
YBR019C	GAL10	UDP-glucose-4-epimerase, catalyzes the interconversion of UDP-galactose and UDP-D-glucose in galactose metabolism; also catalyzes the conversion of alpha-D-glucose or alpha-D-galactose to their beta-anomers
YMR307W	GAS1	Beta-1,3-glucanosyltransferase, required for cell wall assembly and also has a role in transcriptional silencing; localizes to the cell surface via a glycosylphosphatidylinositol (GPI) anchor; also found at the nuclear periphery
YGL020C	GET1	Subunit of the GET complex; involved in insertion of proteins into the ER membrane; required for the retrieval of HDEL proteins from the Golgi to the ER in an ERD2 dependent fashion and for normal mitochondrial morphology and inheritance

YER083C	GET2	Subunit of the GET complex; involved in insertion of proteins into the ER membrane; required for the retrieval of HDEL proteins from the Golgi to the ER in an ERD2 dependent fashion and for meiotic nuclear division
YDR508C	GNP1	High-affinity glutamine permease, also transports Leu, Ser, Thr, Cys, Met and Asn; expression is fully dependent on Grr1p and modulated by the Ssy1p-Ptr3p-Ssy5p (SPS) sensor of extracellular amino acids
YER020W	GPA2	Nucleotide binding alpha subunit of the heterotrimeric G protein that interacts with the receptor Gpr1p, has signaling role in response to nutrients; green fluorescent protein (GFP)-fusion protein localizes to the cell periphery
YJL101C	GSH1	Gamma glutamylcysteine synthetase catalyzes the first step in glutathione (GSH) biosynthesis; expression induced by oxidants, cadmium, and mercury
YOL049W	GSH2	Glutathione synthetase, catalyzes the ATP-dependent synthesis of glutathione (GSH) from gamma-glutamylcysteine and glycine; induced by oxidative stress and heat shock
YGL084C	GUP1	Plasma membrane protein involved in remodeling GPI anchors; member of the MBOAT family of putative membrane-bound O-acyltransferases; proposed to be involved in glycerol transport
YGR223C	HSV2	Phosphatidylinositol 3,5-bisphosphate-binding protein, plays a role in micronucleophagy; predicted to fold as a seven-bladed beta-propeller; displays punctate cytoplasmic localization
YJR118C	ILM1	Protein of unknown function; may be involved in mitochondrial DNA maintenance; required for slowed DNA synthesis-induced filamentous growth
YOL081W	IRA2	GTPase-activating protein that negatively regulates RAS by converting it from the GTP- to the GDP-bound inactive form, required for reducing cAMP levels under nutrient limiting conditions, has similarity to Ira1p and human neurofibromin
YER019W	ISC1	Mitochondrial membrane localized inositol phosphosphingolipid phospholipase C, hydrolyzes complex sphingolipids to produce ceramide; activated by phosphatidylserine, cardiolipin, and phosphatidylglycerol; mediates Na ⁺ and Li ⁺ halotolerance
YKL032C	IXR1	Protein that binds DNA containing intrastrand cross-links formed by cisplatin, contains two HMG (high mobility group box) domains, which confer the ability to bend cisplatin-modified DNA; mediates aerobic transcriptional repression of COX5b
YJL062W	LAS21	Integral plasma membrane protein involved in the synthesis of the glycosylphosphatidylinositol (GPI) core structure; mutations affect cell wall integrity
YHR121W	LSM12	Protein of unknown function that may function in RNA processing; interacts with Pbp1p and Pbp4p and associates with ribosomes; contains an RNA-binding LSM domain and an AD domain; GFP-fusion protein is induced by the DNA-damaging agent MMS
YPR070W	MED1	Subunit of the RNA polymerase II mediator complex; associates with core polymerase subunits to form the RNA polymerase II holoenzyme; essential for transcriptional regulation

YNL076W	MKS1	Pleiotropic negative transcriptional regulator involved in Ras-CAMP and lysine biosynthetic pathways and nitrogen regulation; involved in retrograde (RTG) mitochondria-to-nucleus signaling
YGL124C	MON1	Protein required for fusion of cvt-vesicles and autophagosomes with the vacuole; associates, as a complex with Ccz1p, with a perivacuolar compartment; potential Cdc28p substrate
YNL297C	MON2	Peripheral membrane protein with a role in endocytosis and vacuole integrity, interacts with Arl1p and localizes to the endosome; member of the Sec7p family of proteins
YMR224C	MRE11	Subunit of a complex with Rad50p and Xrs2p (MRX complex) that functions in repair of DNA double-strand breaks and in telomere stability, exhibits nuclease activity that appears to be required for MRX function; widely conserved
YKL009W	MRT4	Protein involved in mRNA turnover and ribosome assembly, localizes to the nucleolus
YHR004C	NEM1	Probable catalytic subunit of Nem1p-Spo7p phosphatase holoenzyme; regulates nuclear growth by controlling phospholipid biosynthesis, required for normal nuclear envelope morphology and sporulation; homolog of the human protein Dullard
YGL151W	NUT1	Component of the RNA polymerase II mediator complex, which is required for transcriptional activation and also has a role in basal transcription
YLR338W	OPI9	Dubious open reading frame unlikely to encode a protein, based on available experimental and comparative sequence data; partially overlaps the verified ORF VRP1/YLR337C
YDL232W	OST4	Subunit of the oligosaccharyltransferase complex of the ER lumen, which catalyzes protein asparagine-linked glycosylation; type I membrane protein required for incorporation of Ost3p or Ost6p into the OST complex
YOR360C	PDE2	High-affinity cyclic AMP phosphodiesterase, component of the cAMP-dependent protein kinase signaling system, protects the cell from extracellular cAMP, contains readthrough motif surrounding termination codon
YOR153W	PDR5	Plasma membrane ATP-binding cassette (ABC) transporter, multidrug transporter actively regulated by Pdr1p; also involved in steroid transport, cation resistance, and cellular detoxification during exponential growth
YER149C	PEA2	Coiled-coil polarisome protein required for polarized morphogenesis, cell fusion, and low affinity Ca ²⁺ influx; forms polarisome complex with Bni1p, Bud6p, and Spa2p; localizes to sites of polarized growth
YNL003C	PET8	S-adenosylmethionine transporter of the mitochondrial inner membrane, member of the mitochondrial carrier family; required for biotin biosynthesis and respiratory growth
YDR244W	PEX5	Peroxisomal membrane signal receptor for the C-terminal tripeptide signal sequence (PTS1) of peroxisomal matrix proteins, required for peroxisomal matrix protein import; also proposed to have PTS1-receptor independent functions
YMR205C	PFK2	Beta subunit of heterooctameric phosphofructokinase involved in glycolysis, indispensable for anaerobic growth, activated by fructose-2,6-bisphosphate and AMP, mutation inhibits glucose induction of cell cycle-related genes

YDR276C	PMP3	Small plasma membrane protein related to a family of plant polypeptides that are overexpressed under high salt concentration or low temperature, not essential for viability, deletion causes hyperpolarization of the plasma membrane potential
YAL023C	PMT2	Protein O-mannosyltransferase, transfers mannose residues from dolichyl phosphate-D-mannose to protein serine/threonine residues; acts in a complex with Pmt1p, can instead interact with Pmt5p in some conditions; target for new antifungals
YDR314C	RAD34	Protein involved in nucleotide excision repair (NER); homologous to RAD4
YMR274C	RCE1	Type II CAAX prenyl protease involved in the proteolysis and maturation of Ras and the a-factor mating pheromone
YMR154C	RIM13	Calpain-like cysteine protease involved in proteolytic activation of Rim101p in response to alkaline pH; has similarity to A. nidulans palB
YFL033C	RIM15	Glucose-repressible protein kinase involved in signal transduction during cell proliferation in response to nutrients, specifically the establishment of stationary phase; identified as a regulator of IME2; substrate of Pho80p-Pho85p kinase
YOR275C	RIM20	Protein involved in proteolytic activation of Rim101p in response to alkaline pH; PalA/AIP1/Alix family member; interaction with the ESCRT-III subunit Snf7p suggests a relationship between pH response and multivesicular body formation
YNL294C	RIM21	Component of the RIM101 pathway, has a role in cell wall construction and alkaline pH response; has similarity to A. nidulans PalH
YMR063W	RIM9	Protein of unknown function, involved in the proteolytic activation of Rim101p in response to alkaline pH; has similarity to A. nidulans PalI; putative membrane protein
YBR246W	RRT2	Putative protein of unknown function; non-essential gene identified in a screen for mutants with increased levels of rDNA transcription; null mutants display a weak carboxypeptidase Y missorting/secretion phenotype
YGL244W	RTF1	Subunit of the RNA polymerase II-associated Paf1 complex; directly or indirectly regulates DNA-binding properties of Spt15p and relative activities of different TATA elements; involved in telomere maintenance
YOR216C	RUD3	Golgi matrix protein involved in the structural organization of the cis-Golgi; interacts genetically with COG3 and USO1
YCR009C	RVS161	Amphiphysin-like lipid raft protein; interacts with Rvs167p and regulates polarization of the actin cytoskeleton, endocytosis, cell polarity, cell fusion and viability following starvation or osmotic stress
YDR388W	RVS167	Actin-associated protein, interacts with Rvs161p to regulate actin cytoskeleton, endocytosis, and viability following starvation or osmotic stress; homolog of mammalian amphiphysin
YDR469W	SDC1	Subunit of the COMPASS (Set1C) complex, which methylates lysine 4 of histone H3 and is required in chromatin silencing at telomeres; contains a Dpy-30 domain that mediates interaction with Bre2p; similar to C. elegans and human DPY-30

YBR171W	SEC66	Non-essential subunit of Sec63 complex (Sec63p, Sec62p, Sec66p and Sec72p); with Sec61 complex, Kar2p/BiP and Lhs1p forms a channel competent for SRP-dependent and post-translational SRP-independent protein targeting and import into the ER
YOR140W	SFL1	Transcriptional repressor and activator; involved in repression of flocculation-related genes, and activation of stress responsive genes; negatively regulated by cAMP-dependent protein kinase A subunit Tpk2p
YCL010C	SGF29	Probable subunit of SAGA histone acetyltransferase complex
YBR077C	SLM4	Component of the EGO complex, which is involved in the regulation of microautophagy, and of the GSE complex, which is required for proper sorting of amino acid permease Gap1p; gene exhibits synthetic genetic interaction with MSS4
YDR477W	SNF1	AMP-activated serine/threonine protein kinase found in a complex containing Snf4p and members of the Sip1p/Sip2p/Gal83p family; required for transcription of glucose-repressed genes, thermotolerance, sporulation, and peroxisome biogenesis
YGL115W	SNF4	Activating gamma subunit of the AMP-activated Snf1p kinase complex (contains Snf1p and a Sip1p/Sip2p/Gal83p family member); activates glucose-repressed genes, represses glucose-induced genes; role in sporulation, and peroxisome biogenesis
YCR033W	SNT1	Subunit of the Set3C deacetylase complex that interacts directly with the Set3C subunit, Sif2p; putative DNA-binding protein
YCL037C	SRO9	Cytoplasmic RNA-binding protein that associates with translating ribosomes; involved in heme regulation of Hap1p as a component of the HMC complex, also involved in the organization of actin filaments; contains a La motif
YDR310C	SUM1	Transcriptional repressor required for mitotic repression of middle sporulation-specific genes; also acts as general replication initiation factor; involved in telomere maintenance, chromatin silencing; regulated by pachytene checkpoint
YPL057C	SUR1	Probable catalytic subunit of a mannosylinositol phosphorylceramide (MIPC) synthase, forms a complex with probable regulatory subunit Csg2p; function in sphingolipid biosynthesis is overlapping with that of Csh1p
YDR297W	SUR2	Sphinganine C4-hydroxylase, catalyses the conversion of sphinganine to phytosphingosine in sphingolipid biosynthesis
YAR042W	SWH1	Protein similar to mammalian oxysterol-binding protein; contains ankyrin repeats; localizes to the Golgi and the nucleus-vacuole junction
YLR182W	SWI6	Transcription cofactor, forms complexes with DNA-binding proteins Swi4p and Mbp1p to regulate transcription at the G1/S transition; involved in meiotic gene expression; localization regulated by phosphorylation; potential Cdc28p substrate
YNL081C	SWS2	Putative mitochondrial ribosomal protein of the small subunit, has similarity to E. coli S13 ribosomal protein; participates in controlling sporulation efficiency
YOL018C	TLG2	Syntaxin-like t-SNARE that forms a complex with Tlg1p and Vti1p and mediates fusion of endosome-derived vesicles with the late Golgi; binds Vps45p, which prevents Tlg2p degradation and also facilitates t-SNARE complex formation

YNL079C	TPM1	Major isoform of tropomyosin; binds to and stabilizes actin cables and filaments, which direct polarized cell growth and the distribution of several organelles; acetylated by the NatB complex and acetylated form binds actin most efficiently
YML028W	TSA1	Thioredoxin peroxidase, acts as both a ribosome-associated and free cytoplasmic antioxidant; self-associates to form a high-molecular weight chaperone complex under oxidative stress; deletion results in mutator phenotype
YOR006C	TSR3	Putative protein of unknown function; green fluorescent protein (GFP)-fusion protein localizes to both the cytoplasm and the nucleus
YLL039C	UBI4	Ubiquitin, becomes conjugated to proteins, marking them for selective degradation via the ubiquitin-26S proteasome system; essential for the cellular stress response; encoded as a polyubiquitin precursor comprised of 5 head-to-tail repeats
YER151C	UBP3	Ubiquitin-specific protease that interacts with Bre5p to co-regulate anterograde and retrograde transport between endoplasmic reticulum and Golgi compartments; inhibitor of gene silencing; cleaves ubiquitin fusions but not polyubiquitin
YFR010W	UBP6	Ubiquitin-specific protease situated in the base subcomplex of the 26S proteasome, releases free ubiquitin from branched polyubiquitin chains; works in opposition to polyubiquitin elongation activity of Hul5p
YNL229C	URE2	Nitrogen catabolite repression transcriptional regulator that acts by inhibition of GLN3 transcription in good nitrogen source; has glutathione peroxidase activity and can mutate to acquire GST activity; altered form creates [URE3] prion
YOR106W	VAM3	Syntaxin-related protein required for vacuolar assembly; functions with Vam7p in vacuolar protein trafficking; member of the syntaxin family of proteins
YDL077C	VAM6	Vacuolar protein that plays a critical role in the tethering steps of vacuolar membrane fusion by facilitating guanine nucleotide exchange on small guanosine triphosphatase Ypt7p
YHL035C	VMR1	Protein of unknown function that may interact with ribosomes, based on co-purification experiments; member of the ATP-binding cassette (ABC) family; potential Cdc28p substrate; detected in purified mitochondria in high-throughput studies
YKR001C	VPS1	Dynamin-like GTPase required for vacuolar sorting; also involved in actin cytoskeleton organization, late Golgi-retention of some proteins, regulating peroxisome biogenesis
YOR089C	VPS21	GTPase required for transport during endocytosis and for correct sorting of vacuolar hydrolases; localized in endocytic intermediates; detected in mitochondria; geranylgeranylation required for membrane association; mammalian Rab5 homolog
YKL041W	VPS24	One of four subunits of the endosomal sorting complex required for transport III (ESCRT-III); forms an ESCRT-III subcomplex with Did4p; involved in the sorting of transmembrane proteins into the multivesicular body (MVB) pathway
YNR006W	VPS27	Endosomal protein that forms a complex with Hse1p; required for recycling Golgi proteins, forming luminal membranes and sorting ubiquitinated proteins destined for degradation; has Ubiquitin Interaction Motifs which bind ubiquitin (Ubi4p)

YPR173C	VPS4	AAA-ATPase involved in multivesicular body (MVB) protein sorting, ATP-bound Vps4p localizes to endosomes and catalyzes ESCRT-III disassembly and membrane release; ATPase activity is activated by Vta1p; regulates cellular sterol metabolism
YDR080W	VPS41	Vacuolar membrane protein that is a subunit of the homotypic vacuole fusion and vacuole protein sorting (HOPS) complex; essential for membrane docking and fusion at the Golgi-to-endosome and endosome-to-vacuole stages of protein transport
YKR020W	VPS51	Component of the GARP (Golgi-associated retrograde protein) complex, Vps51p-Vps52p-Vps53p-Vps54p, which is required for the recycling of proteins from endosomes to the late Golgi; links the (VFT/GARP) complex to the SNARE Tlg1p
YJL029C	VPS53	Component of the GARP (Golgi-associated retrograde protein) complex, Vps51p-Vps52p-Vps53p-Vps54p, which is required for the recycling of proteins from endosomes to the late Golgi; required for vacuolar protein sorting
YAL002W	VPS8	Membrane-associated protein that interacts with Vps21p to facilitate soluble vacuolar protein localization; component of the CORVET complex; required for localization and trafficking of the CPY sorting receptor; contains RING finger motif
YOR043W	WHI2	Protein required, with binding partner Psr1p, for full activation of the general stress response, possibly through Msn2p dephosphorylation; regulates growth during the diauxic shift; negative regulator of G1 cyclin expression
YML001W	YPT7	GTPase; GTP-binding protein of the rab family; required for homotypic fusion event in vacuole inheritance, for endosome-endosome fusion, similar to mammalian Rab7
YMR294W-A		Dubious open reading frame unlikely to encode a functional protein, substantially overlaps YMR295C; deletion causes sensitivity to unfolded protein response-inducing agents
YOR062C		Protein of unknown function; similar to YKR075Cp and Reg1p; expression regulated by glucose and Rgt1p; GFP-fusion protein is induced in response to the DNA-damaging agent MMS
YNL296W		Dubious open reading frame unlikely to encode a functional protein; deletion adversely affects sporulation; deletion mutant exhibits synthetic phenotype under expression of mutant huntingtin fragment, but gene does not have human ortholog
YGR250C		Putative RNA binding protein; localizes to stress granules induced by glucose deprivation; interacts with Rbg1p in a two-hybrid
YLR374C		Dubious open reading frame unlikely to encode a protein, based on available experimental and comparative sequence data; partially overlaps the uncharacterized ORF STP3/YLR375W
YMR295C		Protein of unknown function that associates with ribosomes; green fluorescent protein (GFP)-fusion protein localizes to the cell periphery and bud; YMR295C is not an essential gene
YDR186C		Putative protein of unknown function; may interact with ribosomes, based on co-purification experiments; green fluorescent protein (GFP)-fusion protein localizes to the cytoplasm

YDR199W		Dubious open reading frame unlikely to encode a protein, based on available experimental and comparative sequence data; partially overlaps the verified gene VPS64; computationally predicted to have thiol-disulfide oxidoreductase activity
YNR071C		Putative protein of unknown function
YOR059C		Hypothetical protein
YCL042W		Putative protein of unknown function; epitope-tagged protein localizes to the cytoplasm
YOL013W-A		Putative protein of unknown function; identified by SAGE
YML012C-A		Dubious open reading frame unlikely to encode a protein, based on available experimental and comparative sequence data; partially overlaps the verified gene SEL1

Table B.6: Lovastatin + Δ hmg2 Δ xxx PE interactions

YDL243C	AAD4	Putative aryl-alcohol dehydrogenase with similarity to <i>P. chrysosporium</i> aryl-alcohol dehydrogenase, involved in the oxidative stress response; expression induced in cells treated with the mycotoxin patulin
YMR282C	AEP2	Mitochondrial protein, likely involved in translation of the mitochondrial OLI1 mRNA; exhibits genetic interaction with the OLI1 mRNA 5'-untranslated leader
YCL025C	AGP1	Low-affinity amino acid permease with broad substrate range, involved in uptake of asparagine, glutamine, and other amino acids; expression is regulated by the SPS plasma membrane amino acid sensor system (Ssy1p-Ptr3p-Ssy5p)
YMR003W	AIM34	Protein of unknown function; GFP-fusion protein localizes to the mitochondria; null mutant is viable and displays reduced frequency of mitochondrial genome loss
YHR126C	ANS1	Putative protein of unknown function; transcription dependent upon Azflp
YDL074C	BRE1	E3 ubiquitin ligase, forms heterodimer with Rad6p to monoubiquitinate histone H2B-K123, which is required for the subsequent methylation of histone H3-K4 and H3-K79; required for DSBR, transcription, silencing, and checkpoint control
YBR131W	CCZ1	Protein involved in vacuolar assembly, essential for autophagy and the cytoplasm-to-vacuole pathway
YER164W	CHD1	Nucleosome remodeling factor that functions in regulation of transcription elongation; contains a chromo domain, a helicase domain and a DNA-binding domain; component of both the SAGA and SLIK complexes
YBR023C	CHS3	Chitin synthase III, catalyzes the transfer of N-acetylglucosamine (GlcNAc) to chitin; required for synthesis of the majority of cell wall chitin, the chitin ring during bud emergence, and spore wall chitosan
YDL155W	CLB3	B-type cyclin involved in cell cycle progression; activates Cdc28p to promote the G2/M transition; may be involved in DNA replication and spindle assembly; accumulates during S phase and G2, then targeted for ubiquitin-mediated degradation
YLR087C	CSF1	Protein required for fermentation at low temperature; the authentic, non-tagged protein is detected in highly purified mitochondria in high-throughput studies
YCR017C	CWH43	Putative sensor/transporter protein involved in cell wall biogenesis; contains 14-16 transmembrane segments and several putative glycosylation and phosphorylation sites; null mutation is synthetically lethal with <i>pkc1</i> deletion
YIR023W	DAL81	Positive regulator of genes in multiple nitrogen degradation pathways; contains DNA binding domain but does not appear to bind the dodecanucleotide sequence present in the promoter region of many genes involved in allantoin catabolism
YKR024C	DBP7	Putative ATP-dependent RNA helicase of the DEAD-box family involved in ribosomal biogenesis; essential for growth under anaerobic conditions
YAL013W	DEP1	Transcriptional modulator involved in regulation of structural phospholipid biosynthesis genes and metabolically unrelated genes, as well as maintenance of telomeres, mating efficiency, and sporulation

YOR245C	DGA1	Diacylglycerol acyltransferase, catalyzes the terminal step of triacylglycerol (TAG) formation, acylates diacylglycerol using acyl-CoA as an acyl donor, localized to lipid particles
YKL213C	DOA1	WD repeat protein required for ubiquitin-mediated protein degradation, forms complex with Cdc48p, plays a role in controlling cellular ubiquitin concentration; also promotes efficient NHEJ in postdiauxic/stationary phase
YBR078W	ECM33	GPI-anchored protein of unknown function, has a possible role in apical bud growth; GPI-anchoring on the plasma membrane crucial to function; phosphorylated in mitochondria; similar to Sps2p and Pst1p
YDR414C	ERD1	Predicted membrane protein required for the retention of luminal endoplasmic reticulum proteins; mutants secrete the endogenous ER protein, BiP (Kar2p)
YMR202W	ERG2	C-8 sterol isomerase, catalyzes the isomerization of the delta-8 double bond to the delta-7 position at an intermediate step in ergosterol biosynthesis
YLR056W	ERG3	C-5 sterol desaturase, catalyzes the introduction of a C-5(6) double bond into episterol, a precursor in ergosterol biosynthesis; mutants are viable, but cannot grow on non-fermentable carbon sources
YML008C	ERG6	Delta(24)-sterol C-methyltransferase, converts zymosterol to fecosterol in the ergosterol biosynthetic pathway by methylating position C-24; localized to both lipid particles and mitochondrial outer membrane
YBR041W	FAT1	Fatty acid transporter and very long-chain fatty acyl-CoA synthetase, may form a complex with Faa1p or Faa4p that imports and activates exogenous fatty acids
YBR019C	GAL10	UDP-glucose-4-epimerase, catalyzes the interconversion of UDP-galactose and UDP-D-glucose in galactose metabolism; also catalyzes the conversion of alpha-D-glucose or alpha-D-galactose to their beta-anomers
YMR307W	GAS1	Beta-1,3-glucanosyltransferase, required for cell wall assembly and also has a role in transcriptional silencing; localizes to the cell surface via a glycosylphosphatidylinositol (GPI) anchor; also found at the nuclear periphery
YGL020C	GET1	Subunit of the GET complex; involved in insertion of proteins into the ER membrane; required for the retrieval of HDEL proteins from the Golgi to the ER in an ERD2 dependent fashion and for normal mitochondrial morphology and inheritance
YER083C	GET2	Subunit of the GET complex; involved in insertion of proteins into the ER membrane; required for the retrieval of HDEL proteins from the Golgi to the ER in an ERD2 dependent fashion and for meiotic nuclear division
YDR508C	GNP1	High-affinity glutamine permease, also transports Leu, Ser, Thr, Cys, Met and Asn; expression is fully dependent on Grr1p and modulated by the Ssy1p-Ptr3p-Ssy5p (SPS) sensor of extracellular amino acids
YJL101C	GSH1	Gamma glutamylcysteine synthetase catalyzes the first step in glutathione (GSH) biosynthesis; expression induced by oxidants, cadmium, and mercury
YOL049W	GSH2	Glutathione synthetase, catalyzes the ATP-dependent synthesis of glutathione (GSH) from gamma-glutamylcysteine and glycine; induced by oxidative stress and heat shock
YGL084C	GUP1	Plasma membrane protein involved in remodeling GPI anchors; member of the MBOAT family of putative membrane-bound O-acyltransferases; proposed to be involved in glycerol transport

YOR038C	HIR2	Subunit of the HIR complex, a nucleosome assembly complex involved in regulation of histone gene transcription; recruits Swi-Snf complexes to histone gene promoters; promotes heterochromatic gene silencing with Asf1p
YJR118C	ILM1	Protein of unknown function; may be involved in mitochondrial DNA maintenance; required for slowed DNA synthesis-induced filamentous growth
YMR035W	IMP2	Catalytic subunit of the mitochondrial inner membrane peptidase complex, required for maturation of mitochondrial proteins of the intermembrane space; complex contains Imp1p and Imp2p (both catalytic subunits), and Som1p
YIL002C	INP51	Phosphatidylinositol 4,5-bisphosphate 5-phosphatase, synaptojanin-like protein with an N-terminal Sac1 domain, plays a role in phosphatidylinositol 4,5-bisphosphate homeostasis and in endocytosis; null mutation confers cold-tolerant growth
YOL081W	IRA2	GTPase-activating protein that negatively regulates RAS by converting it from the GTP- to the GDP-bound inactive form, required for reducing cAMP levels under nutrient limiting conditions, has similarity to Ira1p and human neurofibromin
YER019W	ISC1	Mitochondrial membrane localized inositol phosphosphingolipid phospholipase C, hydrolyzes complex sphingolipids to produce ceramide; activated by phosphatidylserine, cardiolipin, and phosphatidylglycerol; mediates Na ⁺ and Li ⁺ halotolerance
YKL032C	IXR1	Protein that binds DNA containing intrastrand cross-links formed by cisplatin, contains two HMG (high mobility group box) domains, which confer the ability to bend cisplatin-modified DNA; mediates aerobic transcriptional repression of COX5b
YJL062W	LAS21	Integral plasma membrane protein involved in the synthesis of the glycosylphosphatidylinositol (GPI) core structure; mutations affect cell wall integrity
YOL009C	MDM12	Mitochondrial outer membrane protein, required for transmission of mitochondria to daughter cells; component of the ERMES complex that links the ER to mitochondria; may influence import and assembly of outer membrane beta-barrel proteins
YKL009W	MRT4	Protein involved in mRNA turnover and ribosome assembly, localizes to the nucleolus
YOL112W	MSB4	GTPase-activating protein of the Ras superfamily that acts primarily on Sec4p, localizes to the bud site and bud tip, has similarity to Msb3p; msb3 msb4 double mutation causes defects in secretion and actin organization
YDR277C	MTH1	Negative regulator of the glucose-sensing signal transduction pathway, required for repression of transcription by Rgt1p; interacts with Rgt1p and the Snf3p and Rgt2p glucose sensors; phosphorylated by Yck1p, triggering Mth1p degradation
YLR338W	OPI9	Dubious open reading frame unlikely to encode a protein, based on available experimental and comparative sequence data; partially overlaps the verified ORF VRP1/YLR337C

YDL232W	OST4	Subunit of the oligosaccharyltransferase complex of the ER lumen, which catalyzes protein asparagine-linked glycosylation; type I membrane protein required for incorporation of Ost3p or Ost6p into the OST complex
YHL013C	OTU2	Protein of unknown function that may interact with ribosomes, based on co-purification experiments; member of the ovarian tumor-like (OTU) superfamily of predicted cysteine proteases; shows cytoplasmic localization
YDR071C	PAA1	Polyamine acetyltransferase; acetylates polyamines (e.g. putrescine, spermidine, spermine) and also aralkylamines (e.g. tryptamine, phenylethylamine); may be involved in transcription and/or DNA replication
YOR360C	PDE2	High-affinity cyclic AMP phosphodiesterase, component of the cAMP-dependent protein kinase signaling system, protects the cell from extracellular cAMP, contains readthrough motif surrounding termination codon
YGL013C	PDR1	Zinc cluster protein that is a master regulator involved in recruiting other zinc cluster proteins to pleiotropic drug response elements (PDREs) to fine tune the regulation of multidrug resistance genes
YOR153W	PDR5	Plasma membrane ATP-binding cassette (ABC) transporter, multidrug transporter actively regulated by Pdr1p; also involved in steroid transport, cation resistance, and cellular detoxification during exponential growth
YER149C	PEA2	Coiled-coil polarisome protein required for polarized morphogenesis, cell fusion, and low affinity Ca ²⁺ influx; forms polarisome complex with Bni1p, Bud6p, and Spa2p; localizes to sites of polarized growth
YNL003C	PET8	S-adenosylmethionine transporter of the mitochondrial inner membrane, member of the mitochondrial carrier family; required for biotin biosynthesis and respiratory growth
YAL023C	PMT2	Protein O-mannosyltransferase, transfers mannose residues from dolichyl phosphate-D-mannose to protein serine/threonine residues; acts in a complex with Pmt1p, can instead interact with Pmt5p in some conditions; target for new antifungals
YDR314C	RAD34	Protein involved in nucleotide excision repair (NER); homologous to RAD4
YHL027W	RIM101	Transcriptional repressor involved in response to pH and in cell wall construction; required for alkaline pH-stimulated haploid invasive growth and sporulation; activated by proteolytic processing; similar to A. nidulans PacC
YMR154C	RIM13	Calpain-like cysteine protease involved in proteolytic activation of Rim101p in response to alkaline pH; has similarity to A. nidulans palB
YFL033C	RIM15	Glucose-repressible protein kinase involved in signal transduction during cell proliferation in response to nutrients, specifically the establishment of stationary phase; identified as a regulator of IME2; substrate of Pho80p-Pho85p kinase
YMR063W	RIM9	Protein of unknown function, involved in the proteolytic activation of Rim101p in response to alkaline pH; has similarity to A. nidulans PalI; putative membrane protein
YPL089C	RLM1	MADS-box transcription factor, component of the protein kinase C-mediated MAP kinase pathway involved in the maintenance of cell integrity; phosphorylated and activated by the MAP-kinase Slk2p

YOR312C	RPL20B	Protein component of the large (60S) ribosomal subunit, nearly identical to Rpl20Ap and has similarity to rat L18a ribosomal protein
YJL136C	RPS21B	Protein component of the small (40S) ribosomal subunit; nearly identical to Rps21Ap and has similarity to rat S21 ribosomal protein
YHR021C	RPS27B	Protein component of the small (40S) ribosomal subunit; nearly identical to Rps27Ap and has similarity to rat S27 ribosomal protein
YGL244W	RTF1	Subunit of the RNA polymerase II-associated Paf1 complex; directly or indirectly regulates DNA-binding properties of Spt15p and relative activities of different TATA elements; involved in telomere maintenance
YOR216C	RUD3	Golgi matrix protein involved in the structural organization of the cis-Golgi; interacts genetically with COG3 and USO1
YCR009C	RVS161	Amphiphysin-like lipid raft protein; interacts with Rvs167p and regulates polarization of the actin cytoskeleton, endocytosis, cell polarity, cell fusion and viability following starvation or osmotic stress
YDR388W	RVS167	Actin-associated protein, interacts with Rvs161p to regulate actin cytoskeleton, endocytosis, and viability following starvation or osmotic stress; homolog of mammalian amphiphysin
YDR469W	SDC1	Subunit of the COMPASS (Set1C) complex, which methylates lysine 4 of histone H3 and is required in chromatin silencing at telomeres; contains a Dpy-30 domain that mediates interaction with Bre2p; similar to C. elegans and human DPY-30
YBR171W	SEC66	Non-essential subunit of Sec63 complex (Sec63p, Sec62p, Sec66p and Sec72p); with Sec61 complex, Kar2p/BiP and Lhs1p forms a channel competent for SRP-dependent and post-translational SRP-independent protein targeting and import into the ER
YCL010C	SGF29	Probable subunit of SAGA histone acetyltransferase complex
YLR079W	SIC1	Inhibitor of Cdc28-Clb kinase complexes that controls G1/S phase transition, preventing premature S phase and ensuring genomic integrity; phosphorylation targets Sic1p for SCF(CDC4)-dependent turnover; functional homolog of mammalian Kip1
YBR077C	SLM4	Component of the EGO complex, which is involved in the regulation of microautophagy, and of the GSE complex, which is required for proper sorting of amino acid permease Gap1p; gene exhibits synthetic genetic interaction with MSS4
YDR477W	SNF1	AMP-activated serine/threonine protein kinase found in a complex containing Snf4p and members of the Sip1p/Sip2p/Gal83p family; required for transcription of glucose-repressed genes, thermotolerance, sporulation, and peroxisome biogenesis
YGL115W	SNF4	Activating gamma subunit of the AMP-activated Snf1p kinase complex (contains Snf1p and a Sip1p/Sip2p/Gal83p family member); activates glucose-repressed genes, represses glucose-induced genes; role in sporulation, and peroxisome biogenesis
YCR033W	SNT1	Subunit of the Set3C deacetylase complex that interacts directly with the Set3C subunit, Sif2p; putative DNA-binding protein
YDR297W	SUR2	Sphinganine C4-hydroxylase, catalyses the conversion of sphinganine to phytosphingosine in sphingolipid biosynthesis
YHR181W	SVP26	Integral membrane protein of the early Golgi apparatus and endoplasmic reticulum, involved in COP II vesicle transport; may also function to promote retention of proteins in the early Golgi compartment

YLR182W	SWI6	Transcription cofactor, forms complexes with DNA-binding proteins Swi4p and Mbp1p to regulate transcription at the G1/S transition; involved in meiotic gene expression; localization regulated by phosphorylation; potential Cdc28p substrate
YOL018C	TLG2	Syntaxin-like t-SNARE that forms a complex with Tlg1p and Vti1p and mediates fusion of endosome-derived vesicles with the late Golgi; binds Vps45p, which prevents Tlg2p degradation and also facilitates t-SNARE complex formation
YER090W	TRP2	Anthranilate synthase, catalyzes the initial step of tryptophan biosynthesis, forms multifunctional hetero-oligomeric anthranilate synthase:indole-3-glycerol phosphate synthase enzyme complex with Trp3p
YKL211C	TRP3	Bifunctional enzyme exhibiting both indole-3-glycerol-phosphate synthase and anthranilate synthase activities, forms multifunctional hetero-oligomeric anthranilate synthase:indole-3-glycerol phosphate synthase enzyme complex with Trp2p
YML028W	TSA1	Thioredoxin peroxidase, acts as both a ribosome-associated and free cytoplasmic antioxidant; self-associates to form a high-molecular weight chaperone complex under oxidative stress; deletion results in mutator phenotype
YOR006C	TSR3	Putative protein of unknown function; green fluorescent protein (GFP)-fusion protein localizes to both the cytoplasm and the nucleus
YLL039C	UBI4	Ubiquitin, becomes conjugated to proteins, marking them for selective degradation via the ubiquitin-26S proteasome system; essential for the cellular stress response; encoded as a polyubiquitin precursor comprised of 5 head-to-tail repeats
YER151C	UBP3	Ubiquitin-specific protease that interacts with Bre5p to co-regulate anterograde and retrograde transport between endoplasmic reticulum and Golgi compartments; inhibitor of gene silencing; cleaves ubiquitin fusions but not polyubiquitin
YFR010W	UBP6	Ubiquitin-specific protease situated in the base subcomplex of the 26S proteasome, releases free ubiquitin from branched polyubiquitin chains; works in opposition to polyubiquitin elongation activity of Hul5p
YOR106W	VAM3	Syntaxin-related protein required for vacuolar assembly; functions with Vam7p in vacuolar protein trafficking; member of the syntaxin family of proteins
YDL077C	VAM6	Vacuolar protein that plays a critical role in the tethering steps of vacuolar membrane fusion by facilitating guanine nucleotide exchange on small guanosine triphosphatase Ypt7p
YGL212W	VAM7	Component of the vacuole SNARE complex involved in vacuolar morphogenesis; SNAP-25 homolog; functions with a syntaxin homolog Vam3p in vacuolar protein trafficking
YLR373C	VID22	Glycosylated integral membrane protein localized to the plasma membrane; plays a role in fructose-1,6-bisphosphatase (FBPase) degradation; involved in FBPase transport from the cytosol to Vid (vacuole import and degradation) vesicles
YKR001C	VPS1	Dynamin-like GTPase required for vacuolar sorting; also involved in actin cytoskeleton organization, late Golgi-retention of some proteins, regulating peroxisome biogenesis

YKL041W	VPS24	One of four subunits of the endosomal sorting complex required for transport III (ESCRT-III); forms an ESCRT-III subcomplex with Did4p; involved in the sorting of transmembrane proteins into the multivesicular body (MVB) pathway
YNR006W	VPS27	Endosomal protein that forms a complex with Hse1p; required for recycling Golgi proteins, forming luminal membranes and sorting ubiquitinated proteins destined for degradation; has Ubiquitin Interaction Motifs which bind ubiquitin (Ubi4p)
YPR173C	VPS4	AAA-ATPase involved in multivesicular body (MVB) protein sorting, ATP-bound Vps4p localizes to endosomes and catalyzes ESCRT-III disassembly and membrane release; ATPase activity is activated by Vta1p; regulates cellular sterol metabolism
YDR080W	VPS41	Vacuolar membrane protein that is a subunit of the homotypic vacuole fusion and vacuole protein sorting (HOPS) complex; essential for membrane docking and fusion at the Golgi-to-endosome and endosome-to-vacuole stages of protein transport
YKR020W	VPS51	Component of the GARP (Golgi-associated retrograde protein) complex, Vps51p-Vps52p-Vps53p-Vps54p, which is required for the recycling of proteins from endosomes to the late Golgi; links the (VFT/GARP) complex to the SNARE Tlg1p
YJL029C	VPS53	Component of the GARP (Golgi-associated retrograde protein) complex, Vps51p-Vps52p-Vps53p-Vps54p, which is required for the recycling of proteins from endosomes to the late Golgi; required for vacuolar protein sorting
YML097C	VPS9	A guanine nucleotide exchange factor involved in vesicle-mediated vacuolar protein transport; specifically stimulates the intrinsic guanine nucleotide exchange activity of Vps21p/Rab5: similar to mammalian ras inhibitors; binds ubiquitin
YLR337C	VRP1	Proline-rich actin-associated protein involved in cytoskeletal organization and cytokinesis; related to mammalian Wiskott-Aldrich syndrome protein (WASP)-interacting protein (WIP)
YOR043W	WHI2	Protein required, with binding partner Psr1p, for full activation of the general stress response, possibly through Msn2p dephosphorylation; regulates growth during the diauxic shift; negative regulator of G1 cyclin expression
YML001W	YPT7	GTPase; GTP-binding protein of the rab family; required for homotypic fusion event in vacuole inheritance, for endosome-endosome fusion, similar to mammalian Rab7
YBR111C	YSA1	Nudix hydrolase family member with ADP-ribose pyrophosphatase activity; shown to metabolize O-acetyl-ADP-ribose to AMP and acetylated ribose 5'-phosphate
YJL211C		Dubious open reading frame unlikely to encode a protein, based on available experimental and comparative sequence data; partially overlaps the verified gene YJL210W/PEX2
YHR210C		Putative protein of unknown function; non-essential gene; highly expressed under anaerobic conditions; sequence similarity to aldose 1-epimerases such as GAL10

YOR062C		Protein of unknown function; similar to YKR075Cp and Reg1p; expression regulated by glucose and Rgt1p; GFP-fusion protein is induced in response to the DNA-damaging agent MMS
YPL041C		Protein of unknown function involved in maintenance of proper telomere length
YBR174C		Dubious open reading frame unlikely to encode a protein, based on available experimental and comparative sequence data; partially overlaps the verified ORF YBR175W; null mutant is viable and sporulation defective
YGR250C		Putative RNA binding protein; localizes to stress granules induced by glucose deprivation; interacts with Rbg1p in a two-hybrid
YMR295C		Protein of unknown function that associates with ribosomes; green fluorescent protein (GFP)-fusion protein localizes to the cell periphery and bud; YMR295C is not an essential gene
YNL170W		Dubious open reading frame unlikely to encode a functional protein, based on available experimental and comparative sequence data
YGR122W		Probable ortholog of <i>A. nidulans</i> PalC, which is involved in pH regulation and binds to the ESCRT-III complex; null mutant does not properly process Rim101p and has decreased resistance to rapamycin; GFP-fusion protein is cytoplasmic
YER119C-A		Dubious open reading frame, not conserved in closely related <i>Saccharomyces</i> species; deletion mutation blocks replication of Brome mosaic virus in <i>S. cerevisiae</i> , but this is likely due to effects on the overlapping gene SCS2
YHL012W		Putative protein of unknown function, has some homology to Ugp1p, which encodes UDP-glucose pyrophosphorylase
YCL042W		Putative protein of unknown function; epitope-tagged protein localizes to the cytoplasm